Reaction kinetics of the pyrolysis of urea phosphate

P.A. Broodryk


ORCid ID: https://orcid.org/0000-0001-8392-1793

Dissertation submitted in fulfilment of the requirements for the degree *Master of Engineering in Chemical Engineering* at the North-West University

Supervisor: Mr. A.F. van der Merwe

Co-supervisor: Prof. H.W.J.P. Neomagus

Examination March 2019

Student number: 24150738

Declaration

I, Pieter Andri Broodryk, hereby declare that the dissertation entitled: Reaction kinetics of the pyrolysis of urea phosphate, which was done for the completion of a Masters Degree in Chemical Engineering, is my own work.

P.A. Broodryk

Date

Abstract

In this study, the pyrolysis reaction of urea phosphate for the production of the liquid fertiliser ammonium di-phosphate (ADP) was investigated. The liquid fertiliser ADP is a promising alternative to the increasing demand of nitrogen and phosphorus fertilisers in Africa, and it also the first clear liquid fertiliser being produced in South Africa. Although ADP can be produced in various ways, the pyrolysis of urea phosphate is the preferred route. Urea phosphate decomposes upon melting, and forms ADP, as well as longer chain ammonium polyphosphates (APP). Two reactions were focussed on within this study, namely the production of ADP from urea (U) and phosphoric acid (PA), and the consecutive reaction to ammonium tri-phosphate (ATP).

The reactions were monitored by determining the mass loss, heat effects and CO_2 formation transiently in a TGA-DSC couples to an FTIR. The liquid composition of the final product was determined by NMR analysis. The experiments were carried out at atmospheric pressure, and both isothermal and non-isothermal conditions within the temperature range of 115 – 140°C.

The process is found to be initially exothermic, producing only ammonium diphosphate and carbon dioxide as products. At higher conversions, the process becomes endothermic, also producing ammonium tri-phosphate and ammonia gas. At longer reaction times, some longer chain APP's were also observed.

By adopting a mechanism from literature, kinetic parameters were fitted to the experimental data. The ADP formation reaction was found to be described by the kinetic rate equation

$$r_1 = A_1 \exp(\frac{-E_{A1}}{RT}) C_U$$

with $A_1 = 1.4 \times 10^{13}$ min^{-1} and $E_{A1} = 113$ kJ mol^{-1} The consumption of ADP to produce ATP follows the kinetic rate equation

$$r_2 = A_2 \exp(\frac{-E_{A2}}{RT}) C_{ADP} C_{PA}$$

with $A_2 = 1.3 \times 10^{38}$ L mol^{-1}min^{-1} and $E_{A2} = 311$ kJmol^{-1}. Where C_x is the concentration of species x.

1

[1]Keywords: pyrolysis, reaction kinetics, urea phosphate, ammonium polyphosphate

Contents

Declaration i

Abstract ii

Nomenclature xi

1 Introduction 1
- 1.1 Background of this study . . . 1
- 1.2 Problem Statement . . . 2
- 1.3 Objectives and scope of this work . . . 3
  - 1.3.1 Objectives . . . 3
- 1.4 Scope of the work . . . 3
  - 1.4.1 Dissertation layout . . . 4

2 Literature review 5
- 2.1 Background and manufacturing of Ammonium polyphosphate . . . 5
  - 2.1.1 Mono- and polyphosphates . . . 5
  - 2.1.2 Manufacturing of ammonium polyphosphates: a historical perspective . . . 6
- 2.2 Chemistry of the pyrolysis of urea phosphate . . . 7
  - 2.2.1 Decomposition of urea . . . 7
  - 2.2.2 Condensation of phosphates . . . 8
  - 2.2.3 Decomposition of urea phosphate . . . 11
  - 2.2.4 Reaction mechanism of urea phosphate decomposition . . . 12
- 2.3 Reaction kinetics . . . 14
  - 2.3.1 Analysis of experimentally generated kinetic data . . . 14
  - 2.3.2 Complex kinetics . . . 17
- 2.4 Analytical methods . . . 17
  - 2.4.1 NMR . . . 17
  - 2.4.2 FTIR . . . 18
- 2.5 Summary of literature and relevance to this study . . . 19

3 Experimental procedure 21
- 3.1 Materials used . . . 21
- 3.2 TGA-DSC experiments . . . 22
  - 3.2.1 Overview of the experiment . . . 22
  - 3.2.2 Operation of the TGA and product analysis . . . 22
- 3.3 NMR analysis . . . 23
- 3.4 Experimental plan . . . 24

3.5 Calculations . . . 24
3.5.1 Experimental error . . . 24
3.5.2 NMR . . . 25
3.5.3 Quality of fit calculation . . . 27

4 Model Development **28**
4.1 Assumptions . . . 28
4.1.1 Reversibility of reactions . . . 28
4.1.2 Urea phosphate purity . . . 28
4.1.3 Condensing of only di- and tri-phosphates . . . 28
4.1.4 Gas produced . . . 29
4.1.5 Liquid density . . . 29
4.1.6 Well mixed reactor . . . 29
4.2 Design equations . . . 30
4.3 Mole balance . . . 32
4.3.1 NMR balance . . . 32
4.3.2 TGA balance . . . 32
4.4 Reaction rate equations . . . 33
4.4.1 Parameter fitting . . . 33

5 Results and discussion **36**
5.1 Thermogravimetric analysis . . . 36
5.2 FTIR analysis . . . 39
5.2.1 Non-isothermal experiments . . . 39
5.2.2 Isothermal experiments . . . 40
5.3 Model fitting . . . 42
5.4 NMR corellation with TG measurements . . . 46
5.5 Energy analysis . . . 47
5.5.1 Non-isothermal experiments . . . 47
5.5.2 Isothermal experiments . . . 48

6 Conclusions and recommendations **50**
6.1 Conclusions . . . 50
6.1.1 Reaction mechanism . . . 50
6.1.2 Model development and fit . . . 50
6.2 Contribution to science . . . 51
6.3 Recommendations . . . 51

A Purity Analysis results **55**
A.1 ICP-OES results . . . 55
A.2 XRD analysis results . . . 57

B FTIR Calibration **61**

C Mechanism derivation **63**
C.1 Ammonium di-phosphate mechanism . . . 63
C.2 Ammonium tri-phosphate mechanism . . . 65
C.3 Matlab Code for solution to pseudo steady state equations . . . 67

D Matlab Code **69**

D.1 Derive . . . 69
D.2 Model display . . . 71
D.3 Options . . . 72
D.4 Data load . . . 73
D.5 Integrated . . . 77
D.6 dNdt . . . 80
D.7 Quality of Fit . . . 82
D.8 Graphing . . . 83
D.9 Graph export . . . 86

E Experimental data 106
E.1 TGA Data . . . 106
E.1.1 0.5 K/min . . . 107
E.1.2 1 K/min . . . 108
E.1.3 2 K/min . . . 110
E.1.4 3 K/min . . . 111
E.1.5 4 K/min . . . 111
E.1.6 5 K/min . . . 112
E.1.7 Isothermal, 119 °C . . . 112
E.1.8 Isothermal, 122 °C . . . 113
E.1.9 Isothermal, 125 °C . . . 114
E.1.10 Isothermal 130 °C . . . 114
E.2 Mass balances . . . 116
E.2.1 0.5 K/min . . . 116
E.2.2 1 K/min . . . 118
E.2.3 2 K/min . . . 121
E.2.4 3 K/min . . . 122
E.2.5 4 K/min . . . 123
E.2.6 5 K/min . . . 124
E.2.7 Isothermal 119 °C . . . 125
E.2.8 Isothermal 122 °C . . . 126
E.2.9 Isothermal 125 °C . . . 128
E.2.10 Isothermal 130 °C . . . 129
E.3 FTIR data . . . 130
E.3.1 Calibration run . . . 131
E.3.2 0.5 K/min . . . 132
E.3.3 1 K/min . . . 133
E.3.4 2 K/min . . . 135
E.3.5 3 K/min . . . 136
E.3.6 4 K/min . . . 137
E.3.7 5 K/min . . . 138
E.3.8 130 °C isothermal . . . 139
E.4 NMR results . . . 140

List of Figures

1.1 Schematic representation of the structure of the reagent and the product of interest for the reaction investigated. (Adapted from [7], [9], [10]) . . . 2

2.1 Chemical structure of diphosphate [7] . . . 9
2.2 Chemical structure of urea phosphate . . . 12
2.3 Chemical structure of ammonium polyphosphate . . . 12
2.4 Reaction scheme for equation 2.13 [18] . . . 14
2.5 Mono-phosphate ion . . . 18
2.6 Tri-phosphate . . . 18

3.1 TGA-DSC schematic . . . 23
3.2 Repeatability and experimental error calculation for 5 repeats of 1 K/min between the temperature range of 120 and 140°C . . . 26

4.1 Matlab algorithm used for finding kinetic parameters . . . 35

5.1 Normalised mass loss as a function of temperature and heating rate on a temperature range of 120 – 140°C . . . 37
5.2 Normalised mass loss as a function of temperature and heating rate on a temperature range of 120 – 140°C . . . 37
5.3 Mass loss as a function of time of different temperatures on a temperature range of 119 – 130°C and a total residence time of 60 min . . . 38
5.4 Total mass loss and mass loss due to CO_2 formation for a constant heating rate of 5 K/min . . . 39
5.5 Total Mass loss and mass loss due to CO_2 formation for a constant heating rate of 0.5 K/min . . . 40
5.6 Total mass loss and mass loss due to CO_2 formation for a constant temperature of 122°C . . . 40
5.7 Total mass loss and mass loss due to CO_2 formation for a constant temperature of 130°C . . . 41
5.8 Mass loss measured and predicted for various different heating rates . . . 43
5.9 Measured mass loss due to CO_2 formation and predicted for various different heating rates . . . 44
5.10 Mass loss measured and predicted for various different temperatures . . . 45
5.11 Reaction rates for a 1 K/min experiment within the temperature range of 120°C and 140°C . . . 45
5.12 TGA-DSC and FTIR data output of a constant heating rate of 5 K/min . . . 47
5.13 TGA-DSC output and mass loss due to CO_2 for a constant heating rate of 0.5 K/min . . . 48

5.14 TGA-DSC and FTIR data output of a constant temperature of 122°C . . . 48
5.15 TGA-DSC and FTIR data output of a constant temperature of 130°C . . . 49

E.1 Mass loss and thermal effects of the pyrolysis of urea phosphate at a constant heating rate of 0.5 K/min run # 1 . . . 107
E.2 Mass loss and thermal effects of the pyrolysis of urea phosphate at a constant heating rate of 0.5 K/min run # 2 . . . 107
E.3 Mass loss and thermal effects of the pyrolysis of urea phosphate at a constant heating rate of 1 K/min run # 1 . . . 108
E.4 Mass loss and thermal effects of the pyrolysis of urea phosphate at a constant heating rate of 1 K/min run # 2 . . . 108
E.5 Mass loss and thermal effects of the pyrolysis of urea phosphate at a constant heating rate of 1 K/min run # 3 (10mg) . . . 109
E.6 Mass loss and thermal effects of the pyrolysis of urea phosphate at a constant heating rate of 1 K/min run # 4 . . . 109
E.7 Mass loss and thermal effects of the pyrolysis of urea phosphate at a constant heating rate of 1 K/min run # 5 . . . 110
E.8 Mass loss and thermal effects of the pyrolysis of urea phosphate at a constant heating rate of 2 K/min run # 1 . . . 110
E.9 Mass loss and thermal effects of the pyrolysis of urea phosphate at a constant heating rate of 3 K/min run # 1 . . . 111
E.10 Mass loss and thermal effects of the pyrolysis of urea phosphate at a constant heating rate of 4 K/min run # 1 . . . 111
E.11 Mass loss and thermal effects of the pyrolysis of urea phosphate at a constant heating rate of 5 K/min run # 1 . . . 112
E.12 Mass loss and thermal effects of the pyrolysis of urea phosphate at a constant temperature of 119 °C run # 1 . . . 112
E.13 Mass loss and thermal effects of the pyrolysis of urea phosphate at a constant temperature of 122 °C run # 1 . . . 113
E.14 Mass loss and thermal effects of the pyrolysis of urea phosphate at a constant temperature of 122 °C run # 2 . . . 113
E.15 Mass loss and thermal effects of the pyrolysis of urea phosphate at a constant temperature of 125 °C run # 1 . . . 114
E.16 Mass loss and thermal effects of the pyrolysis of urea phosphate at a constant temperature of 130 °C run # 1 . . . 114
E.17 Mass loss and thermal effects of the pyrolysis of urea phosphate at a constant temperature of 130 °C run # 2 . . . 115
E.18 Mass CO_2 produced during the pyrolysis of urea phosphate at a constant heating rate of 0.5 K/min run # 1 . . . 116
E.19 Mass loss of predicted and experimental measurements as a constant heating rate of 0.5 K/min run # 1 . . . 116
E.20 Mass CO_2 produced during the pyrolysis of urea phosphate at a constant heating rate of 0.5 K/min run # 2 . . . 117
E.21 Mass loss of predicted and experimental measurements as a constant heating rate of 0.5 K/min run # 2 . . . 117
E.22 Mass CO_2 produced during the pyrolysis of urea phosphate at a constant heating rate of 1 K/min run # 2 . . . 118
E.23 Mass loss of predicted and experimental measurements as a constant heating rate of 1 K/min run # 2 . . . 118

E.24 Mass CO_2 produced during the pyrolysis of urea phosphate at a constant heating rate of 1 K/min run # 3 119
E.25 Mass loss of predicted and experimental measurements as a constant heating rate of 1 K/min run # 3 119
E.26 Mass CO_2 produced during the pyrolysis of urea phosphate at a constant heating rate of 1 K/min run # 5 120
E.27 Mass loss of predicted and experimental measurements as a constant heating rate of 1 K/min run # 5 120
E.28 Mass CO_2 produced during the pyrolysis of urea phosphate at a constant heating rate of 2 K/min run # 1 121
E.29 Mass loss of predicted and experimental measurements as a constant heating rate of 2 K/min run # 1 121
E.30 Mass CO_2 produced during the pyrolysis of urea phosphate at a constant heating rate of 3 K/min run # 1 122
E.31 Mass loss of predicted and experimental measurements as a constant heating rate of 3 K/min run # 1 122
E.32 Mass CO_2 produced during the pyrolysis of urea phosphate at a constant heating rate of 4 K/min run # 1 123
E.33 Mass loss of predicted and experimental measurements as a constant heating rate of 4 K/min run # 1 123
E.34 Mass CO_2 produced during the pyrolysis of urea phosphate at a constant heating rate of 5 K/min run # 1 124
E.35 Mass loss of predicted and experimental measurements as a constant heating rate of 5 K/min run # 1 124
E.36 Mass CO_2 produced during the pyrolysis of urea phosphate at a constant temperature of 119 °C run # 1 125
E.37 Mass loss of predicted and experimental measurements as a constant temperature of 119 °C run # 1 125
E.38 Mass CO_2 produced during the pyrolysis of urea phosphate at a constant temperature of 122 °C run # 1 126
E.39 Mass loss of predicted and experimental measurements as a constant temperature of 122 °C run # 1 126
E.40 Mass CO_2 produced during the pyrolysis of urea phosphate at a constant temperature of 122 °C run # 2 127
E.41 Mass loss of predicted and experimental measurements as a constant temperature of 122 °C run # 2 127
E.42 Mass CO_2 produced during the pyrolysis of urea phosphate at a constant temperature of 122 °C run # 1 128
E.43 Mass loss of predicted and experimental measurements as a constant temperature of 125 °C run # 1 128
E.44 Mass CO_2 produced during the pyrolysis of urea phosphate at a constant temperature of 130 °C run # 1 129
E.45 Mass loss of predicted and experimental measurements as a constant temperature of 130 °C run # 1 129
E.46 Mass CO_2 produced during the pyrolysis of urea phosphate at a constant temperature of 130 °C run # 2 130
E.47 Mass loss of predicted and experimental measurements as a constant temperature of 130 °C run # 2 130
E.48 CO_2 Calibration run FTIR feed 131

E.49 0.5 K/min run # 1 FTIR feed 132
E.50 1 K/min run # 2 FTIR feed 133
E.51 1 K/min run # 3 (10 mg) FTIR feed 134
E.52 1 K/min run # 5 FTIR feed 134
E.53 2 K/min run # 1 FTIR feed 135
E.54 3 K/min run # 1 FTIR feed 136
E.55 4 K/min run # 1 FTIR feed 137
E.56 5 K/min run # 1 FTIR feed 138
E.57 130 °C isothermal run # 1 FTIR feed 139
E.58 130 °C isothermal run # 2 FTIR feed 140
E.59 NMR spectrum of the 122 °C isothermal 30 min sample 140
E.60 NMR spectrum of the 122 °C isothermal 60 min sample 141
E.61 NMR spectrum of the 0.5K/min sample 141
E.62 NMR spectrum of the 1K/min sample 142
E.63 NMR spectrum of the 4K/min sample 142

List of Tables

2.1 Classification of phosphate ions, adapted from Gard [7] 10

3.1 Materials used during the experimental programme 21
3.2 Summary of non-isothermal experiments and analysis done 24
3.3 Summary of isothermal experiments and analysis done 24
3.4 Experimental Error calculation 25

5.1 Rate law comparisson 42
5.2 Best fit kinetic parameters 43
5.3 NMR Integrated peak area percentages 46
5.4 Comparisson between TGA mass loss and NMR calculated mass loss . . . 46

B.1 Summary of the values for c_{FTIR} for each experiment conducted 62

Nomenclature

List of Abbreviations

ADP	Ammonium di-phosphate
APP	Ammonium polyphosphate
ATP	Ammonium triphosphate
DOF	Degrees of freedom
DSC	Differential scanning saloriemeter
FTIR	Fourier transform infrared spectroscopy
IC	Ion Chromatography
ICP-OES	Inductively coupled plasma - optical emission spectrometry
MFC	Microparticle free control
Mt	Million tonnes
NMR	Nuclear magnetic resonance
ODE	Ordinary differential equation
PA	Phosphoric acid
RMSE	Root mean squared error
TGA	Thermogravimetric Analysis
TGA-DSC	Thermogravimetric analysis and differential scanning caloriemeter
U	Urea
UP	Urea phosphate
XRD	X-ray diffraction

List of Symbols

α	Conversion fraction	
β	Heating rate	K/min
ΔH_{rxn}	Heat of Reaction	$\frac{J}{mol}$
ρ	Density	$\frac{kg}{m^3}$

ξ	Extent of reaction	various
A	Pre-exponential factor	
C_i	Concentration of specie i	$\frac{mol}{L}$
E_A	Activation energy	$\frac{J}{mol}$
I_{end}	percentage of phosphorus atoms in an end group position	
I_{mid}	percentage of phosphorus atoms in a mid group position	
I_{mono}	percentage of phosphorus atoms as mono-phosphate	
k(T)	Rate Constant/Specific rate	
M	Normalised mass	$\frac{m}{m_0}$
m_i	mass of specie i	mg
MW_i	Molecular weight of chemical specias i	$\frac{g}{mol}$
N	Number of data points	
n_i	molar amount of specie i	mol
$n_{i(0)}$	initial molar amount of specie i	mol
q	Energy input required	$\frac{J}{min}$
R	Universal gas constant	$8.314 \frac{J}{mol\ K}$
r_A	Reaction rate	$\frac{mol}{L\ min}$
SS_{res}	Sum of squares of residuals	
SS_{tot}	Total sum of squares	
T	Absolute temperature	K
V	Volume	m^3
x_{ADP}	mole fraction ammonium di-phosphate	
x_{ATP}	mole fraction ammonium tri-phosphate	
x_P	mole fraction phosphoric acid	
$\bar{y}$	Average value of data set	
$\hat{y}_i$	Predicted value at point i	
y_i	experimental data point i	

Chapter 1: Introduction

This chapter introduces the study and serves to provide an overview of the necessity for the research conducted. The introductory information consists of three sections, providing (i) the background to the study, (ii) the objectives of the study and (iii) the scope of the investigation.

1.1 Background of this study

Fertilisers are essential in today's society for managing the fertility of soil which allows for the cultivation of crops large enough to sustain the growing population in modern society. The Cambridge dictionary defines a fertiliser as:" any substance that can be applied to soil that makes plants grow well" [2]. Heffer and Prud'homme [1] stated that the global annual demand for fertiliser was 186 million tonnes (Mt) for 2016/17 and is expected to grow to 199 Mt in 2020/21. The demand for phosphorus and potassium in fertilisers is expected to increase, while nitrogen demand is expected to steadily decline as improved fertiliser management practices are adopted by farmers globally [1]. With Africa being the largest contributor to the increase in global demand with an expected growth of 3.6% per annum [1], it is important for African companies and institutions to keep track of these trends and to develop improved methods of producing fertilisers which can cope with the demand.

Fertilisers are produced and applied as either a granular solid or as a liquid [3]. Both forms of fertilisers have advantages and disadvantages with the main disadvantages that liquid fertilisers conventionally have over dry granules being the high cost of reagents, the corrosive nature of the liquid fertiliser that leads to increased storage costs and limited plant food availability [3]–[5]. Some innate advantages of liquid fertilisers include the elimination of water evaporation and bagging costs, simplification of applying the liquid to the soil by eliminating material-handling difficulties due to segregation and caking, and it provides the plant immediate access to the nutrients. Condensed phosphates with an ammonium cation are referred to as ammonium polyphosphates and these ammonium polyphosphates (APP), when of sufficiently short chain length ($n < 10$), are highly water soluble [6], rendering it of value as a liquid fertiliser. Ammonium polyphosphates start to form a crystalline structure at longer chain lengths, greatly reducing its solubility in water, thus making it not suitable for use as a fertiliser [6]. These non-soluble polyphosphates are frequently applied as fire retardant coatings [7].

When the granular fertiliser urea phosphate is heated to temperatures above its melting point, the mono-phosphoric acid reacts to produce a polyphosphate with an ammonium

cation [8], which is soluble in water and usable as a liquid fertiliser [3]–[5].

While the APP chain length is short enough for the product to be water-soluble, the resulting liquid solution, when free of impurities, is a clear liquid. This substance can be produced in various ways, with the preferred method being the pyrolysis reaction of urea phosphate [3]. The pyrolysis route is preferred as it reduces the required reaction temperatures and provides an exothermic reaction pathway to the final product, which greatly reduces the energy input requirement and consequently the cost of production [8].

This reaction, excluding any potential by-products, is schematically represented in Figure 1.1 with the reagent being urea phosphate and the product being ammonium polyphosphate, with n denoting the chain length of the phosphate in the formed product.

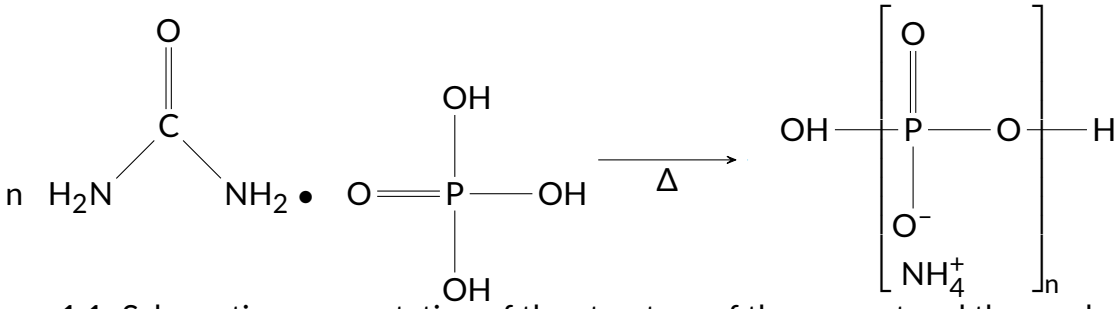

Figure 1.1: Schematic representation of the structure of the reagent and the product of interest for the reaction investigated. (Adapted from [7], [9], [10])

The solubility reduces with an increase in chain length [6] and longer chain length APP is coupled with nitrogen loss due to NH_3 production as well as an endothermic nature [9]. The optimal production scheme of APP would thus be to maximise the first condensing reaction, ammonium di-phosphate (ADP) production, as this minimises nitrogen loss due to NH_3 production, reduces energy input required and maximises solubility in water.

The kinetics of any chemical reaction is an integral part of the process of designing a commercial reactor to produce such a chemical from its less valuable natural resources [11, p.1]. An extensive literature survey yielded very little useful information on reaction kinetics for the pyrolysis of urea phosphate. This lack of information limits the attempts to design pilot scale and industrial scale reactors for the production of ammonium polyphosphate.

1.2 Problem Statement

The pyrolysis of urea phosphate has only received little attention in literature, with only a limited number of papers published on this specific reaction in the late 1960s to the late 1970s [9], [12]–[18]. Sarbaev and Koryakin [16] proposed a reaction mechanism for the condensing of mono-phosphoric acid into ammonium polyphosphates while McCullough, Sheridan, and Frederick [9] investigated the pyrolysis at lower temperature ranges, in order to quantify the polyphosphates produced. There is, however, at this stage no proof found of published reaction kinetics for this specific reaction. This study will attempt to build on current knowledge by focusing on determining the kinetics of the pyrolysis reaction of urea phosphate. The kinetics could then be used in the design

of an industrial reactor for the production of ADP. For this, a mathematical model for the rate law governing the reaction kinetics is derived yielding access to the determination of the accompanying rate constants.

1.3 Objectives and scope of this work

The aim of this study is to characterise the pyrolysis reaction of urea phosphate by proposing rate equations and determining the associated kinetic constants.

1.3.1 Objectives

In order to arrive at a kinetic model and accompanying kinetic parameters that can describe the reaction the following objectives were set:

1. To propose a possible reaction mechanism along with accompanying rate equations to aid in determining reaction kinetics
2. To design and commission an experimental procedure for generating kinetic data.
3. To experimentally study the reaction by measuring the mass loss as a result of pyrolysis.
4. To fit reaction kinetic parameters associated with the pyrolysis of urea phosphate into ADP from experimentally obtained isothermal and non-isothermal data.
5. To determine the reaction kinetics of the further condensing of ADP into ammonium tri-phosphate (ATP).

1.4 Scope of the work

This thesis shows the investigation into the reaction kinetics of the pyrolysis of urea phosphate, with focus on the production of ADP and the consecutive reaction of ADP to ATP. The rate data for the investigation was generated with merchant grade urea phosphate and the use of a simultaneous thermogravimetry and differential scanning calorimetry (TGA-DSC) analyser connected to a Fourier transform infrared spectroscopy analyser (FTIR). The investigation comprised of varying heating rates, within the temperature ranging between 120 and 140°C. The liquid product was analysed using a nuclear magnetic resonance (NMR) analyser which used ^{31}P as standard. The reaction conditions were carefully chosen to allow only the first two reactions, i.e. the pyrolysis of urea phosphate into ADP and ATP, to dominate.

A mechanism for the formation of ADP and ATP is proposed from the rate laws, experimental data and relevant literature. Non-linear regression techniques were conducted on the obtained data to find the applicable reaction rate law and accompanying kinetic parameters.

1.4.1 Dissertation layout

The results of this investigation are reported in this thesis in the following 6 chapters:

Introduction: This chapter provides a short background on the relevance of the study, elaborating on the focus points for the investigation and listing the objectives achieved.

Literature: An overview on the accumulated knowledge of the reaction being investigated is presented in this chapter. Included are the history on the production of ammonium polyphosphates as liquid fertilisers followed by an investigation on how the addition of urea to the phosphoric acid reaction mixture affects the formed products, a review of phosphate chemistry and finally an overview of the field of reaction kinetics relevant to this study.

Experimental procedures: This chapter provides the reader with the outline of the experiments that were conducted, how to replicate the obtained results as well as the experimental plan that was followed. The analytical methods used and calculations done on the raw data for model development are also elaborated on in this chapter.

Model development: This section details the analytical derivation of the model for the parameter fit done in this study, which is followed by a comprehensive discussion on how the model was employed to predict the experimental data.

Results and discussion: In this chapter, the experimental results as well as the obtained kinetic parameters and rate laws obtained from the model and validated using experimental results are discussed in detail, and a proposed reaction mechanism for the reactions is being discussed.

Conclusions and recommendations: This section concludes the report stating firstly the conclusions drawn in this investigation and, secondly, the recommendations for building upon the obtained knowledge of this study.

Appendices: The addenda are attached to this document, containing additional information relevant to the investigation as well as all the raw data produced during this study.

Chapter 2: Literature review

This chapter is divided into four sections. Section 2.1 provides an historical overview of the patented processes of the production of urea phosphate.

Section 2.2 shifts the focus to the chemistry of the pyrolysis reaction of urea phosphate starting with the chemistry of the decomposition of urea (section 2.2.1) followed by chemistry of condensed phosphates in section 2.2.2. Section 2.2.3 details the research conducted on the pyrolysis of urea phosphate and how these two chemicals interact with each other while section 2.2.4 provides insight into a proposed reaction mechanism for the decomposition of urea phosphate during pyrolysis.

Methods to determine reaction kinetics for this pyrolysis reaction receives attention in section 2.3 and the chapter concludes with a discussion on the analytical methods employed (section 2.4) in this study in order to obtain a rate law and accompanying rate constants from experimental data.

2.1 Background and manufacturing of Ammonium polyphosphate

2.1.1 Mono- and polyphosphates

Corbridge [19] defines a phosphate as any compound that contains a pentavalent phosphorus ion that contains at least one P – O bond. This makes phosphoric acid (H_3PO_4) the most basic form of a phosphate. Phosphoric acid in this form is also commonly called orthophosphoric acid in literature [19], although the commonly accepted naming of this molecule is mono-phosphoric acid [20]. Another, more complex form of a phosphate, is a polyphosphate, which consists of a combination of several H_3PO_4 molecules in a similar way as carbon atoms form chains. Durif [20] stated that the easiest way to define this class of phosphates is that any phosphoric anion, which contains a P – O – P bond would be considered a condensed phosphoric acid anion.

Gard [7] classifies a compound that contains monomeric PO_4^{3-} ions as an mono-phosphate. Mono-phosphoric acid is the most basic form of phosphorus from which all other phosphates are derived. Mono-phosphoric acid is condensed into the various classes of phosphates through either polymerisation or neutralisation reactions [7]. Polymerisation entails the dehydration of the orthophosphoric acid, leading to a $(P – O – P)_n$ chain, which is very susceptible to hydrolysis [7].

Condensed phosphates are classified into 3 groups, namely polyphosphates, meta-phosphates and ultra-phosphates. Gard [7] states that a linear chain of condensed phosphates is known as polyphosphates, cyclic P – O – P chains are known as metaphosphates, and branched polymeric chemicals containing at least one tri-bonded phosphate are named ultra-phosphates.

2.1.2 Manufacturing of ammonium polyphosphates: a historical perspective

Direct ammoniation of phosphoric acid

Potts, Stinson, and Striplin [4] were the first to patent a method of producing ammonium polyphosphates as a liquid fertiliser solution. These researchers described the investigated method as the direct and intimate mixing of purified phosphoric acid with ammonia gas and water within a controlled reaction zone. The ammonia gas saturated the phosphoric acid and formed polyphosphate chains. The major improvements that this method exhibited over alternative liquid fertilisers were that solutions greater than 33 wt.% fertiliser could be produced in water and the control over the pH of the solution has lead to reduced corrosiveness and thus reduces storage and handling costs [4].

Young [21] has found that merchant grade phosphoric acid (54 $\%_{mass} H_3PO_4$) can be purified through evaporation to a concentration of between 60 $\%_{mass}$ and 80 $\%_{mass}$. The impurities present in the feed phosphoric acid can be kept in solution at higher concentrations. Getsinger [5] has found that by directly heating merchant grade phosphoric acid and utilising the heat of ammoniation to evaporate the free water in the phosphoric acid, the acid can be upgraded to higher concentrations without the use of expensive additional fuels for heating. These methods demonstrated the disadvantage that the feed phosphoric acid must contain low quantities of metallic impurities in order to provide high plant food availability.

Stinson [8] discovered that adding urea as a condensing agent, the total energy input in terms of heating and mechanical agitation can be reduced to a large extent. This direct ammoniation of phosphoric acid method had the disadvantage of having all the impurities present in the original phosphoric acid in the final product, which negatively impacts the solubility and opacity of the ammonium polyphosphate solution [3]. Stinson [8] found that it is possible to get 90% impurity removal [6] by adding urea to the phosphoric acid mother liquor and separating the urea phosphate (UP) crystals from the liquid, followed by subsequent heating of the crystals to form ammonium polyphosphate. This bypassed the need of the more expensive super-phosphoric acid as a base reagent for the process and produced a product that is highly soluble in water (in the order of 430g/) [22].

Pyrolysis of urea phosphate method

Keens [23] was the first to purify super-phosphoric acid by means of separation with the crystallisation of urea phosphate. Gittenait [24] used the method described by Keens [23] but on merchant grade phosphoric acid (meaning $54\%_{mass} P_2O_5$) followed by ammoniation of said crystals at elevated temperatures. This leads to the production of

diphosphates (previously referred to as pyrophosphates), and the free heat of the ammoniation reaction can be used to execute this process in auto-thermal conditions. Young [25] added low amounts of acid (specifically sulphuric, nitric or hydrochloric acid) to the mixture as it improved the solubility of impurities present.

Stinson and Burnell [3] proposed that the process is performed batch-wise in a single reactor vessel using urea phosphate, an ammonium polyphosphate melt and ammonia gas. The heat of ammoniation provided enough heat to operate the process in auto thermal conditions.

2.2 Chemistry of the pyrolysis of urea phosphate

2.2.1 Decomposition of urea

. The thermal decomposition of urea phosphate is understood via the lens of the thermal degradation of urea amongst other things in which shows that the hydrolysis of urea within the phosphoric acid is the main driving mechanism for the pyrolysis reaction of urea phosphate. Schaber, Colson, Higgins, *et al.* [26] investigated the thermal decomposition of urea. These authors have found that the decomposition products of urea are biuret (NH_2 – CO – NH – CO – NH_2), cyanuric acid(NH – CO – NH – CO – NH – CO), ammelide (NH – CO – NH – CO – $C(NH)_2$), ammeline (NH – CO – $C(NH)_2$ – $C(NH)_2$), melamine ($C(NH)_2$ – $C(NH)_2$ – $C(NH)_2$), with only biuret and cyanuric acid being present in appreciable amounts below 200°C.

Schaber, Colson, Higgins, *et al.* [26] suggested that cyanuric acid, ammelide and ammeline are decomposition products of biuret rather than being direct decomposition products of urea at temperatures in excess of 190°C, where biuret is a product of cyanic acid (HNCO) and urea. Cyanic acid is produced as urea decomposes according to the following equation 2.1:

$$CO(NH_2)_2 \rightarrow NH_4^+NCO^- \leftrightarrows NH_3 + HNCO \tag{2.1}$$

Investigations into the hydrolysis of urea have been made by various authors, [27]–[31]. The production of ammonium polyphosphates at temperatures between the melting point and 200°C falls within the temperature range of hydrolysis [27], [29], [30] and thermal decomposition [26], [32] of urea, which will very likely have an effect on the mechanism of ammonium polyphosphate production.

Warner [27] suggests that after reaction 2.1 occurs, free H_3O^+ reacts with HNCO to produce ammonia (NH_3) and carbon dioxide (CO_2). Since it is essentially the only reaction occurring in the presence of water [27], the formation of cyanic acid is the only quantifiably significant reaction pathway.

The pyrolysis is a rather complex system as several processes compete for the production of the same products [26]. Schaber, Colson, Higgins, *et al.* [32] found that urea decomposition begins at 152°C, which is seen by rapid gas formation from the melt. At this temperature, biuret also starts to form as cyanic acid is produced from the decomposition of urea, and follows the reaction as shown in equation 2.2, followed by cyanuric acid and ammelide production at 175°C [32].

The following reaction equations show possible decomposition products expected at temperatures higher than 150°C within the urea and phosphorus mixture:

$$CO(NH_2)_2 + HNCO \leftrightarrows H_2NCONHCONH_2 \tag{2.2}$$

$$H_2NCONHCONH_2 + HNCO \rightarrow (CONH)_3 + NH_3 \tag{2.3}$$

$$H_2NCONHCONH_2 + HNCO \rightarrow C_3H_4N_4O_2 + H_2O \tag{2.4}$$

The formed biuret further reacts with the cyanic acid, and produces either cyanuric acid or ammelide, with ammonia gas or water as by-products respectively [32]. Equations 2.2, 2.3 and 2.4 are the dominant reactions up until 190°C.

The hydrolysis of urea was originally believed to be acid catalysed [28], [31], although Shaw and Bordeaux [29] concluded that the specific rate of urea hydrolysis is independent of pH, indicating that the presence of an acid does not affect the activation energy of the reaction. This observation was later proved by Lee, Kim, and Lee [30] when an in-depth study on the hydrolysis mechanism of urea hydrolysis was done. Lee, Kim, and Lee [30] managed to reproduce and confirm the observations made by, Shaw and Bordeaux [29], while also characterising the activated complex and determining the rate-limiting step of urea hydrolysis. Since urea phosphate decomposes into liquid phosphoric acid and dissolved urea upon melting [7], [9], [16], the hydrolysis of urea would seem to be what primarily drives the pyrolysis reaction of urea phosphate rather than the acidic nature of the solution.

2.2.2 Condensation of phosphates

Phosphoric acid solutions up to a P_2O_5 concentration of 68 wt.% contain H_3PO_4 as the only acid species in the solution [7]. At higher concentrations, the acid undergoes condensation after which it is referred to as superphosphoric acid.

When a phosphate condenses into a polyphosphate it releases an H_2O molecule, according to

$$nH_3PO_4 \leftrightharpoons (n-1)H_2O + H_{n+2}P_nO_{3n+1} \tag{2.5}$$

where n is classified as the degree of condensation [20], [33]. This elementary condensing reaction synergises with the decomposition of urea. As stated in the previous section, the presence of an H_2O molecule provides urea with another preferred reaction route into producing ammonia gas and CO_2, shifting the condensing equilibrium to the right.

The nomenclature of polyphosphates has been a source of confusion as these were initially erroneously named based on invalid assumptions. Renaming was later done as knowledge on the structures and geometry accumulated. Durif [20] lists the most recently accepted naming of polyphosphates, where naming is primarily based on the degree of condensation (n). For short chain lengths the Greek numeral prefix is used with 2 = di-, 3 = tri- , 4= tetraphosphate etc. The group of polyphosphates of a relatively small degree of condensing ($n \leq 20$) is referred to as *oligophospates*. For larger degrees of condensation, the polyphosphates are simply referred to as long-chain polyphosphates in literature. While polyphosphates forming cyclic rings rather than chains were for the longest period of time referred to as metaphosphates, it is currently accepted to refer to

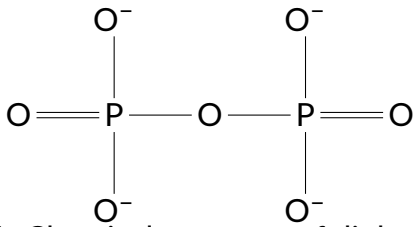

Figure 2.1: Chemical structure of diphosphate [7]

them by the more descriptive names of cyclo-phosphates. As an example, the polyphosphate ring with three phosphorus atoms in the ring is referred to as a cyclotri-phosphate.

At high concentrations (concentrations higher than $68\%_{mass}$ in water), phosphoric acid starts to condense into phosphoric acid chains [7], [10], [23]. After the existence of some condensed phosphates was established, new analytical methods had to be developed to quantitatively analyse these polyphosphates in the presence of one another [20]. Jones [34] proposed a method to separate short chain polyphosphates (mono-, di-, tri-, tetra-, and cyclo-phosphates) based on precipitation. A better analytical method used was paper chromatography. Kubasova [10] states that this paper chromatography technique was able to separate and quantify polyphosphate chains of up to 9 phosphorus atoms. Paper chromatography could only separate phosphates with an oxide ratio of 1.5 in superphosphoric acid, while lower ratios could not be quantitatively determined [10]. The chemical structure of some condensed phosphates is shown in Table 2.1.

The oxide ratio of a phosphate is based on its empirical formula. This can be calculated as the ratio of $H_2O : P_2O_5$ [7]. A meta-phosphate for example has the empirical formula HPO_3 which can be written as $\frac{1}{2}H_2O + \frac{1}{2}P_2O_5$, which translates into an oxide ratio of 1. Phosphates have an oxide ratio that is roughly at a value of 3, polyphosphoric acid has an oxide ratio between 1 and 2, a metaphosphate's oxide ratio is exactly 1 and ultra-phosphoric acid has an oxide ratio lower than 1 [7]. In long polyphosphate chains, the composition and oxide ratio of the molecule approaches that of a cyclo-phosphate ring structure (the oxide ratio approaches 1), which has led to these often being named meta-phosphates or cyclo-phosphates in literature, even though not cyclic in nature [7], [10].The empirical formula of various phosphates and the oxide ratios are also shown in Table 2.1.

Ammonium phosphates of the form $(NH_4)_2HPO_4$ (also known as diammonoium phosphate) forms at room temperature, but the formation of the condensed form $H[(NH_4)PO_3]_2OH$ (ammonium di-phosphate) is more stable at higher temperatures, and is thus the preferred product when forming at temperatures above room temperature. Durif [20] stated that according to current knowledge, all monovalent cation (such as NH_4^+) cyclo-phosphates undergo the transition into its corresponding chain polyphosphate under elevated temperatures. Some exceptions exist where the cylo-phosphates stay stable up to their melting points. According to Durif [20], there has not been a single monovalent cation ultraphosphate reported on in literature. Gard [7] states that a compound containing a single P – O – P bond is also considered a condensed phosphate, thus the substance diphosphate (also known as pyrophosphate) shown in figure 2.1 is the most elementary condensed phosphate. Both Sarbaev and Koryakin [16] and Gard [7] states that molten phosphoric acid undergoes a reorganisation according to the equilibrium equation shown in equation 2.6, where, when left to reach equilibrium, approximately $6\%_{mol}$ of diphosphoric acid is present in the liquid.

Table 2.1: Classification of phosphate ions, adapted from Gard [7]

Designation	Oxide Ratio	Empirical formula	Structure
Phosphate	≥ 3	PO_4^{3-}	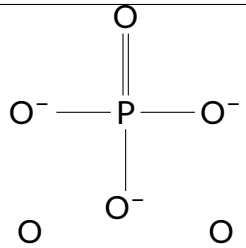
diphosphate	2	$P_2O_7^{4-}$	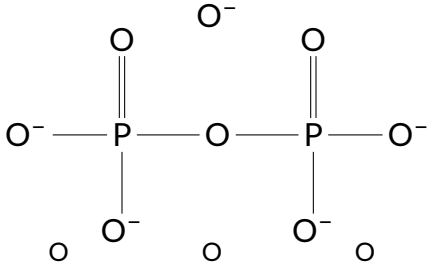
Triphosphate	1.67	$P_3O_{10}^{5-}$	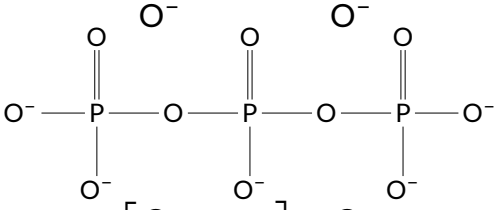
Polyphosphates	1-2	$P_nO_{3n+1}^{(n+2)-}$	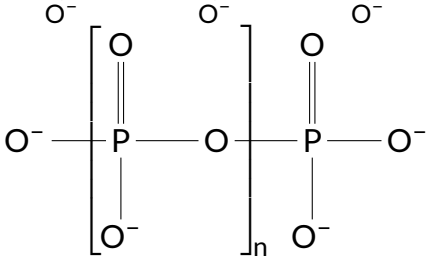
Cyclophosphates	1	$(PO_3)_n$	cyclic
Ultraphosphates	0-1	$P_2O_5(O^{2-})$	cross-linked chains and/or rings
Phosphorus pentoxide	0	$(P_2O_5)_n$	P_4O_{10} or continuous structures

$$2H_3PO_4 \leftrightarrows H_4P_2O_7 + H_2O \tag{2.6}$$

As the chain length of polyphosphates increases, their properties become more and more similar to such an extent that mixtures of polyphosphates behave like pure substances and occur as amorphous glassy structures [7]. At very long chain lengths, a crystal lattice begins to form, and Shen, Stahlheber, and Dyroff [18] have identified five different crystal forms for ammonium polyphosphates. Morgan and Wilkie [35] stated that polyphosphates of crystalline form 1 are believed to have a chain length of 30-150 phosphate units (P – O – P links) and polyphosphate chains of a shorter chain length are believed to have an amorphous shape. It was also found that the solubility of ammonium polyphosphate crystalline form 1 is much lower at 83.8 g/L [36] than that of the amorphous polyphosphate, which is at 430 g/L [22]. Producing these long chains requires high temperatures and residence times in the order of 280°C and 16 hours respectively [18]. Since the goal of this study is to maximise the production of water-

soluble polyphosphates, this provides an upper limit to the temperature and residence times to be investigated.

2.2.3 Decomposition of urea phosphate

In two articles published by Sarbaev, Gerbert, and Koryakin [17],[16] possible mechanisms for the thermal decomposition of urea phosphate were investigated. These researchers [16] used thermogravimetric analysis (TGA) to investigate and propose a reaction mechanism for the thermal decomposition within the temperature range of 20 to 400°C. The mechanism proposed is described in more detail in section 2.2.4. The use of urea as an ammoniating agent reduces the temperature required to produce polyphosphate chains [18], [37]. This could be likely to the production of an H_2O molecule that is liberated when two mono-phosphoric acid molecules bind to each other, enabling the CO_2 producing reaction rather than the cyanic acid producing pathway found with the pyrolysis of urea. The urea is able to consume the water produced by reaction 2.6 [20], [27], shifting the equilibrium towards a higher degree of condensing. The reason for this shift is twofold. Firstly, the urea hydrolysis reaction consumes water, producing a larger concentration of diphosphates. Secondly, the hydrolysis products include ammonia gas, which neutralises the diphosphate, thus consuming the second product in reaction 2.6. The observation of Warner [27] indicates that the activation energy of hydrolysis is much lower than that of the pyrolysis of urea, thus the condensing of phosphoric acid increases the decomposition rate of urea.

McCullough, Sheridan, and Frederick [9] investigated the pyrolysis reaction of urea phosphate to a maximum temperature of 200°C. It was found that urea phosphate forms a relatively stable melt at 112°C, but increasing the temperature caused the melt to form a foam, while an increase in viscosity was noted which progressed with an increase in both time and temperature [9, p.671]. McCullough, Sheridan, and Frederick [9] describes ammonium polyphosphates at room temperature as a soft taffy-like mass at low levels of polyphosphate condensation and hard, almost glass-like at higher levels of condensation. Under microscopic examination, ammonium polyphosphate was found to be amorphous in shape, but the unreacted urea formed micro-crystalline structures [9].

The results presented by McCullough, Sheridan, and Frederick [9] show that condensation of phosphates into ammonium polyphosphate doesn't occur without the decomposition of the stoichiometric amount of urea, even in the presence of ammonia. This reinforces the suggestion that the water molecule liberated by the condensing of phosphates provides a significantly lower energy pathway for the decomposition of urea. McCullough, Sheridan, and Frederick [9] notes that originally all the ammonia formed is fixed to the phosphates until they are completely saturated, which corresponds with the first reaction step, as shown in equation 2.13, which is also the exothermic step as noted by McCullough, Sheridan, and Frederick [9] and Sarbaev and Koryakin [16]. The reaction scheme shown in Figure 2.4 also shows this. After the phosphates in the melt have been saturated with ammonia, ammonia is present in the gas phase in the reactor vessel [16], amounting to a linear correlation with NH_3 reduction in the liquid phase and average polyphosphate chain length [9], which corresponds to the endothermic step shown by equation 2.17. McCullough, Sheridan, and Frederick [9] noted that the reaction rate increases sharply at roughly 126°C, while Sarbaev and Koryakin [16] notes a sharp exothermic effect directly after melting at 117°C. Both these groups of

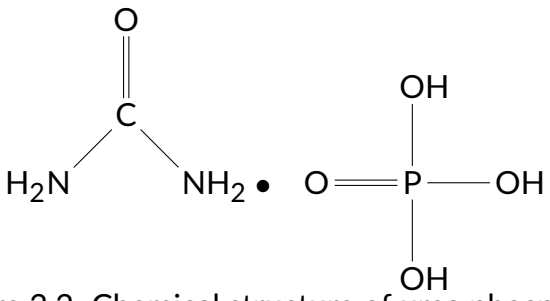

Figure 2.2: Chemical structure of urea phosphate

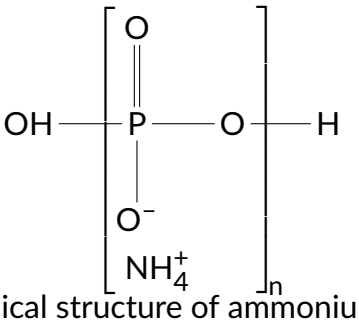

Figure 2.3: Chemical structure of ammonium polyphosphate

authors found that a maximum exothermic effect exists at 155°C after which the onset of ammonia in the gas phase is observed and the melt temperature begins to decrease.

McCullough, Sheridan, and Frederick [9] observed that adding anhydrous ammonia to the urea phosphate melt increases the rate of reaction during the exothermic step, but retards the reaction during the endothermic step, since adding anhydrous ammonia increases its partial pressure, retarding the release of newly formed ammonia gas. This is either an indication of reversibility or a complex nature in the reaction 2.17. The binding of ammonia to the condensed phosphates are thus exothermic, but increasing the partial pressure of NH_3 increases the ammonium concentration in the liquid, thus shifting the decomposition of urea as shown in equation 2.9, retarding the reaction as a whole. This could be an effective method to control the condensing, thus ensuring more complete condensing of monophosphate while keeping the solubility high enough for use as fertiliser. Biuret, which is poisonous to plants, is also found in the solid phase product [9]. It increases with an increase in polymerisation initially, where McCullough, Sheridan, and Frederick [9] found a maximum percentage of 2.7 wt.% after which it started to decrease again as polymerisation continued; a further indication of a complex mechanism for reactions producing longer chain APP, with the decomposition of biuret in an acidic medium adding to the production of polyphosphates.

2.2.4 Reaction mechanism of urea phosphate decomposition

The reaction mechanism, proposed by Sarbaev and Koryakin [16] is presented in this Section. Sarbaev and Koryakin [16] and Gittenait [24] stated that urea phosphate decomposes into its pure components, i.e. urea and phosphoric acid, during melting according to the reaction:

$$CO(NH_2)_2H_3PO_4 \rightarrow CO(NH_2)_2 + H_3PO_4 \tag{2.7}$$

After this, an equilibrium between monophosphate H_3PO_4 and diphosphate $H_4P_2O_7$ occurs [16].

$$2H_3PO_4 \leftrightarrows H_4P_2O_7 + H_2O \tag{2.8}$$

Sarbaev and Koryakin [16] notes that urea is a proton acceptor, and in alignment with this, Schaber, Colson, Higgins, *et al.* [26] and Warner [27] has noted that pure urea decomposes to produce isocyanic acid and ammonia.

$$CO(NH_2)_2 \leftrightarrows NH_3 + HNCO \tag{2.9}$$

$$HNCO + H_2O \rightarrow NH_3 + CO_2 \tag{2.10}$$

Sarbaev and Koryakin [16] proposed that the produced ammonia neutralises the acid and produces mono-ammonium phosphate, which further reacts with ammonia to produce ammonium poly- and cyclo-phosphates. The conversion into cyclo-phosphates occurs in the 360 – 380°C temperature range [16].

$$2NH_3 + H_4P_2O_7 \rightarrow HO - PO_3NH_4PO_3H - H \tag{2.11}$$

$$2NH_3 + HO - PO_3NH_4PO_3H - H \rightarrow HO(PO_3NH_4)_2H \tag{2.12}$$

The net reaction occurring thus reduces to the following reaction equation

$$CO(NH_2)_2 + 2H_3PO_4 \rightarrow HO(PO_3NH_4)_2H + CO_2 \tag{2.13}$$

Equation 2.13 is the first step of this reaction, which is exothermic [16], [24]. After the phosphates have been fully saturated with NH_3, the mixture starts releasing ammonia into the gas phase along with CO_2. Further condensing of the diphosphate can change reaction 2.8 into

$$H_3PO_4 + HO(PO_3NH_4)_2H \leftrightarrows HO(PO_3H)(PO_3NH_4)_2H + H_2O \tag{2.14}$$

wherein only 1 of the 2 liberated NH_3 molecules from urea decomposition are required to react with the intermediate compound ($HO(PO_3H)(PO_3NH_4)_2H$) in an intermediate reaction to produce an ammonium triphosphate. The net reaction occurring then reduces to the equation shown below.

$$HO[PO_3NH_4]_2H + H_3PO_4 + CO(NH_2)_2 \rightarrow HO(PO_3NH_4)_3H + CO_2 + NH_3 \tag{2.15}$$

The logic for equation 2.14, can be applied to the general case where $n \geq 2$

$$H_3PO_4 + HO[PO_3NH_4]_nH \leftrightarrows HO(PO_3H)(PO_3NH_4)_nH + H_2O \tag{2.16}$$

and the net reaction can be generalised to

$$HO(PO_3NH_4)_nH + H_3PO_4 + CO(NH_2)_2 \rightarrow HO(PO_3NH_4)_{(n+1)}H + CO_2 + NH_3 \tag{2.17}$$

McCullough, Sheridan, and Frederick [9] demonstrated that the production of CO_2 and NH_3 does in fact account for the full mass loss of the urea phosphate system. Trace amounts of biuret have been detected in the produced APP, according to McCullough, Sheridan, and Frederick [9], which had the effect of producing slightly more NH_3 then what the pure condensing of phosphates with urea predicts, according to:

$$2CO(NH_2) \rightarrow NH_2CONHCONH_2 + NH_3 \tag{2.18}$$

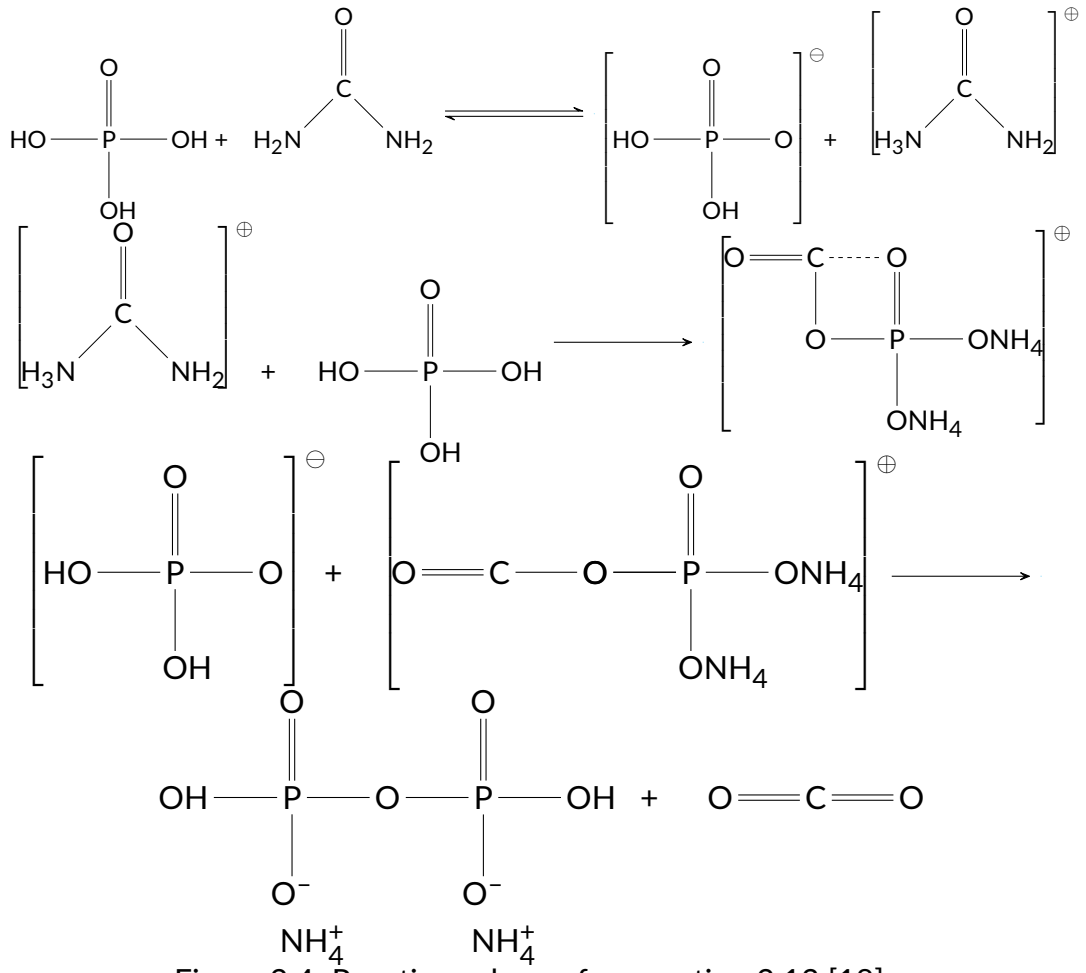

Figure 2.4: Reaction scheme for equation 2.13 [18]

McCullough, Sheridan, and Frederick [9] has additionally found that with a 99% confidence interval, the extra ammonia produced does not significantly alter the amount of NH_3 expected to form as predicted by equations 2.13 - 2.17. It is thus not statistically significant to bring into account the production of biuret. A possible reaction scheme is proposed by Shen, Stahlheber, and Dyroff [18] and is shown in figure 2.4, wherein the urea and phosphoric acid initially undergoes a proton exchange to positively charge the urea. The positively charged urea then reacts with phosphoric acid to produce a reaction intermediate, which then reacts with another phosphoric acid molecule to produce ammonium diphosphate and carbon dioxide.

2.3 Reaction kinetics

2.3.1 Analysis of experimentally generated kinetic data

The field of chemical kinetics is the collection of empirical studies on the effects of concentration, temperature, and in some cases pressure on the rate of reactions of various types[28]. There are thus two main goals in a study on the kinetics of a reaction. Firstly, to determine the relationship between the rate or velocity and the factors named previously [28], and secondly, to interpret this relationship in terms of a reaction mechanism [28]. In order to achieve this, data needs to be collected, where Fogler [11, p. 253] lists

six methods of analysing chemical rate data: 1. the differential method, 2. the integral method, 3. the method of half-lives, 4. the method of the initial rate, 5. linear regression and 6. non-linear regression. With the differential and integral methods mostly being used for batch reactor data [11], this, however, is mostly applicable to isothermal experimental conditions. The rate law is defined as the rate of change of the concentration of a reagent or product, $\frac{dC_A}{dt}$ [11], [31]. By definition, the units of a rate law should be moles per unit volume per unit of time. In the hypothetical reaction of $\alpha A + \beta B \rightarrow \theta C + \delta D$ the rate of consumption of A can be written as:

$$-r_A = \frac{dC_A}{dt} = k(T)f(C_A, C_B, ...) \tag{2.19}$$

with

- r_A = rate of consumption of A,
- C_A = Concentration of A
- k(T) = the rate constant, which is a function of temperature shown in equation 2.20.

The relationship between the rate of reaction and the concentration can be any function of the concentrations of the chemical species present in the reacting space. When considering the reaction:

$$\alpha A + \beta B \rightarrow \theta C + \delta D$$

a common form of the concentration dependence of the rate law is $C_A^{\alpha} C_B^{\beta}$, where the reaction is termed αth order in A and βth order in B, and the overall reaction order (n) is defined as $\alpha + \beta$ [11], [31]. The rate constant has units dependant on the overall order of the reaction meaning that it has the units of

$$\frac{\text{moles/unit volume}}{\text{unit time(moles/unit volume)}^n}$$

where n represents the overall reaction order [31]. This reduces to

$$\frac{(\text{moles})^{1-n}}{(\text{unit volume})^{1-n}(\text{unit time})}.$$

This temperature-dependent function follows the form

$$k(T) = Ae^{\frac{-E_A}{RT}} \tag{2.20}$$

Where:

- A = pre-exponential factor
- E_A = activation energy (J/mole)
- R = universal gas constant (8.314 J/mole K)
- T = absolute temperature (K)

The reaction of focus in this study is exothermic in nature [9], [16], and thus increases in temperature spontaneously, complicating isothermal operation for a pure system. Dilution of the substance into an inert solvent is generally the preferred way of achieving isothermal conditions. The integral

$$\int e^{\frac{1}{x}} dx \tag{2.21}$$

does not have an analytical solution [38], which complicates the determination of kinetic parameters for non-isothermal reaction data. Hence, non-isothermal techniques need to be employed in solving for the rate law and reaction constant parameters. Isothermal and non-isothermal studies rely on different assumptions and methods for linearizing and solving for kinetic parameters [39].

Writing the rate law in terms of the conversion fraction, α, equation 2.19 becomes:

$$\frac{d\alpha}{dt} = Ae^{\frac{-E_a}{RT}}(1-\alpha)^n \tag{2.22}$$

The integral method attempts to integrate equation 2.19. Starting from equation 2.22 and adding the assumption that the rate of change in temperature is a constant, $dT/dt = \beta$, it can be rearranged and simplified:

$$\int \frac{d\alpha}{(1-\alpha)^n} = \int Ae^{\frac{-E_a}{RT}} dt \tag{2.23}$$

And substituting $dt = dT/\beta$ the following is obtained:

$$\int_0^\alpha \frac{d\alpha}{(1-\alpha)^n} = \int_0^T \frac{Ae^{\frac{-E_a}{RT}} dT}{\beta} \tag{2.24}$$

with A and β being constants:

$$\int_0^\alpha \frac{d\alpha}{(1-\alpha)^n} = \frac{A}{\beta}\int_0^T e^{\frac{-E_a}{RT}} dT \tag{2.25}$$

As stated previously, the right-hand side of equation 2.25 has no exact integral. Hillier, Bezzant, and Fletcher [39] and Li, Chen, Zhang, *et al.* [40] proposed alternative methods for the determination of kinetic parameters that outperforms the differential and integral methods when used on non-isothermal data, e.g. when using TGA data.

The method of Hillier, Bezzant, and Fletcher [39] relies on a numerical integration of the right-hand side of equation 2.25. In solving the equation:

$$\int_0^\alpha \frac{d\alpha}{(1-\alpha)^n} = \int_{t_0}^t Ae^{\frac{-E_a}{RT}} dt \tag{2.26}$$

in the case of $n = 1$:

$$(1-\alpha) = -\exp\left(\int_0^t Ae^{\frac{-E_a}{RT}}\right)dt \tag{2.27}$$

in the case of $n \neq 1$:

$$\frac{(1-\alpha)^{1-n}}{n-1} = \frac{(1)^{1-n}}{n-1} + \left(\int_0^t Ae^{\frac{-E_a}{RT}}\right)dt \tag{2.28}$$

with the integral term being calculated numerically. Since this is a non-linear equation, a parameter search is to be employed to find the best fit of the data [39]. Hillier, Bezzant, and Fletcher [39] has demonstrated that this method is also applicable to a dataset where the heating rate

$$\frac{dT}{dt} \neq \text{constant}$$

.

In another method, published by Li, Chen, Zhang, *et al.* [40], DSC measurements are employed in solving the heat transfer equation:

$$q = \Delta H_{rxn} r_A = \Delta H_{rxn} A e^{\frac{-E_a}{RT}} f(\alpha)^n \tag{2.29}$$

Linearized, it becomes:

$$\ln(\frac{q}{(1-\alpha)^n}) = \ln(\Delta H_{rxn} A) - \frac{E_a}{RT} \tag{2.30}$$

where values for q, α and T can be obtained directly from the TGA-DSC. Using these values, equation 2.30 can be used to determine the values of E_a and $\Delta H_{rxn}A$ graphically. This method was found to be quantitatively comparable to previously used basket heating methods, but also cheaper and quicker to execute [40].

2.3.2 Complex kinetics

As stated in previous sections, urea and phosphoric acid combine to form ammonium di-phosphate, followed by the ammonium di-phosphate product reacting further with more urea and phosphoric acid to form ammonium tri-phosphate and so forth producing ammonium polyphosphate chains. The reaction between urea and phosphoric acid is not a simple reaction but forms various intermediates as shown in Figure 2.4. Fogler [11, p.3] states that a rate law is considered elementary when the stoichiometric coefficients are identical to the powers in the rate law. This indicates, but does not necessarily prove, that the reaction occurs in a single step. Laidler [28] defines a complex reaction as one that does not occur by a simple rearrangement of atoms in a single stage, but rather by a series of well-defined steps, which, when combined, form the stoichiometric equation of the overall reaction. When the rate law of a chemical system does not agree with the stoichiometric equation, it is an indication that the reaction occurs in multiple steps, each with their own rates, and the reaction is then considered to be complex [11], [28].

It is then necessary to set up the various rate equations and solve the set of differential equations [28]. Although integration of these equations can often prove near impossible or in fact not possible, Laidler [28] suggests that numerical methods may be the last resort.

2.4 Analytical methods

2.4.1 NMR

^{31}P NMR spectroscopy is a quantitative analytical method that can distinguish between differently bonded phosphorous atoms [41], [42]. According to Crutchfield, Callis, Irani,

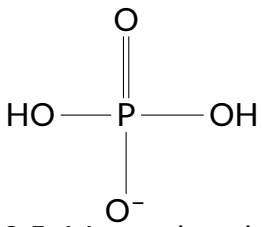

Figure 2.5: Mono-phosphate ion

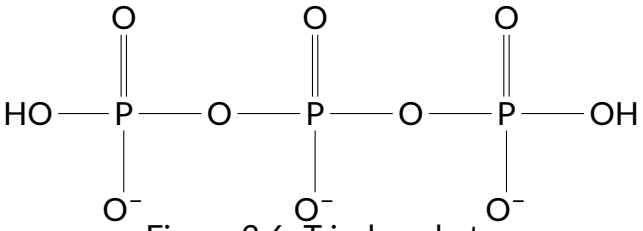

Figure 2.6: Tri-phosphate

et al. [42], polyphosphates can have peaks at 3 distinct shift ranges corresponding to either mono-, mid- or end-group phosphates. These peaks are observed in a set range depending on the pH of the solution, with mono-phosphate detectable at a chemical shift of between 0 and -5 ppm. End group phosphates will show a peak between -6 and -11 ppm, and middle groups can be found between -20 and -23 ppm, with the magnitude of the shift increasing with increasing pH in all cases [42].

A mono bound phosphate is where the phosphorous atom is not directly bound to any other phosphorous atoms through a P – O bond in the molecule (corresponding to a magnetic shift of 0 to -5 ppm), and is shown in Figure 2.5. Figure 2.6 shows a tri-phosphate, which has two phosphorous atoms in end group positions, meaning it has two phosphorous atoms that are linked to another phosphorous atom via a P – O bond (corresponding to a shift of -6 to -11 ppm), and 1 phosphorous atom is in a mid group position, meaning it is directly connected to two additional phosphorous atoms via a P – O bond (corresponding to a shift of -20 and -23 ppm)[42].

An NMR spectrum is interpreted by rather considering the area underneath a peak than the amplitude [41]. An NMR spectrum of a pure tri-phosphate species would thus report an integrated peak percentage of 66% for the peak between -5 and -11 ppm, and the remaining 33% of the total integrated area would be the peak in the range from -20 to -23 ppm.

This leads to ^{31}P NMR being able to quantify polymerisation of phosphates, but being limited to only giving average chain lengths. The average chain length can be determined from the ratio of the integrated areas of the 3 peaks. If, however, only one polyphosphate is present with a mid-group phosphate with a known structure, all the phosphate species present in a sample can be quantified using this technique.

2.4.2 FTIR

Fourier transform infrared spectroscopy (FTIR) is an analytical technique that uses absorption or emissions of specific wavelengths to identify chemical species [43]. The absorbance of light can directly be related to the concentration of a certain species, with the use of the Beer-Lambert law [44]. It is, in fact, a combination of the observa-

tions made by J.H. Lambert and August Beer [45], [46]. Lambert [45] discovered that the absorbance of a sample is directly proportional to the length of the path the light follows, and Beer [46] found that the absorbance is also directly proportional to the concentration of the attenuating species. These two correlations are combined in the Beer-Lambert law, which is given as:

$$A = \log_{10}\frac{I}{I_0} = \varepsilon l c \tag{2.31}$$

where

- A = absorbance
- I = light intensity
- ε = absorptivity constant of species ($Lcm^{-1}mol^{-1}$)
- l = length of the medium through which the light passes (cm)
- c = concentration of chemical species (mol/L)

Once a sample has been characterised using FTIR, the absorptivity constant for a species at a specific wavelength can be obtained and the absorbance at that wavelength can be used to quantify the concentration of the material in the said sample.

Under the correct circumstances, the combination of the Beer-Lambert law with FTIR data can be used to quantify concentrations of species in a sample.

2.5 Summary of literature and relevance to this study

There is a growing need for the production of better fertilisers, especially in Africa [1]. Potts, Stinson, and Striplin [4] have demonstrated that by adding urea to merchant grade phosphoric acid and by subsequent heating of the produced urea phosphate crystals overcomes virtually all difficulties encountered with previous methods of producing ammonium polyphosphate fertilisers. McCullough, Sheridan, and Frederick [9] as well as Sarbaev and Koryakin [16] have investigated the reaction in more detail.

The additional characterisation of this reaction in terms of its kinetics would be of value for the production of ammonium polyphosphates on an industrial scale. The exothermic nature of this reaction [9] paired with the product's high viscosity [3], [14] poses problems for isothermal operation. These factors combined with limited analytical techniques available for phosphorus analysis [7] require the employment of indirect methods for obtaining rate data, and new non-isothermal methods of determining kinetics [11], [40], [41], [44]. The reactions under investigation in this study produces two gas products, namely CO_2 and NH_3 [9], [16]. These gases evaporate from the reaction mixture, and thus leads to a nett decrease in weight. TG analysis can be employed to accurately quantify this mass loss due to gas production, and DSC measurements can be incorporated to ensure that kinetic data is only obtained for exothermic reaction conditions. This ensures that the production of mainly ammonium di-phosphate occur, and with relative certainty, the assumption can be made that the only condensing reaction beyond the formation of ammonium diphosphate is the production of ammonium tri-phosphate

[9]. The gas produced can be quantified with the use of the Beer-Lambert law [44], and these readings can be validated with NMR analysis of the final product [41], [42].

It is evident from literature that, in addition to the multiple steps in the suggested reaction mechanism, the condensing reactions that occur during the pyrolysis of urea phosphate interact with each other, leading to complex kinetics [9], [18], which requires complex methods of determining the reaction kinetics [28], [40], [47].

Chapter 3: Experimental procedure

This chapter is subdivided into multiple sections, each describing separate aspects of the experimental plan with the respective goals of each in achieving the objectives. Section 3.1 describes the raw materials used in the study while section 3.2 elaborates the thermo-gravimetric analysis (TGA) methodology employed. Section 3.3 provides insight into how NMR analysis was performed on the UP and APP samples. Section 3.4 summarises the actual experiments performed and how the variables have been investigated, and finally, section 3.5 details the calculations used on the raw data in order to obtain a kinetics model.

3.1 Materials used

The materials listed in table 3.1 were used during the execution of the experimental plan.

Table 3.1: Materials used during the experimental programme

Material	Supplier	Purity	Usage
Urea phosphate N:P:K rating(18-44-0)	SQM	95%	Reagent / feed material
Deuterium oxide (D_2O)	Merck	99.9%	Sample preparation for NMR analysis
Nitrogen gas (N_2)	Afrox	99.999%	Used as carrier gas through the TGA
Liquid Nitrogen (LN_2)	Afrox	99.999%	Used as coolent in the TGA

The urea phosphate was analysed with ICP-OES and XRD analysis. A fairly low impurity level is detected within each of these analyses. The impurities identified with ICP analysis are 1.68 wt.%. The most notable impurity is magnesium oxide, accounting for 10 % of all impurities detected within the sample.

XRD analysis only reported UP present in the sample and no other substance was detected, suggesting that individual impurities are below 0.5-3 wt.%. This is consistent with the results from the ICP analysis, supporting the idea that the urea phosphate is around 98% pure. The analyses results and methodology are given in Appendix A.

3.2 TGA-DSC experiments

3.2.1 Overview of the experiment

A NETZSCH STA 449F3 set to TGA-DSC mode, connected to a Bruker Vertex 80 FTIR was employed to characterise the reaction under isothermal and non-isothermal conditions. The full setup is represented in Figure 3.1. Platinum sample (A) and reference (B) crucibles were placed on a 0.5 mm sapphire disc and covered with a lid. Platinum crucibles were chosen as it would be inert under the conditions investigated. A blank correction run was performed for each heating profile investigated prior to performing any pyrolysis experiments. For all the experiments conducted, the TGA was programmed to do 1 evacuation cycle, with a 10 min equilibration before commencing with any measurements.

The TGA was set to heat to 80°C, after which measurements on the set heating profile is to begin. The initial ramp to 80°C was to ensure that the overshoot from the high heating rate would stabilise well before melting and the subsequent reaction would occur. All the non-isothermal runs were terminated at 140°C in order to limit the amount of NH_3 gas produced from the pyrolysis reaction, as ammonium gas is indicative of further condensing.

Nitrogen was used as a purge gas (D) through the TGA with a flow rate of 20 Nml/min on all the experiments, with a protective microparticle free control (MFC) (E) flow rate of 50 Nml/min, for a combined total of 70 Nml/min. Sample temperature control (STC) was enabled in the TGA program in order to minimise temperature variations while the reaction was occurring. Reproducibility was tested by doing a total of 5 repeats of the 1 K/min experiment.

An FTIR analyser connected to the TGA (F) was used as an on-line technique to quantify the amount of CO_2 gas produced. The gas cell used was a stainless steel beam conforming gas cell, investigating the wavelength range of 2500 to 25000 nm, and using transfer lines at an angle of 250°. Liquid nitrogen (E) was used to rapidly cool down the sample, and immediately quenche the reaction at the termination temperature.

3.2.2 Operation of the TGA and product analysis

A sample of 3 ± 1 mg of urea phosphate crystals was placed inside the Pt TGA pan and heated to a maximum temperature of 140°C at various pre-defined heating rates. Once the final temperature was reached, the reacting liquid was quenched by rapid cooling of the TGA chamber with liquid nitrogen, solidifying the APP mixture, halting the reaction. The full contents of the crucible was subsequently dissolved in D_2O, and subjected to ^{31}P NMR analysis.

The purge and MFC gas flow directed through the FTIR was used to quantify the amount of CO_2 gas produced. As explained in chapter 2, the Beer-Lambert law, can be used to quantify a known material based on the fraction of light absorbed when passing through the sample [43]. As baseline nitrogen gas was used as a purge gas, and the only gases produced inside the TGA are CO_2 and NH_3, the only gases affecting the absorbance inside the FTIR are these 3 gases. CO_2 has a peak absorbance at a wavelength of

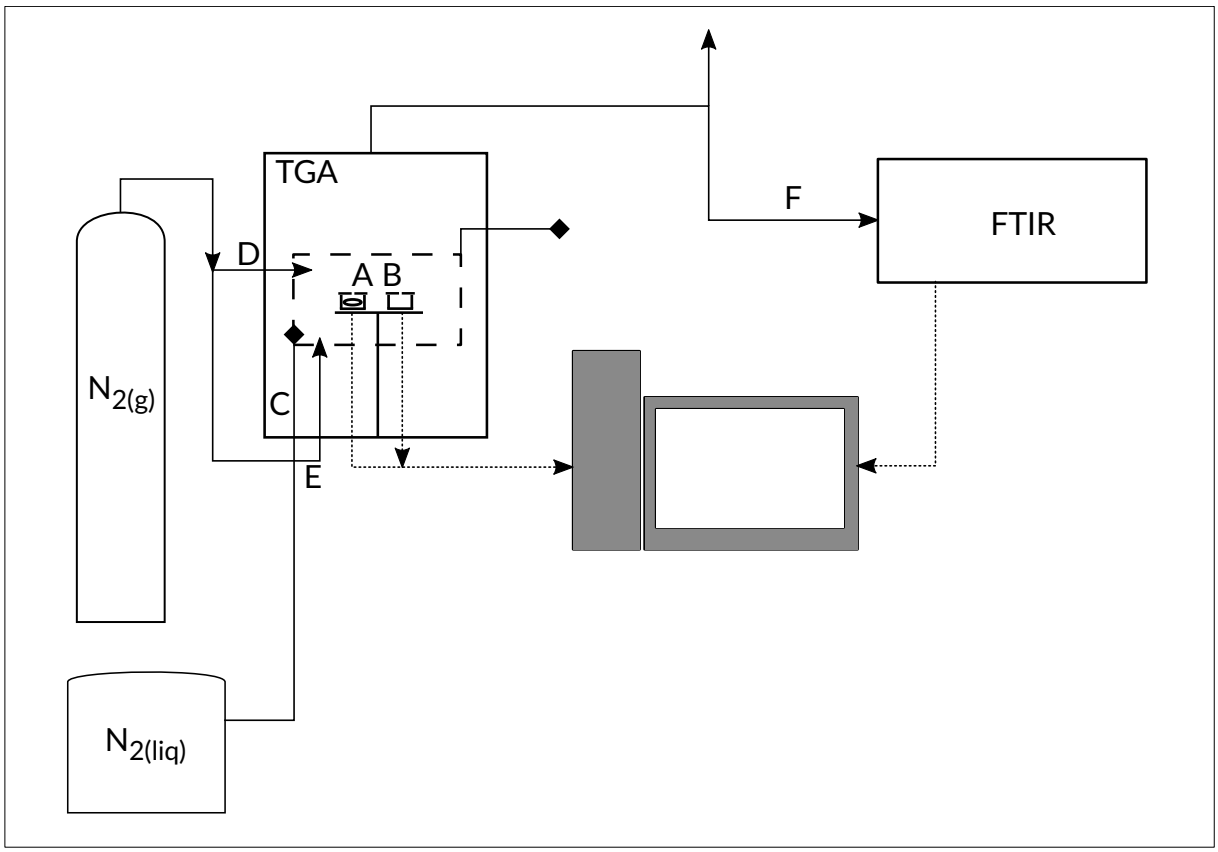

Figure 3.1: TGA-DSC schematic

2360 cm^{-1}, which coincides with the presence of a double bond between carbon and oxygen [43]. The C = O bond is not present in any of the other gases expected to be present in the purge gas mixture, thus the total absorbance at this wavelength is due to carbon dioxide. Using this assumption and the Beer-Lambert law, the FTIR data can be used to quantify the mass of CO_2 produced inside the TGA. Under the assumption of no other gases present, the mass of NH_3 gas produced can subsequently be derived by completing the mass balance. The amount of ammonia is then quantified as the difference between the total mass loss and mass loss due to CO_2.

3.3 NMR analysis

The reaction products originating from the TGA analysis were dissolved in 1.00 ml D_2O and placed inside thin-walled precision tubes with an outer diameter of 5 mm. The prepared vials were then placed into a 600 MHz Bruker Avance III NMR spectrometer. The spectrometer was used to record ^{31}P spectra, using a broadband gradient observation probe (PA BBO 600S3 BB-H-D-05 Z).

Results of these samples were then locked against D_2O as a reference, and the spectra recorded over a spectral width of 396 ppm. 512 scans with a soft pulse 30° flip angle were performed on each sample. These spectra were recorded with power-gated decoupling of the proton channel. Since the TGA samples were relatively small, i.e. in the range of ± 3 mg it was possible to dissolve the full content in D_2O for NMR analysis, eliminating representative uncertainty when having to divide a sample for analysis.

The NMR analysis is then interpreted by integrating the relative area of the peaks observed. These peak area percentages then correlate to the percentage of phosphorus atoms bound in a specific configuration. There are 3 peaks expected to be observed within this system [42], namely a mono-phosphorus peak (I_{mono}), an end group phosphorus peak (I_{end}) and a mid group phosphorus peak (I_{mid}).

3.4 Experimental plan

As stated, a sample of roughly 3 mg was used for TGA-DSC analysis, with various heating rates, as summarised in Table 3.2. In order to ensure that the mass loading did not affect the results, one repeat of the 1 K/min experiment was conducted on a 10 mg sample.

Table 3.2: Summary of non-isothermal experiments and analysis done

Heating rate (K/min)	Start temp (°C)	End temp (°C)	Repeats	TG	DSC	FTIR	NMR
				No. analysis done			
0.5	80	135	2	2	2	1	1
1	80	140	5	5	5	3	1
2	80	140	1	1	1	1	0
3	80	140	1	1	1	1	0
4	80	140	1	1	1	1	1
5	80	140	1	1	1	1	0

An additional set of isothermal experiments were conducted with the TGA, wherein the temperature was set to a set temperature and residence time at the constant temperature. These experiments are summarised in Table 3.3.

Table 3.3: Summary of isothermal experiments and analysis done

Temp (°C)	Time (min)	TG	DSC	FTIR	NMR
119	60	1	1	1	0
122	30	1	1	1	1
122	60	1	1	1	1
125	60	1	1	1	0
130	60	1	1	1	0
130	60	1	1	1	0

3.5 Calculations

3.5.1 Experimental error

The experimental error is determined by taking the final data point obtained from the TGA on the 5 data sets done with a 1 K/min heating rate. The mass loss was normalised using the following equation to account for the difference in mass loading:

$$M = \frac{m}{m_0} \tag{3.1}$$

The experimental error calculation is based on the t-test method [48, p. 313], with critical t-values obtained from Devore [48, p. 566]. The fraction of mass loss was used rather than the mass fraction remaining, in order to more accurately portray true deviation between samples. The error was calculated for a 95% confidence interval. The resulting error from this method is shown in Table 3.4.

The following equations explain how the results were obtained. The standard deviation (Stdev) is calculated based on the sample size (N) of 5. Degrees of freedom (DOF), for obtaining critical t-values, and the standard deviation is determined using equations 3.2 and 3.3.:

$$DOF = N - 1 \tag{3.2}$$

$$Stdev = \sqrt{\frac{\sum_{i=1}^{N}(x_i - \bar{x})}{DOF}} \tag{3.3}$$

The uncertainty is then calculated using:

$$\varepsilon = \frac{t \times Stdev}{\sqrt{N}} \tag{3.4}$$

Converting the uncertainty to a relative percentage is done with the following equation:

$$\varepsilon_{95}\% = \frac{\varepsilon}{\bar{x}} \times 100\% \tag{3.5}$$

Table 3.4 details the error analysis based on the equations above, while Figure 3.2 displays the normalised mass of all the repeats as well as the predicted mass loss from the regression data. Run # 3 was done with a 10 mg initial mass load wherein all the other four experiments used a 3 ± 1 mg initial load. This shows that mass transfer effects can be neglected in the investigation, and the data acquired is indeed within the rate limiting regime. An average mass loss of 15 wt.% is observed with a 1.03 wt.% variance. This means that the experimental error is 8.5% within the 95% confidence interval, verifying the reproducibility of the data obtained with the method used.

Table 3.4: Experimental Error calculation

Mass loss Fraction at t(f)		**Mass loading (mg)**	**Experimental Error Analysis**	
1 K/min R1	0.159	3.49	Average	0.1503
1 K/min R2	0.133	3.34	Stdev	0.0103
1 K/min R3	0.150	2.91	N	5
1 K/min R4	0.154	10.17	Crit t-value (95%)	2.776
1 K/min R5	0.156	3.91		
		ε (95%)	0.01	
		ε_{95} (%)	8.5%	

3.5.2 NMR

NMR analysis reports an atom balance on the ^{31}P atom, showing the percentage of P atoms being bound to 0, 1 or 2 other P atoms. From the balanced equations in 2.13 and

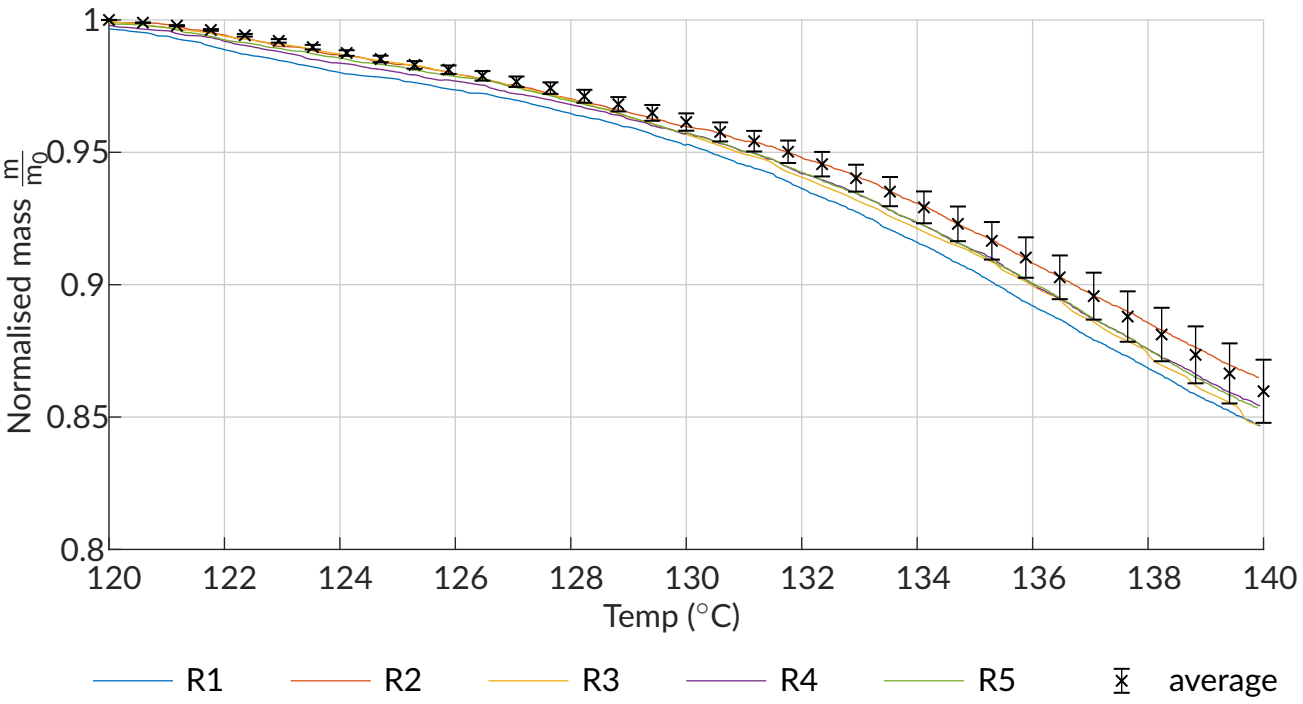

Figure 3.2: Repeatability and experimental error calculation for 5 repeats of 1 K/min between the temperature range of 120 and 140°C

2.17, it can be seen that PA represents a P atom bound to no other P atoms, ADP has 2 P atoms bound to one another (thus bound to 1 P) and ATP consists of 3 P atoms, 2 on the ends, bound to 1 P (the one in the middle) and 1 P bound to 2 other P atoms.

Since urea phosphate contains only un-condensed phosphoric acid, the starting point is 100% mono-phosphate. The percentage of mono-phosphates present after the reaction is then regarded as the un-reacted fraction of original mono-phosphates. Although it is not the fraction of mono-phosphates in the sample, as 2 terminal phosphorus are required for 1 condensed phosphate and for larger condensation mid-groups phosphates, determining the mole fractions of mono- di- and triphosphate (P, ADP and ATP) can be done through the use of equations 3.6 - 3.8.

$$x_P = \frac{I_{mono}}{I_{mono} + \frac{I_{end} - 2I_{mid}}{2} + I_{mid}} \tag{3.6}$$

$$x_{ADP} = \frac{\frac{I_{end} - 2I_{mid}}{2}}{I_{mono} + \frac{I_{end} - 2I_{mid}}{2} + I_{mid}} \tag{3.7}$$

$$x_{ATP} = \frac{I_{mid}}{I_{mono} + \frac{I_{end} - 2I_{mid}}{2} + I_{mid}} \tag{3.8}$$

where x_P, x_{ADP} and x_{ATP} denote the mole fractions of the three compounds, P, ADP and ATP and I_{mono}, I_{end} and I_{mid} the integrated surface area percentage of each peak on the NMR spectroscopy.

3.5.3 Quality of fit calculation

An indication of the quality-of-fit is the coefficient of multiple determination (R^2 value) defined by Devore [48, p. 119] as:

$$R^2 = 1 - \frac{SS_{res}}{SS_{tot}} \tag{3.9}$$

where SS_{res} is the sum of squares of residuals, and SS_{tot} is the total sum of squares, each of these calculated using:

$$SS_{res} = \sum_{i=1}^{N}(y_i - \hat{y}_i)^2 \tag{3.10}$$

$$SS_{tot} = \sum_{i=1}^{N}(y_i - \bar{y})^2 \tag{3.11}$$

where y_i is the experimental data point i, $\bar{y}$ is the average value, and $\hat{y}_i$ is the predicted value point i [48, p. 495]. Thus R^2 becomes:

$$R^2 = 1 - \frac{\sum_{i=1}^{N}(y_i - \hat{y}_i)^2}{\sum_{i=1}^{N}(y_i - \bar{y})^2} \tag{3.12}$$

This value is interpreted as the proportion of variation observed experimentally that can be explained by the proposed model [48].

An error value should be used in conjunction with R^2 to explain the overall quality of a model's fit. The root mean squared error is frequently being used and is defined by [48]:

$$RMSE = \sqrt{\frac{1}{N}\sum_{i=1}^{N}(\hat{y}_i - y)^2} \tag{3.13}$$

Chapter 4: Model Development

This Chapter is divided into 4 main sections. Section 4.1 elaborates on the assumptions made in order to arrive at conclusive results, along with reasons as to why these assumptions were considered. The differential equations that describe the pyrolysis of urea phosphate are listed in Section 4.2. Section 4.3 shows subsequently how the measured variables are used to describe the composition, and how they are implemented on the various types of analyses performed. Section 4.4 explains how the mechanism for the reactions investigated is determined and how the rate laws are formulated from there.

4.1 Assumptions

4.1.1 Reversibility of reactions

Since the products of both reactions consists of liquids and gases, it is assumed that the evolved gases evaporate from the liquid and are removed from the reacting liquid via the sweep gas in the TGA, assuring an irreversible reaction. Conversion is also kept relatively low, neglecting the effect of any backward reactions. Since the reactions are assumed to be irreversible and are non-catalytic, the rate laws are therefore assumed to be only functions of the reagent concentrations.

4.1.2 Urea phosphate purity

As stated in Section 3.1, the urea phosphate being used was of such a low impurity content that, taking them into account, would not make a statistically significant difference in the measured data. The assumption of a pure reagent is, therefore, made.

4.1.3 Condensing of only di- and tri-phosphates

As stated in Section 2.2.4, McCullough, Sheridan, and Frederick [9] have found trace amounts of biuret in the APP that was produced from the pyrolysis reaction. With the highest concentration of biuret at 2.7 wt.% of the produced APP, the amount of additional NH_3 is neglected as it does not have a significant effect on the composition. The relatively low conversion of the experiments also ensure that ADP and ATP dominate as products.

No literature notes any other reaction occurring within this closed system under the conditions investigated. As such, only the formation of ADP and the subsequent formation of ATP are considered, as shown in equations 4.2 and 4.3. As will be seen in the subsequent sections of this chapter, the fact that the model can reasonably well predict the mass loss for both isothermal and non-isothermal conditions, also correlating well with the NMR results, it can be deduced that this is a valid assumption.

4.1.4 Gas produced

The assumption of only producing ammonium di-phosphate (ADP) and ammonium tri-phosphate (ATP) has the direct consequence of only producing CO_2 as by-product during the production of ADP, and equal molar amounts of CO_2 and NH_3 during the production of ATP.

No other gas products are expected to form, when considering the literature sources [9], [16]. If the assumption that only the production of di- and tri-phosphate are considered valid, this follows.

4.1.5 Liquid density

Since liquid densities of ADP and ATP are unknown, the assumption is made that the density of the reacting mixture remains constant. The consequence of this is that the volume is directly proportional to the mass of the reacting liquid.

4.1.6 Well mixed reactor

The liquid under the conditions investigated is assumed to be well mixed, thus having no concentration or temperature gradients.This assumption is validated by the similar rates observed for the 3 and 10 mg experiments.

The assumptions made in this study are summarised as:

1. the reactions occurring are considered irreversible
2. the urea phosphate reagent is pure
3. the only liquid products being produced are ADP and ATP
4. the only gaseous products that evolved in the reaction are CO_2 and NH_3
5. the liquid density of ADP and ATP is constant and equal to that of the urea and phosphoric acid melt density
6. the liquid is considered to be in a well mixed state.

4.2 Design equations

The balanced reaction equations as laid out in chapter 2 will from here on onward be simplified to the following form:

$$UP_{(s)} \rightarrow_{melting} U_{(l)} + PA_{(l)} \quad (4.1)$$

$$U_{(l)} + 2PA_{(l)} \rightarrow ADP_{(l)} + CO_{2(g)} \quad (4.2)$$

$$U_{(l)} + PA_{(l)} + ADP_{(l)} \rightarrow ATP_{(l)} + CO_{2(g)} + NH_{3(g)} \quad (4.3)$$

Here, U represents urea, PA represents phosphoric acid, ADP represents ammonium di-phosphate and ATP represents ammonium tri-phosphate. Using these stoichiometric reaction equations the rates of consumption and formation of each specie can be determined.

A batch reactor design equation, as given in equation 4.4, is used to model the reactive material inside the TGA crucible:

$$\frac{dn_i}{dt} = r_i V \quad (4.4)$$

The mole balance differential equations for urea, phosphoric acid, ammonium di-phosphate and ammonium triphosphate are:

$$\frac{dn_P}{dt} = r_P V \quad (4.5)$$

$$n_{P0} = n_{UP} \quad (4.6)$$

$$\frac{dn_U}{dt} = r_U V \quad (4.7)$$

$$n_{U0} = n_{UP} \quad (4.8)$$

$$\frac{dn_{ADP}}{dt} = r_{ADP} V \quad (4.9)$$

$$n_{ADP0} = 0 \quad (4.10)$$

$$\frac{dn_{ATP}}{dt} = r_{ATP} V \quad (4.11)$$

$$n_{ATP0} = 0 \quad (4.12)$$

$$\frac{dn_{CO_2}}{dt} = r_{CO_2} V \quad (4.13)$$

$$n_{CO_20} = 0 \quad (4.14)$$

$$\frac{dn_{NH_3}}{dt} = r_{NH_3} V \quad (4.15)$$

$$n_{NH_30} = 0 \quad (4.16)$$

The rate equations are only functions of reagent concentrations, as the reaction is considered irreversible.

$$r_1 = k_1(T) f(C_U, C_{PA}) \quad (4.17)$$

$$r_2 = k_2(T) f(C_U, C_{PA}, C_{ADP}) \quad (4.18)$$

From the stoichiometry, the rates of formation/consumption of each species in the system can be determined:

$$r_U = -0.5r_1 - r_2 \tag{4.19}$$
$$r_P = -r_1 - r_2 \tag{4.20}$$
$$r_{ADP} = 0.5r_1 - r_2 \tag{4.21}$$
$$r_{ATP} = r_2 \tag{4.22}$$
$$r_{CO_2} = 0.5r_1 + r_2 \tag{4.23}$$
$$r_{NH_3} = r_2 \tag{4.24}$$

Assuming liquid density to stay constant, the reaction volume can be defined as:

$$V = \frac{m}{\rho} \tag{4.25}$$
$$\frac{V}{V_0} = \frac{m}{m_0} \tag{4.26}$$

With the volume known, the concentrations of all species in the liquid can be determined by:

$$C_i = \frac{n_i}{V} \tag{4.27}$$

Equations for temperature, the rate constants, volume and concentrations are thus:

$$T = T_0 + \beta t \tag{4.28}$$
$$k_1 = A_1 e^{-\frac{E_{A1}}{RT}} \tag{4.29}$$
$$k_2 = A_2 e^{-\frac{E_{A2}}{RT}} \tag{4.30}$$
$$m = n_U MW_U + n_P MW_P + n_{ADP} MW_{ADP} + n_{ATP} MW_{ATP} \tag{4.31}$$
$$V = V_0 \frac{m}{m_0} \tag{4.32}$$
$$C_P = \frac{n_P}{V} \tag{4.33}$$
$$C_U = \frac{n_U}{V} \tag{4.34}$$
$$C_{ADP} = \frac{n_{ADP}}{V} \tag{4.35}$$

The exact form of equations 4.17 and 4.18 is discussed in Section 5.3. Since A_1, E_{A1}, A_2 and E_{A2}, are unknown, numerical integration techniques can be employed along with a non-linear solver to find the unknown parameters that best describe the experimental data obtained from the TGA.

4.3 Mole balance

A complete mole balance of this system, according to equations 4.2 and 4.3, is:

$$n_U = n_{U(0)} - 0.5\xi_1 - \xi_2 \tag{4.36}$$

$$n_{PA} = n_{PA(0)} - \xi_1 - \xi_2 \tag{4.37}$$

$$n_{ADP} = 0.5\xi_1 - \xi_2 \tag{4.38}$$

$$n_{CO_2} = 0.5\xi_1 + \xi_2 \tag{4.39}$$

$$n_{ATP} = \xi_2 \tag{4.40}$$

$$n_{NH_3} = \xi_2 \tag{4.41}$$

$$n_t = n_U + n_{PA} + n_{ADP} + n_{CO_2} + n_{ATP} + n_{NH_3} \tag{4.42}$$

These extent of reaction can then be calculated both from NMR and the TGA + FTIR data data, using equations 4.36 to 4.42.

4.3.1 NMR balance

The full chemical composition of the liquid can be determined from NMR data, by finding ξ_1 and ξ_2 from the phosphorus atom balance, and substituting these into equations 4.36 to 4.42. The percentage of phosphate atoms then containing mid groups corresponds to the percentage of phosphate molecules converted to ATP molecules which, according to the mole balance is equal to ξ_2.

$$\xi_2 = n_{PA0}\frac{I_{mid}}{100} \tag{4.43}$$

The percentage of PA converted to APP is equal to the percentage of P atoms bound to other P atoms.

$$\xi_1 + \xi_2 = n_{PA0}\frac{100 - (I_{mono})}{100} \tag{4.44}$$

4.3.2 TGA balance

The TGA-DSC is connected to an FTIR, thus at any given time during the experiment, both the total mass loss is logged and total CO_2 is quantified by the FTIR. With the total mass loss and the mass of CO_2 known, the composition of he entire reaction mixture can be calculated, with the use of equations 4.36 to 4.42. Equations for the determination of ξ_1 and ξ_2 are derived from the mole balances of NH_3 and CO_2.

$$\xi_2 = \frac{\Delta m - m_{CO_2}}{MW_{NH_3}} \tag{4.45}$$

$$\xi_1 = \frac{\frac{m_{CO_2}}{MW_{CO_2}} - \xi_2}{2} \tag{4.46}$$

With ξ_1 and ξ_2 known, the total mole balance can be calculated. The Calibration for CO_2 quantification is shown in Appendix B.

If the assumptions made are valid, the composition determined from TGA data should be comparable to the composition determined from the NMR results.

4.4 Reaction rate equations

The mechanism for the production of amminium di-phosphate as derived in Appendix C, predics the rate equation for the production of ADP to be one of the following three rate equations:

$$r_1 = k_1[H_3PO_4]^2 \tag{4.47}$$

$$r_1 = k_1[H_3PO_4]^2 - k_2[CO(NH_2)_2] \tag{4.48}$$

$$r_1 = k_1[CO(NH_2)_2] \tag{4.49}$$

The equation here that describes the rate limiting step, should then best describe the mass loss observed in the TGA.

The mechanism for the profuction of ammonium tri-phosphate is summarised by these equations:

$$r_2 = k_3[H_3PO_4][HO(PO_3NH_4)_2H] \tag{4.50}$$

$$r_2 = k_3[H_3PO_4][HO(PO_3NH_4)_2H] - k_4[CO(NH_2)_2] \tag{4.51}$$

$$r_2 = k_3[CO(NH_2)_2] \tag{4.52}$$

Where the rate equation that corresponds with the rate limiting step would be the rate equation that has the best ability to predict mass loss measured within the TGA.

4.4.1 Parameter fitting

Matlab was used for numerical integration and regression. An ordinary differential equation solver (ode113 in Matlab) was set up to solve the set of equations as described in Section 4.2. Matlab has a non-linear least squares solver program (lsqcurvefit) which requires a user-defined function, the parameters to be varied and known x & y data points as the minimum required inputs to perform a regression.

The known x and y data arrays were constructed by joining the raw data of each individual run together, and fed as input to the non-linear least squares solver in order to find the parameter set that can best describe the system at the conditions investigated. The error to be minimised is the combined total mass loss and mass CO_2 values:

$$\text{err} = \sum_{n=1}^{N}\sum_{m=1}^{M}\left((\Delta m_{n,m} - \Delta\hat{m}_{n,m})^2 + (m_{CO_2,n,m} - \hat{m}_{CO_2,n,m})^2\right) \tag{4.53}$$

Where N is the number of experiments performed and M is the number of data points in experiment N. The x data array contained only the time data from the TGA and the y data array consisted of the rest of the recorded data (i.e. temperature, total mass loss and mass CO_2) at the corresponding x values. Since 2 reactions are being quantified, the

objective function required two error values, thus both total mass loss and mass CO_2 is included in the objective function.

The experimental data for each experiment were concatenated and fed to Matlab's non-linear least squares solver program (lsqcurvefit) as the regression data, so that a the single set of parameters can be found that best describe all the experimental data. The differential equations to be solved numerically with ode113 in Matlab, can be seen in Appendix D, Section D.6. This Matlab function was then given as input to Matlab's ordinary differential equation (ODE) solver program at the experimental conditions. The output of the ODE solver at the various reaction conditions are then also concatenated in the same order as the regression data and then sent to Matlab's non-linear solver, where the error between the resulting experimental and regressed arrays are calculated and minimised by varying the parameters used by the ODE solver. The lsqcurvefit function loop terminates once the total error reaches a minimum value or a certain threshold. A flow chart for this solver is shown in Figure 4.1.

Experimental data is fed to a data load function, (A) that extracts reaction data, and concatenates the various experimental runs together for the parameter fit. The extracted boundary conditions are used as input data for the ODE solver (C), which calculates the mass loss and CO_2 generation based on the kinetic parameters recieved from the least square curve fit function in Matlab (F). The various experiments are calculated in the same sequence in which they are read from experimental data and concatenated for error minimisation in the least square curve fit function in matlab (E). The concatenated raw experimental data (D) and concatenated calculated data (E) is then compared, and new kinetic parameters are considered if the error minimisation criteria is not met. On the first loop, user provided kinetic paramters are used (B) for the calculation of modelled data (E). After the kinetic parameters are such that the squared error reached a minimum, the least squares curve fit Matlab function returns the kinetic parameters with the best fit to experimental data (G). The code used to perform the regression can be found in appendix D.

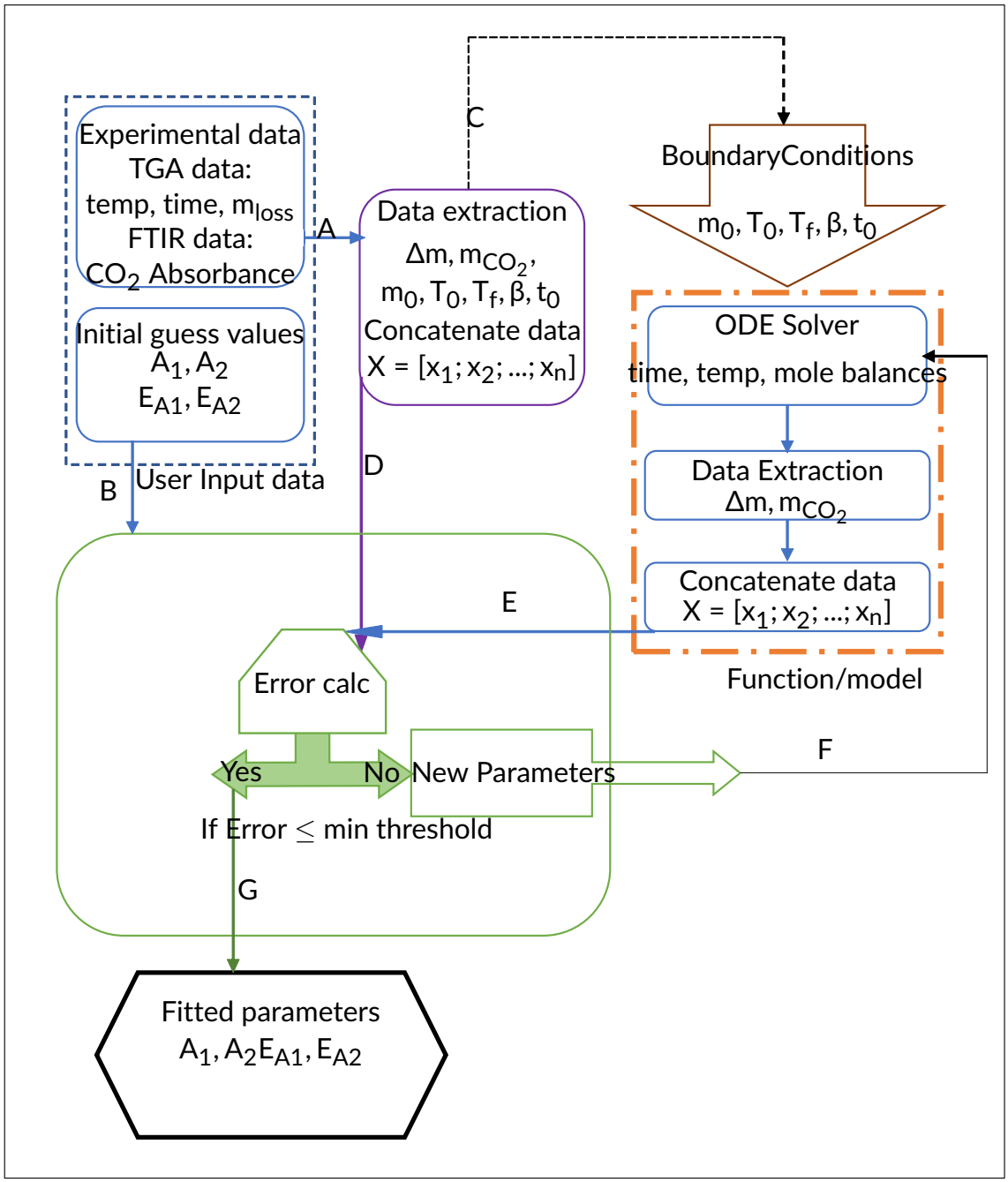

Figure 4.1: Matlab algorithm used for finding kinetic parameters

Chapter 5: Results and discussion

This chapter is divided into 5 sections. Section 5.1 discusses the mass loss measured on tha TGA. Then, section 5.2 shows how the FTIR data corresponds to the mass of CO_2 formed. These two datasets were then used in the regression analysis to fit a model to the observed data, which is discussed in section 5.3. The proposed interpretation of the data used for the regression is validated with NMR analysis, which is further investigated in section 5.4. Finally a qualitative discussion is provided on the DSC measurements made on the system, discussing the exo- and endothermic nature of the reactions investigated, in section 5.5.

5.1 Thermogravimetric analysis

Non-isothermal TGA experiments were conducted at various heating rates, and are summarised in Figures 5.1 and 5.2.

It is evident from this graph that, with an increase in heating rate, a reduction of conversion is observed. This is to be expected as with a higher heating rate, the total reaction time at a certain temperature is reduced. This effect is also seen when the mass loss is plotted against time, here, higher heating rates show a lower conversion but a much more rapid mass loss and a short residence time, while lower heating rates results in longer residence times and thus higher total conversion but a slower rate of mass loss.

Figure 5.3 shows the mass loss observed for urea phosphate at constant temperatures above its melting point for a total time of 60 minutes. It can be seen that with an increase in temperature, the rate of mass loss increases. The 130°C line shows deviation from a rather linear mass loss with a decreasing slope as time goes by, showing a more pronounced first order reaction rate. The same trend would be expected to follow for lower temperatures at longer residence times.

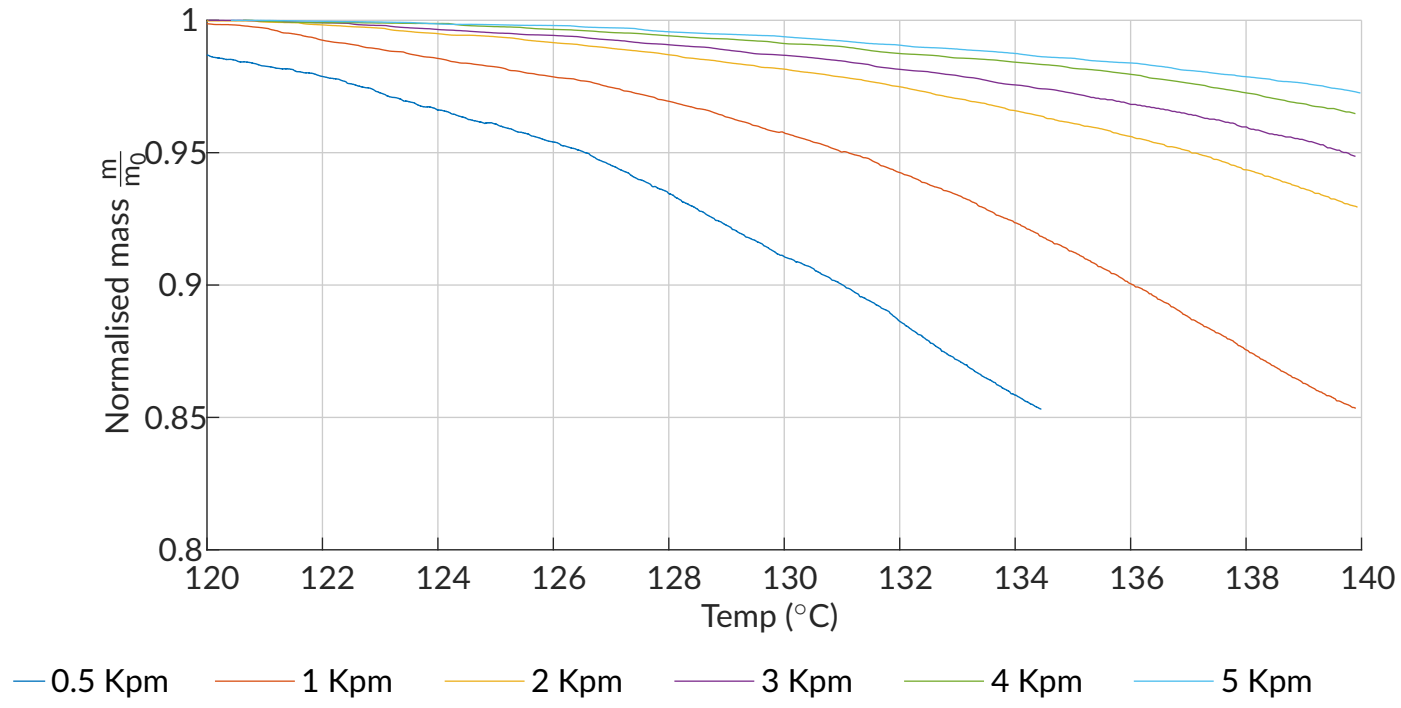

Figure 5.1: Normalised mass loss as a function of temperature and heating rate on a temperature range of 120 – 140°C

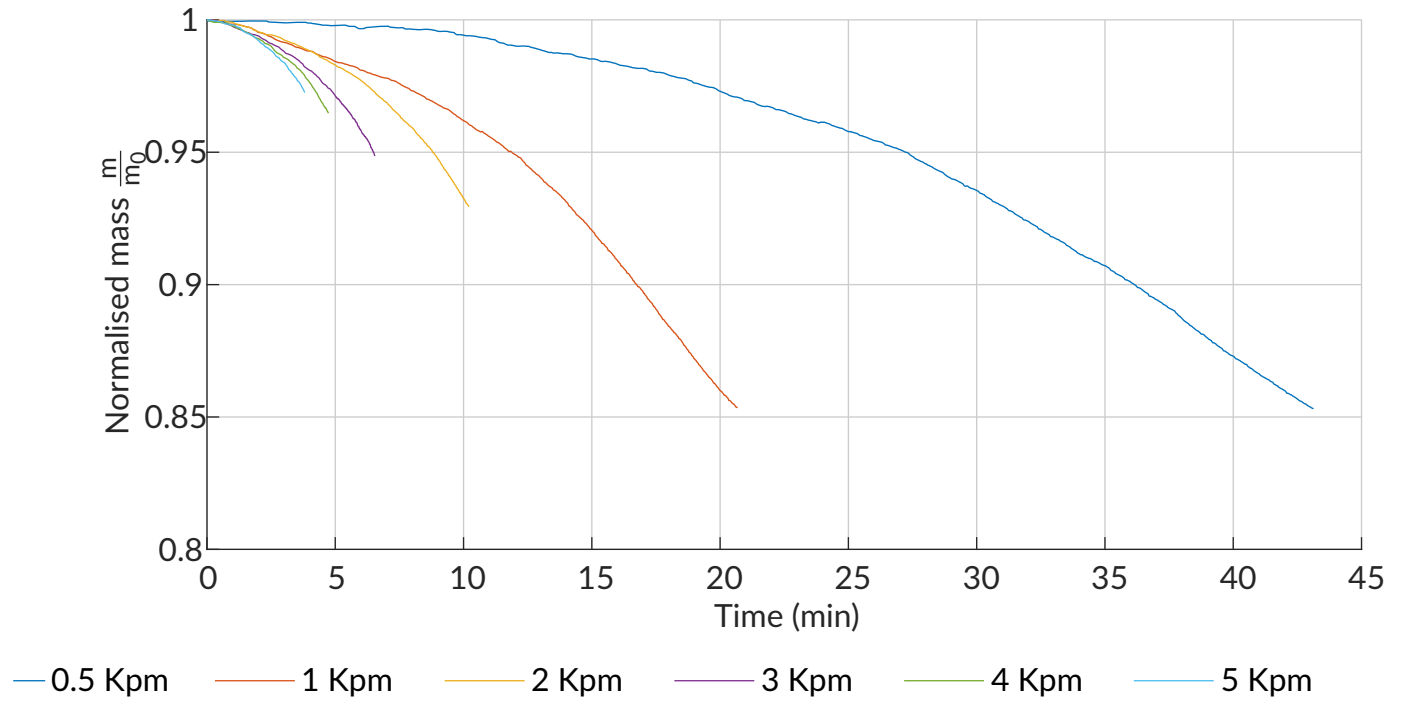

Figure 5.2: Normalised mass loss as a function of temperature and heating rate on a temperature range of 120 – 140°C

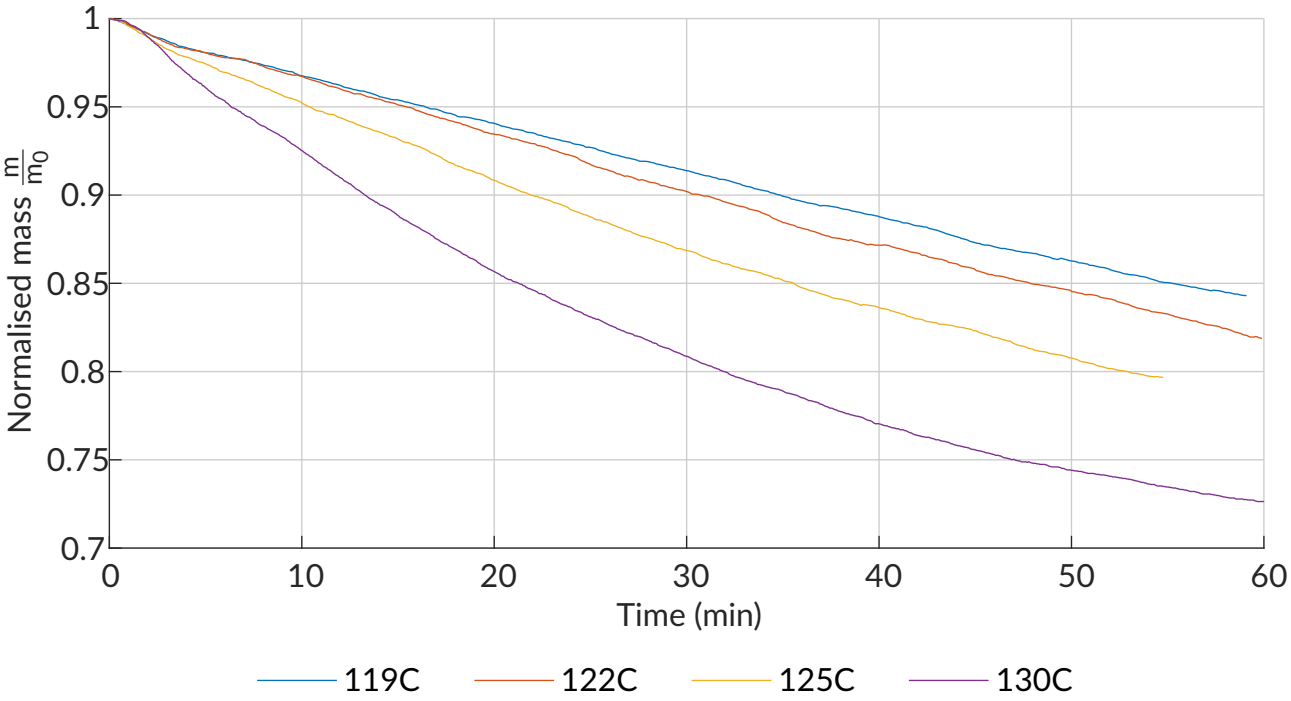

Figure 5.3: Mass loss as a function of time of different temperatures on a temperature range of 119 – 130°C and a total residence time of 60 min

5.2 FTIR analysis

The FTIR data was used to quantify the mass of CO_2 formed, and compared with the total mass loss measured by the TGA, this correlation can be seen in Figures 5.4 and 5.5.

5.2.1 Non-isothermal experiments

At lower heating rates, the effective reaction time is increased, and thus total mass loss is at a maximum at lower heating rates and reducing with an increase in heating rate.

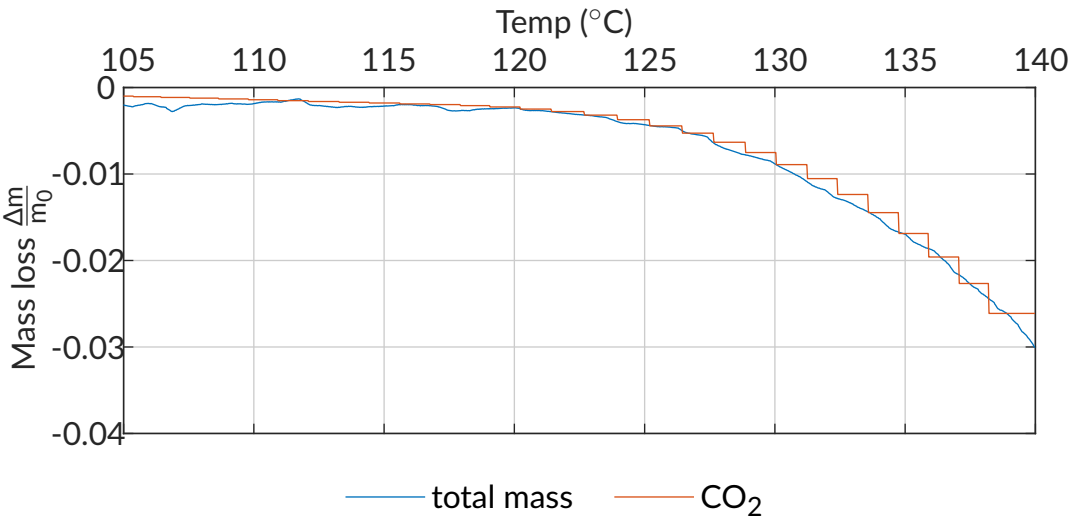

Figure 5.4: Total mass loss and mass loss due to CO_2 formation for a constant heating rate of 5 K/min

Figure 5.4 shows the correlation between total mass loss and CO_2 production for a 5 K/min heating rate within the temperature range of 100 – 140°C. Both the total mass loss and mass loss due to CO_2 formation curves follow the same trend. With the high heating rate, the reaction time is too low for a sufficient amount of ammonium di-phosphate gets produced for the production of ammonium tri-phosphate. The step wise nature of the FTIR data is very evident in Figure 5.4, this is due to the fact that the FTIR only took a measurement roughly once every 13 seconds.

Figure 5.5 shows the mass loss that can be accounted for with CO_2 formation between the temperatures of 100 and 140°C. This shows that initially practically all mass loss is due to CO_2 formation. At higher temperatures, a difference between total mass loss and CO_2 produced becomes apparent, indicating the production of another gas from within the reacting liquid. From literature [9], [16], this additional gas is assumed to be NH_3 gas, and serves as an indicator of the production of ammonium tri-phosphates and longer ammonium polyphosphate chains. The difference between total mass loss and total mass CO_2 produced increases to a significant extent at the higher end of the investigated temperature range, indicating that a significant amount of NH_3 being produced.

When comparing the 5 K/min experiment with the 0.5 K/min experiment, a difference in onset temperature is observed, with 5 K/min experiments only starting to measure a reduction in mass at 120°C while the onset temperature seems to be 117°C at the

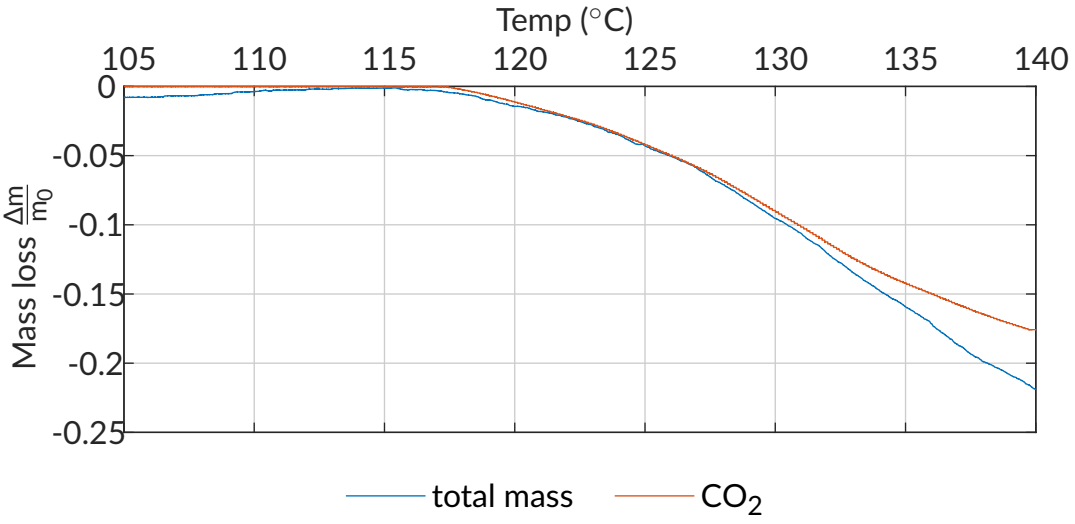

Figure 5.5: Total Mass loss and mass loss due to CO_2 formation for a constant heating rate of 0.5 K/min

0.5 K/min heating rate. This is in accordance with Sarbaev and Koryakin [16]'s claim that the reaction begins to occur with melting. This does, however, contradict the assumption that McCullough, Sheridan, and Frederick [9] made that the reaction only starts to occur at appreciable rates at temperatures in excess of 120°C. The data for the intermediate heating rates are shown in Appendix E.

5.2.2 Isothermal experiments

Isothermal experiments were conducted at 119, 122, 125 and 130°C, with a total reaction time of 60 min at each temperature, found in Appendix E.

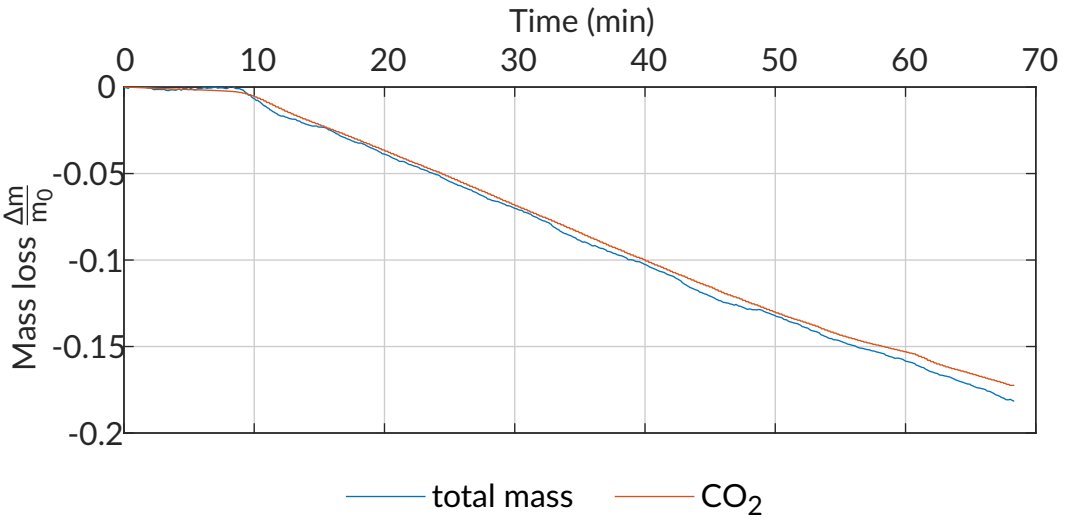

Figure 5.6: Total mass loss and mass loss due to CO_2 formation for a constant temperature of 122°C

Figure 5.6 shows the correlation between total mass loss and mass CO_2 produced. It can be seen that the mass loss can almost entirely be accounted for with CO_2 formation with

a slight deviation being observed near the end of the reaction time, indicating sufficient ADP present for the production of ATP. Isothermal conditions at low temperatures show a much more linear rate of mass loss due to CO_2 production. At higher temperatures, however, it can be seen that the rate of mass loss is non-linear in nature, indicating a concentration dependence in the rate law, for at least one of the reactions occurring.

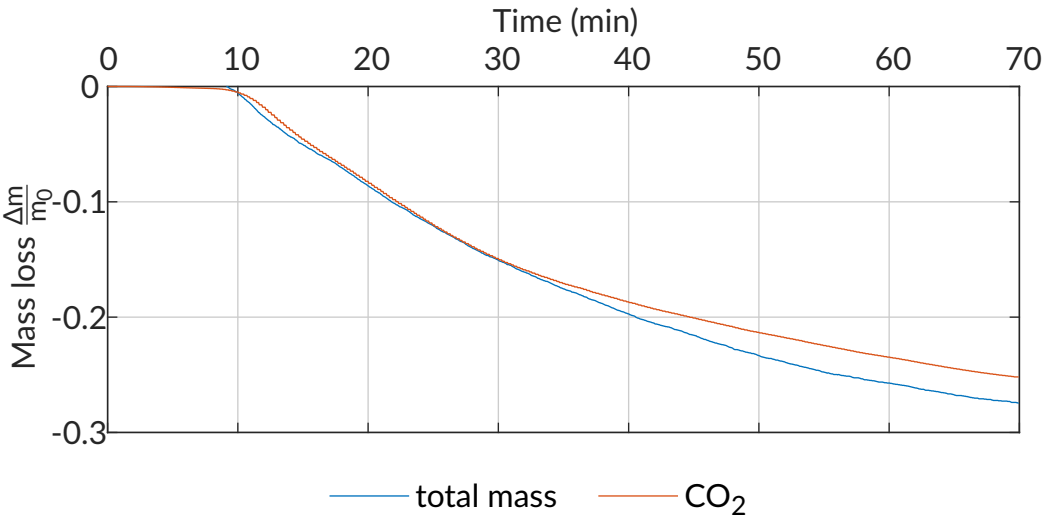

Figure 5.7: Total mass loss and mass loss due to CO_2 formation for a constant temperature of 130°C

Figure 5.5 showed a significant amount of NH_3 being produced at temperatures higher than 130°C. Figure 5.7 shows that the same is true under isothermal conditions, with the mass loss being more than the mass of CO_2 produced as soon as 20 minutes after melting. At this temperature, the rate of mass loss decreases, indicating that the reaction is nearing completion. The maximum amount of CO_2 that can be produced from urea phosphate is 1 mole of CO_2 from 1 mole of UP, which translates to 27.9 wt.%. Looking at Figure 5.7, the mass of CO_2 produced is nearing that limit, thus it is likely that the reduction in the rate of mass loss is due to the low concentration of urea remaining within the reaction mixture.

5.3 Model fitting

From Section 4.4 the first reaction, is described by one of the following reactions.

$$r_1 = k_1[H_3PO_4]^2$$
$$r_1 = k_1[H_3PO_4]^2 - k_2[CO(NH_2)_2]$$
$$r_1 = k_1[CO(NH_2)_2]$$

The mechanism proposed in section 4.4 for the second reaction to be investigated can be described by the following reaction steps:

$$r_2 = k_3[H_3PO_4][HO(PO_3NH_4)_2H]$$
$$r_2 = k_3[H_3PO_4][HO(PO_3NH_4)_2H] - k_4[CO(NH_2)_2]$$
$$r_2 = k_3[CO(NH_2)_2]$$

Table 5.1 shows the average R^2 and RMSE for each of the possible rate law combinations. As can be seen the combination, $r_1 = k_1[CO(NH_2)_2]$ and, either

1. $r_2 = k_3[H_3PO_4][HO(PO_3NH_4)_2H]$ or
2. $r_2 = k_3[H_3PO_4][HO(PO_3NH_4)_2H] - k_3[CO(NH_2)_2]$

shows the best fit and practically identical fit on experimental data along with the lowest average error. This is an indication that the rate-limiting steps for reactions 1 and 2 are one of the equations C.3 - C.6 and reaction C.7 respectively.

Table 5.1: Rate law comparisson

Rate law reaction 1	Rate law reaction 2	R^2	RMSE %
$k_1[PA]^2$	$k_2[PA][ADP]$	0.69	1.05
	$k_2[PA][ADP] - k_3[U]$	0.69	1.05
	$k_2[U]$	0.48	1.29
$k_1[PA] - k_2[U]$	$k_3[P][ADP]$	0.67	1.10
	$k_3[PA][ADP] - k_4[U]$	0.47	2.22
	$k_3[U]$	0.56	1.55
$k_1[U]$	$k_2[PA][ADP]$	0.98	0.79
	$k_2[PA][ADP] - k_3[U]$	0.98	0.79
	$k_2[U]$	0.92	0.53

The best fit is shown in Table 5.1, is

$$r = A_1 \times e^{\frac{-E_{a1}}{RT}}[U] + A_2 \times e^{\frac{-E_{a2}}{RT}}[PA][ADP]$$

The kinetic parameters corresponding to the best fit as shown above are summarised in Table 5.2: These rate equations are shown in Figure 5.8 below, showing the quality of fit for non-isothermal conditions with constant heating rates in the range of 0.5 to 5 K/min.

As can be seen in Figure 5.8, the proposed rate law is capable of accurately describing the mass loss, well within the margins of experimental error under non-isothermal

Table 5.2: Best fit kinetic parameters

parameter	r_1	r_2
A	$1.4 \times 10^{13} \text{min}^{-1}$	$1.3 \times 10^{38} \text{L mol}^{-1}\text{min}^{-1}$
E_a	$113 \frac{\text{kJ}}{\text{mol}}$	$311 \frac{\text{kJ}}{\text{mol}}$

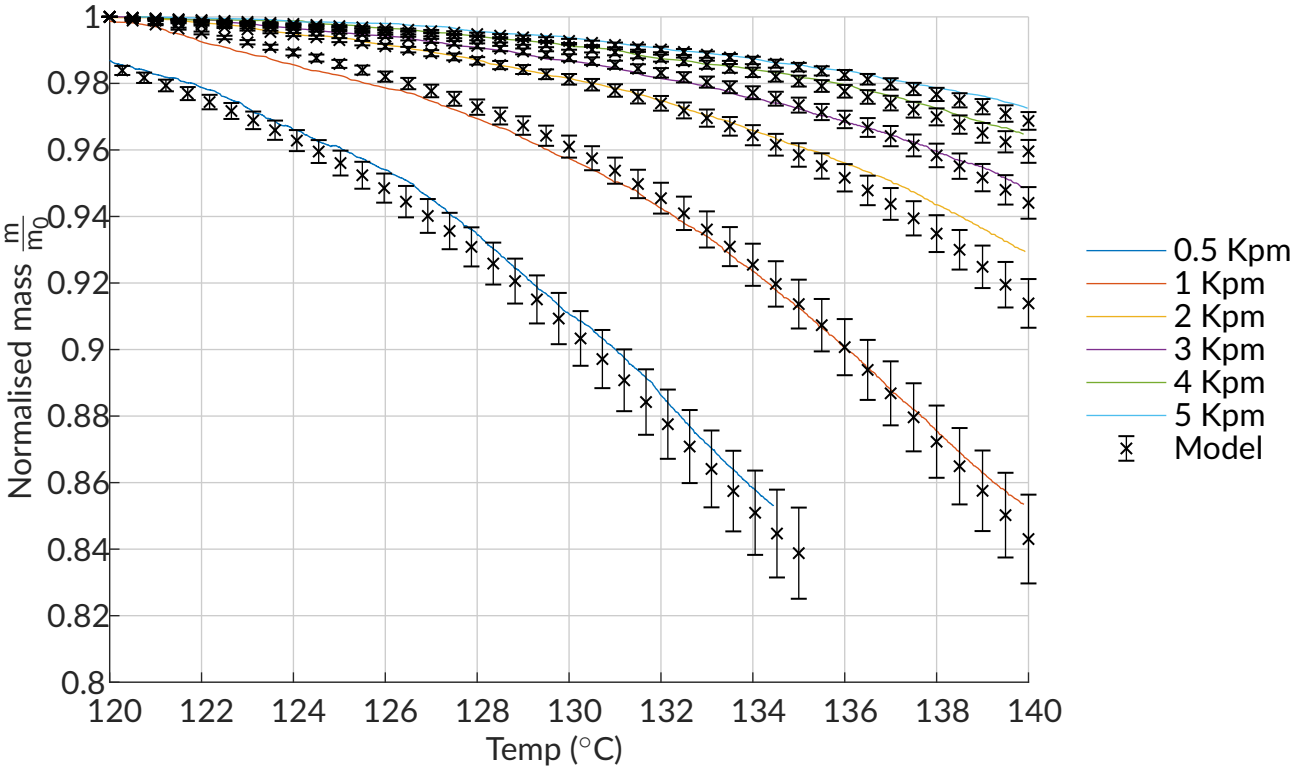

Figure 5.8: Mass loss measured and predicted for various different heating rates

conditions. The equated mass of CO_2 also correlates with the reading from the FTIR as shown in Figure 5.9.

Figure 5.10, shows the proposed rate law's capability of of describing what happens to urea phosphate under isothermal conditions above its melting point. From this graph it is evident that, at longer reaction times the rate law starts to under estimate actual mass loss, this is probably due to either significant urea decomposition, or the further condensing of ammonium polyphosphates, which would lead to more CO_2 and NH_3 forming that what is expected when only ADP and ATP are being produced. At 119°C, the modelled mass loss does not fall within the range expected when comparing it with the experimentally measured mass loss. At this temperature, it could be possible that not all the urea phosphate crystals have melted by the time the reaction mixture reached the set point temperature. This would effectively reduce the volume being used for reacting, reducing the total amount of products being formed, and the energy being liberated from the reaction, would firstly be used for further melting of the crystals rather than allowing more molecules to overcome the activation energy barrier for reacting.

Within the system of pure urea phosphate being pyrolised, the rate of formation of both ammonium di-phosphate and tri-phosphate are calculated by the model developed for a constant heating rate of 1 K/min in Figure 5.11.

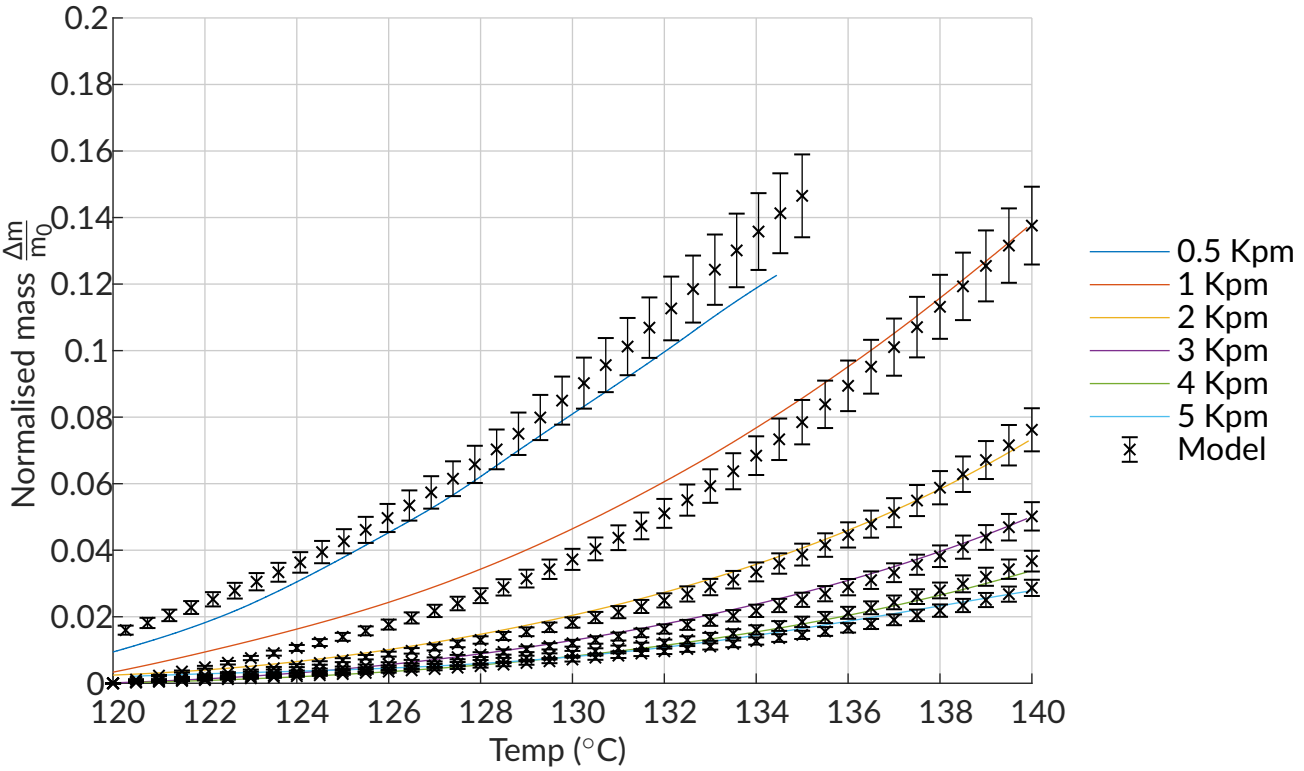

Figure 5.9: Measured mass loss due to CO_2 formation and predicted for various different heating rates

The rate of formation of ADP (reaction 1) starts relatively high, and gradually increases with an increase in temperature, approaching what seems to be a maximum value. While the initial rate of formation of ATP is zero, as no ADP is present at t_0. The rate of ATP production increases sharply near 130°C, where it reaches a maximum, and then falls to a lower rate as the temperature increases to 140°C. This reduction of reaction rate with an increase in temperature is due to the depletion of the limiting reagent, phosphoric acid. Figure 5.11 compares the rates of the modeled rate of the two reactions along with the measured energy measurements from the DSC. An increase of the exothermic effect is observed in Figure 5.11 with an increase in the rate of ADP production (reaction 1) and as the rate of ATP production (reaction 2) increases, a decrease in the exothermic effect is visible, until the total reaction becomes endothermic. The sharp drop to endothermic conditions in the 138 – 140°C range is assumed to be due to further condensing taking place, further contributing to the edothermic nature of the overall reaction at this stage.

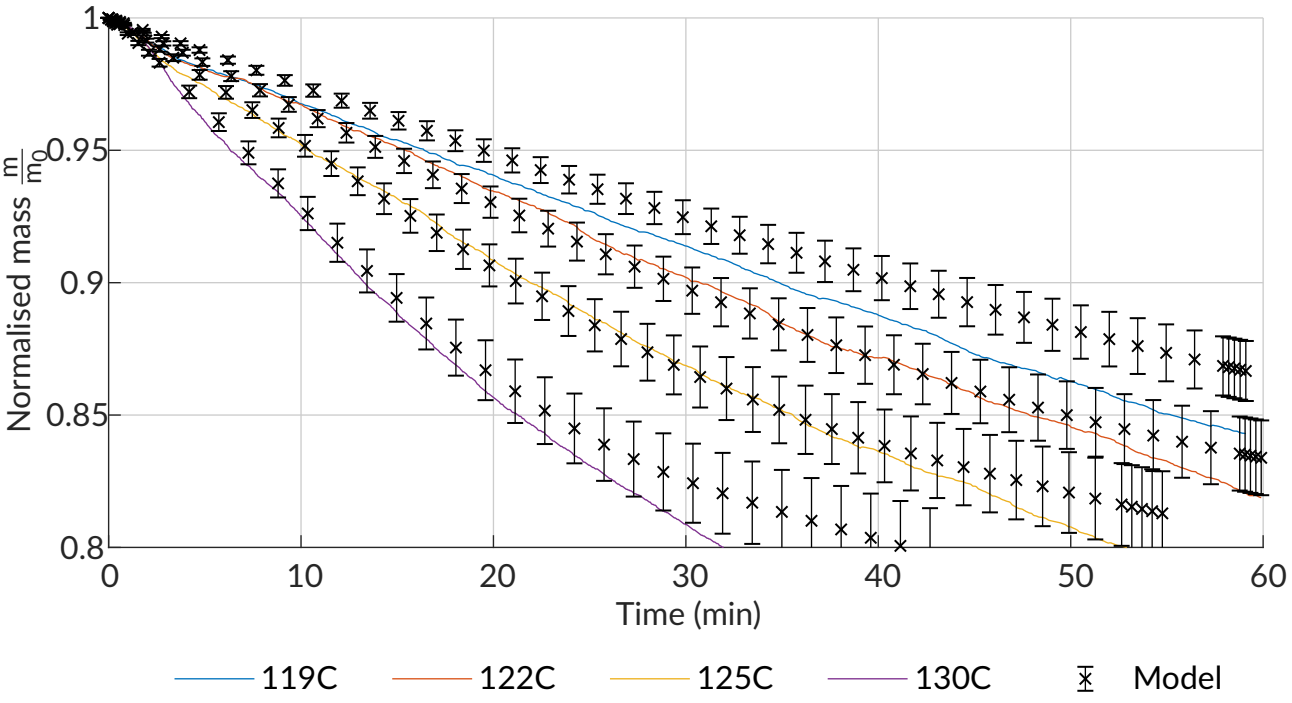

Figure 5.10: Mass loss measured and predicted for various different temperatures

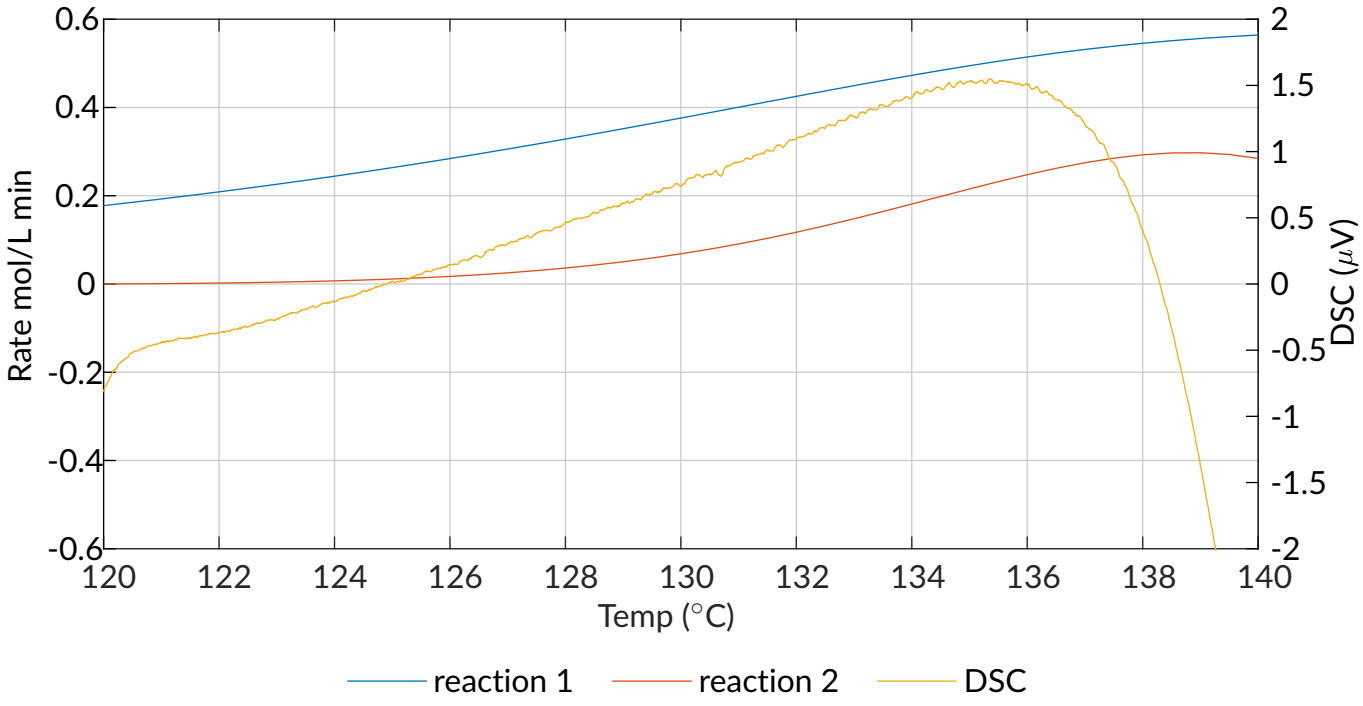

Figure 5.11: Reaction rates for a 1 K/min experiment within the temperature range of 120°C and 140°C

5.4 NMR corellation with TG measurements

TGA-DSC measured the actual mass loss, and the NMR results can be interpreted to calculate the total mass loss, and should in theory then report similar values when compared to the TGA measurement. Table 5.3 below summarises the integrated peak areas for NMR analysis, with all the raw NMR results can be found in the appendix in section E.4.

Table 5.3: NMR Integrated peak area percentages

Reaction conditions	x_{mono}	x_{di}	x_{tri}
0.5 K/min	0.39	0.22	0.40
1.0 K/min	0.28	0.18	0.54
4.0 K/min	0.71	0.29	0
122°C 30min	0.50	0.50	0
122°C 60min	0.31	0.13	0.56

ND = not detected

The mass loss was determined based on the initial mass using the mole balance as set up in section 4.3.1. These two values are compared to each other in Table 5.4.

Table 5.4: Comparisson between TGA mass loss and NMR calculated mass loss

Run (name)	**Mass loss TGA (mg)**	**Mass Loss NMR (mg)**	**Percentage difference (%)**
0.5 K/min	0.74	0.55	26
1 K/min	0.61	0.62	2
4 K/min	0.22	0.19	10
122° C 30 min	0.35	0.31	3
122° C 60 min	0.60	0.59	2

The 0.5 K/min run showed a significant difference of 26% higher mass loss than calculated from the NMR results. This is an indication that at higher temperatures and residence times the assumption that the longest polyphosphate chains forming are triphosphates, no longer holds. The relatively high difference between CO_2 and total mass loss calculated from the TGA and FTIR data is indicative of a significant amount of NH_3, and thus polyphosphates of chain length greater than two forming, or else, a significant amount of urea pyrolysis might be taking place. The rest of the data points show a good correlation between calculated and measured mass loss within experimental error, confirming the validity of the assumptions made. For the isothermal run at 122°C, NMR analysis only shows peaks corresponding to mono- and end-group phosphates. No mid-group phosphates were detected, indicating that no tri-phosphates were produced. Using the mole balance equations as set up for NMR data in section 4.3.1, the total mass loss from NMR data is calculated to be 9.7 wt.%, while the total mass loss measured by the TGA is reported as 10.9 wt.%. These two values differ by 12.9% based on mass loss measured, which is comparable to the experimental error of 8.5%. Based on these observations, it is safe to conclude that reaction 2.13 is adequate in describing these observations.

5.5 Energy analysis

5.5.1 Non-isothermal experiments

Figure 5.12 shows the TGA-DSC and FTIR data obtained for a low conversion at a high heating rate of 5 K/min. At this heating rate, the observed melting point is just below 120°C, with mass loss and CO_2 production seeming to start even slightly before the melting effect completes. After the UP crystals have melted, the DSC reading reaches an exothermic state, and increases with an increase in temperature, indicating an increase in the rate of reaction with an increase in temperature. The exothermic state of the system is an indication that only the first, exothermic reaction occurs under these conditions, which is supported by the FTIR measured data, following the TG mass loss trend exactly for the full temperature range investigated. Thus, the raw TGA data support the assumption that only the first reaction in the condensing of phosphates is occurring at such a low conversion.

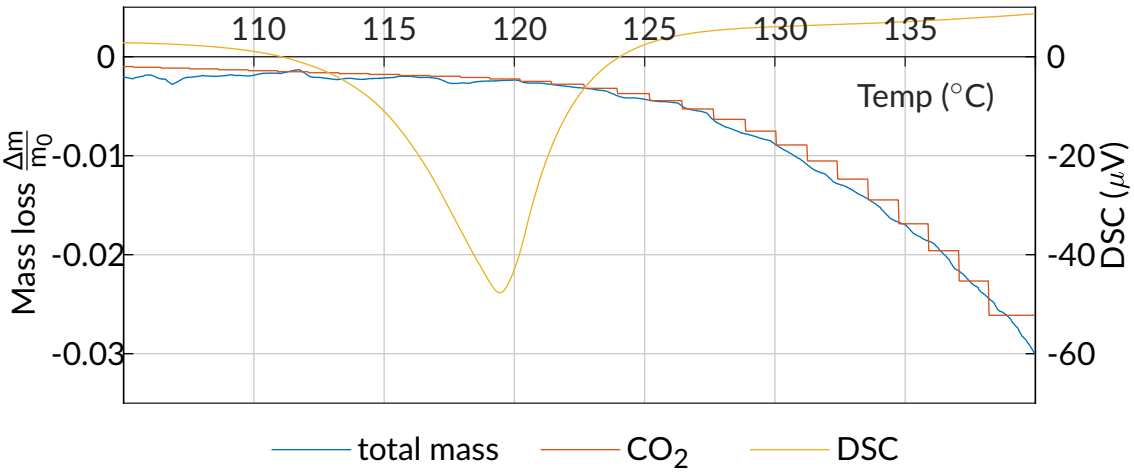

Figure 5.12: TGA-DSC and FTIR data output of a constant heating rate of 5 K/min

Figure 5.13 shows the normalised mass loss, normalised mass of CO_2 formed and the DSC measurements for a constant heating rate of 0.5 K/min. When inspecting the DSC curve in Figure 5.13, the melting point is observed at roughly 116 – 117°C and it can be seen that mass loss and CO_2 formation begins as soon as the endothermic effect of melting stops. It is thus evident that mass loss as well as CO_2 formation starts to occur almost immediately after melting. After that, the DSC shows a shift to an endothermic regime with increasing magnitude as the rate of reaction increases with increasing temperature.

The shift in melting temperature is a result of heat transfer limitation starting to come into play within the system. The TGA curves of all the experiments performed can be found in Appendix E.

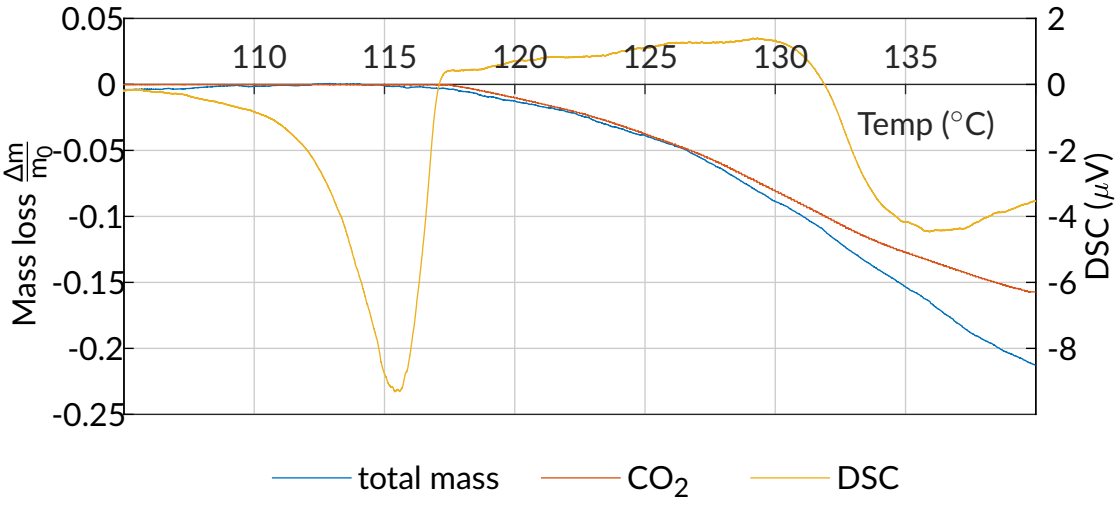

Figure 5.13: TGA-DSC output and mass loss due to CO_2 for a constant heating rate of 0.5 K/min

5.5.2 Isothermal experiments

The DSC curve in Figure 5.14 shows a strong endothermic effect at 10 minutes as the sample melts, which reaches a maximum at about 120°C, after which a relatively constant value is measured in the exothermic region. This could indicate that the first reaction is the predominantly occurring reaction since further condensing is expected to be endothermic in nature [9]. From an inspection of the correlation between the FTIR signal and the mass loss recorded by the TGA, it can be deduced that all mass loss can be accounted for as the formation of CO_2.The mass CO_2 predicted to have formed by the regressed rate law equation for reaction 1 is shown in Figure 5.14 below.

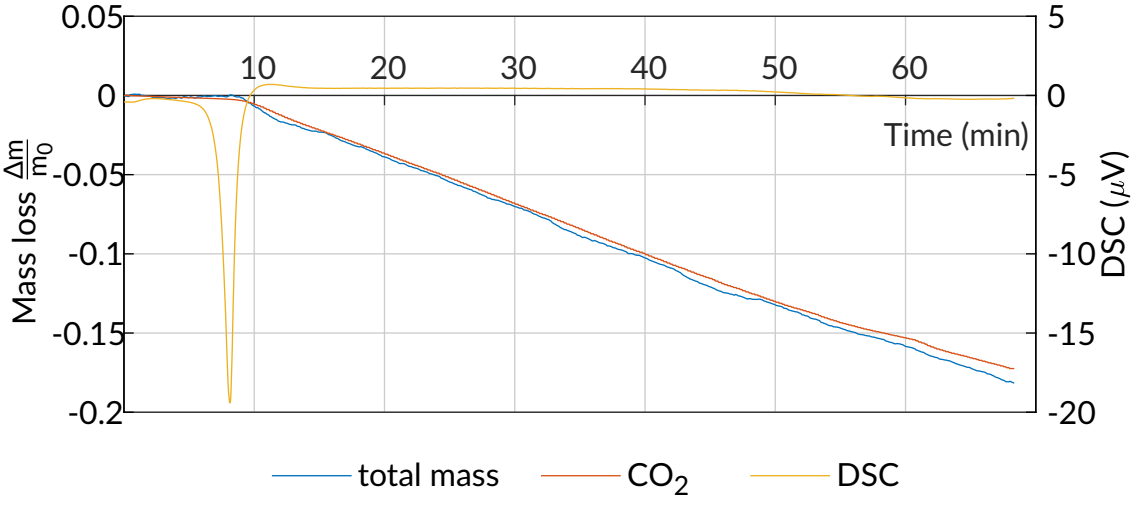

Figure 5.14: TGA-DSC and FTIR data output of a constant temperature of 122°C

Figure 5.14 displays the exact same trend, with a slight difference between the mass loss and CO_2 starting to become apparent around the 60-minute mark. The exothermic DSC reading is also steadily approaching a value of zero, indicating that either the rate

of the first reaction is decreasing with a decrease in reagents or it marks the onset of the endothermic second reaction that is consuming the energy released from the initial exothermic reaction.

At a higher temperature, deviation between total mass loss and mass CO_2 produced become apparent, as soon as the DSC measurement becomes endothermic in nature, indicating a stark increase in the rate of the endothermic production of ammonium tri-phosphate and the production of ammonia gas. This trend is shown in Figure 5.15.

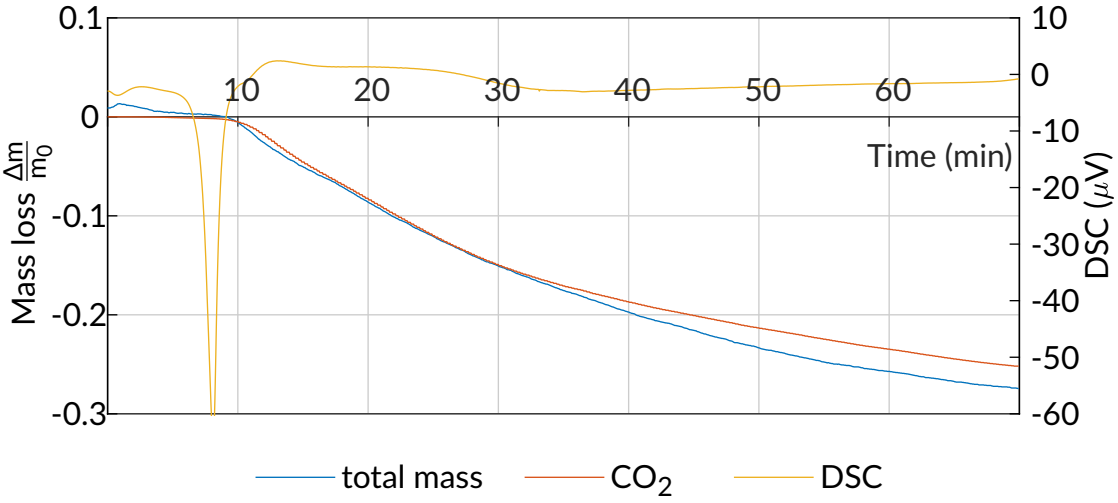

Figure 5.15: TGA-DSC and FTIR data output of a constant temperature of 130°C

When inspecting the DSC curve for the 130°C experiment, it is evident that the exothermic effect of reaction 1 stops at roughly 28 min, and the system demonstrates a slight endothermic regime for the remainder of the time. It can also be visually observed from the graph that, at around the same time that the system becomes endothermic, the mass loss seems to become significantly greater than the amount of CO_2 detected by the FTIR. This is due to NH_3 production, which is in accordance with the findings of McCullough, Sheridan, and Frederick [9] that ammonia release only occurrs once the endothermic reaction starts producing tri-phosphates.

Chapter 6: Conclusions and recommendations

This chapter discusses what the study culminated to and concludes with recommendations for subsequent work on the pyrolysis reaction of urea phosphate.

6.1 Conclusions

6.1.1 Reaction mechanism

By quantifying both mass loss due to pyrolysis and mass loss as CO_2, adequate information on the reaction was gathered to describe the production of ammonium di- and tri-phosphate. This data was used to identify a rate limiting step and to perform a parameter fit. A reaction mechanism for the production of ADP and ATP was proposed,. The rate limiting step was found experimentally as the step that could best describe the experimental data after a marameter fit. The resulting kinetic rate equations could accurately describe the observed mass loss and CO_2 formation within the experimental error range. The composition of the pyrolysis products as predicted by the kinetic model was validated using ^{31}P NMR analysis on the final products of the pyrolysis reaction.

The reaction is initially exothermic in nature followed by an endothermic step, which correlated with the production of ADP and ATP respectively. This observation was made using DSC measurements on the TGA, and the shift from exothermic to endothermic conditions went paired with the release of NH_3 gas, as confirmed by the total mass loss and FTIR data.

6.1.2 Model development and fit

Numerical methods were employed to find kinetic parameters, and the parameters found are able to describe the system at the conditions investigated. Deviation from experimental data is observed at mass loss greater than 15%, suggesting the presence of additional reactions or a change in the reaction mechanism at these conditions. The model can describe the data up to 15% conversion, and is irrespective of isothermal and non-isothermal conditions. At higher conversions measured mass loss and CO_2 formation deviated from the predicted values, indicating the presence of further condensing reactions of the APP. The kinetic model can thus be used for design of a large-scale implementation if the desire is for a high selectivity of short chain ammonium polyphosphates, but

when designing for higher selectivity of ATP and longer chains the kinetic model would need to be expanded upon. The kinetic parameters could describe the mass loss and CO_2 observed within the conditions investigated with a R^2 fit of 0.98 and an a RMSE percentage of 0.8%. The proposed rate law and kinetic parameters could describe the pyrolysis in both isothermal and non-isothermal conditions, as long as the rate of heating did not impose heat transfer limitations.

The production of ADP is described by the rate law equation

$$r_1 = A_1 \exp \frac{-E_{A_1}}{RT} C_U \tag{6.1}$$

and the rate of consumption of ADP to produce ATP is described by the rate law equation

$$r_2 = A_2 \exp \frac{-E_{A_2}}{RT} C_{ADP} C_{PA} \tag{6.2}$$

6.2 Contribution to science

The Rate law and accompanying kinetic parameters for the pyrolysis reaction of urea and phosphoric acid within the mass loss range of 0-15%, is regarded as the contribution to the field of reaction kinetics.

6.3 Recommendations

The data obtained were insufficient to quantify polyphosphate chains of chain length longer than 3, from the literature, it seems that Ion Chromatography (IC) is the most promising analytical technique in quantifying polyphosphate chains. Thus, a subsequent study, performing an investigation into this reaction and employing IC analysis would provide enough information to describe the system at longer residence times and higher temperatures, as higher conversions and longer APP chains are very likely to occur under these conditions.

The pyrolysis of urea phosphate was investigated which means an equimolar feed was the only feed investigated in the present study, the findings of Yang, Li, Luo, *et al.* [22] indicate that increasing urea concentration leads to an increased solubility and improved ability to keep impurities in suspension, thus, it is recommended that an investigation into the reaction with a varying urea mass fraction be done.

When considering industrial scale production, adequate mixing is essential for temperature control, thus an investigation into the thermophysical and thermodynamic properties of APP is recommended.

Bibliography

[1] P. Heffer and M. Prud'homme, "Fertilizer outlook 2016–2020," in *84th IFA Annual Conference, Moscow, Russia*, 2016, pp. 1–5.

[2] S. C. Bacchini, *Cambridge international dictionary of English*. Cambridge University Press, 2013.

[3] J. M. Stinson and J. R. Burnell, *Production of urea-ammonium polyphosphates from urea phosphate*, US Patent 4,292,067, 1981.

[4] J. M. Potts, J. M. Stinson, and J. M. M. Striplin, *Production of liquid fertilizers*, US Patent 2,950,961, 1960.

[5] J. G. Getsinger, *Production of ammonium polyphosphates from wet process phosphoric acid*, US Patent 3,382,059, 1968.

[6] R. H. Adolf and S. Heinz, *Process for the manufacture of catenarily condensed ammonium-phosphates and ammonium-metal-phosphates*, US Patent 3,419,349, 1968.

[7] D. R. Gard, "Phosphoric acids and phosphates," *Kirk-Othmer Encyclopedia of Chemical Technology*, 1996.

[8] S. Stinson, *Process for the production of ammonium polyphosphate*, US Patent 3,540,874, 1970.

[9] J. F. McCullough, R. C. Sheridan, and L. L. Frederick, "Pyrolysis of urea phosphate," *Journal of Agricultural and Food Chemistry*, vol. 26, no. 3, pp. 670–675, 1978.

[10] L. Kubasova, "Polyphosphoric acids and their ammonium salts," *Russian Chemical Reviews*, vol. 40, no. 1, pp. 1–12, 1971.

[11] H. S. Fogler, *Elements of Chemical Reaction Engineering: Pearson New International Edition*, 4th. Pearson, 2013, isbn: 9781292026169.

[12] C. Hodge and T. Motes, "Production of high-quality liquid fertilizers from wet-process acid via urea phosphate," *Nutrient Cycling in Agroecosystems*, vol. 39, no. 1, pp. 59–69, 1994.

[13] H. T. Lewis, T. M. Jones, and J. G. Getsinger, "New routes to clear liquid fertilizers," *Chemical & Engineering News Archive*, vol. 53, no. 35, p. 22, 1975, issn: 0009-2347. doi: 10.1021/cen-v053n035.p022. [Online]. Available: http://dx.doi.org/10.1021/cen-v053n035.p022.

[14] H. T. Lewis, T. M. Jones, and J. R. Burnell, "Two-stage process for crystallization of urea phosphate for production of clear polyphosphate liquid fertilizer," *Industrial & Engineering Chemistry Product Research and Development*, vol. 22, no. 1, pp. 111–117, 1983.

[15] Y. A. Mubarak, "Production of crystalline urea phosphate using," *Dirasat: Engineering Sciences*, vol. 38, no. 1, 2012.

[16] A. Sarbaev and A. Koryakin, "Thermography of carbamide orthophosphate. 3.," *ZHURNAL PRIKLADNOI KHIMII*, vol. 47, no. 4, pp. 717–721, 1974b.

[17] A. Sarbaev, G. Gerbert, and A. Koryakin, “Thermal-decomposition of carbamide orthophosphate at temperatures below its melting-point. 2.,” *ZHURNAL PRIKLADNOI KHIMII*, vol. 47, no. 1, pp. 32–35, 1974a.
[18] C. Y. Shen, N. E. Stahlheber, and D. R. Dyroff, “Preparation and characterization of crystalline long-chain ammonium polyphosphates,” *Journal of the American Chemical Society*, vol. 91, no. 1, pp. 62–67, 1969.
[19] D. E. C. Corbridge, *Structural chemistry of phosphorus*. Elsevier Scientific Pub. Co., 1974.
[20] A. Durif, *Crystal chemistry of condensed phosphates*. Springer Science & Business Media, 2013.
[21] D. C. Young, *Production of ammonium phosphates and product thereof*, US Patent 3,044,851, 1962.
[22] Z. Yang, J. Li, J. Luo, P. Wang, and K. Zhou, “Solid–liquid phase equilibrium for the ternary system urea phosphate+ ammonium dihydrogen phosphate+ water at 25 and 55â° c,” *Fluid Phase Equilibria*, vol. 335, pp. 60–63, 2012.
[23] D. Keens, *Improvements on or relating to the production of urea phosphate*, UK Patent GB1,149,924, 1969.
[24] M. Gittenait, *Reaction of phosphoric acid, urea, and ammonia*, US Patent 3,713,802, 1973.
[25] D. C. Young, *Ammonium polyphosphate production*, US Patent 4,041,133, 1977.
[26] P. M. Schaber, J. Colson, S. Higgins, D. Thielen, B. Anspach, and J. Brauer, “Thermal decomposition (pyrolysis) of urea in an open reaction vessel,” *Thermochimica acta*, vol. 424, no. 1, pp. 131–142, 2004.
[27] R. C. Warner, “The kinetics of the hydrolysis of urea and of arginine,” *Journal of Biological Chemistry*, vol. 142, no. 2, pp. 705–723, 1942.
[28] K. J. Laidler, *Chemical kinetics*, 544.4 LAI. 1987.
[29] W. H. Shaw and J. J. Bordeaux, “The decomposition of urea in aqueous media,” *Journal of the American Chemical Society*, vol. 77, no. 18, pp. 4729–4733, 1955.
[30] I. Lee, C. K. Kim, and B. C. Lee, “Theoretical studies on the hydrolysis of urea in acid solution,” *Journal of Physical Organic Chemistry*, vol. 2, no. 4, pp. 281–299, 1989.
[31] K. Laidler and J. Hoare, “The molecular kinetics of the urea-urease system. i. the kinetic laws,” *Journal of the American Chemical Society*, vol. 71, no. 8, pp. 2699–2702, 1949.
[32] P. M. Schaber, J. Colson, S. Higgins, E. Dietz, D. Thielen, B. Anspach, and J. Brauer, “Study of the urea thermal decomposition (pyrolysis) reaction and importance to cyanuric acid producition,” *American laboratory*, vol. 31, no. 16, pp. 13–21, 1999.
[33] F. Schwarz, “Über eine neue polyphosphorsäure h5p3o10 und einige verbindungen derselben,” *Zeitschrift für anorganische Chemie*, vol. 9, no. 1, pp. 249–266, 1895.
[34] L. Jones, “Estimation of ortho-, pyro-, meta-, and polyphosphates in presence of one another,” *Industrial & Engineering Chemistry Analytical Edition*, vol. 14, no. 7, pp. 536–542, 1942.
[35] A. B. Morgan and C. A. Wilkie, *The Non-halogenated Flame Retardant Handbook*. John Wiley & Sons, 2014.
[36] G. Liu, W. Chen, and J. Yu, “A novel process to prepare ammonium polyphosphate with crystalline form ii and its comparison with melamine polyphosphate,” *Industrial & Engineering Chemistry Research*, vol. 49, no. 23, pp. 12 148–12 155, 2010.
[37] K. Schrödter, G. Bettermann, T. Staffel, T. Klein, and T. Hofmann, “Phosphoric acid and phosphates,” *Ullmann’s encyclopedia of industrial chemistry*, 2008.

[38] A. W. Coats and J. Redfern, "Kinetic parameters from thermogravimetric data," *Nature*, vol. 201, no. 4914, p. 68, 1964.
[39] J. Hillier, T. Bezzant, and T. H. Fletcher, "Improved method for the determination of kinetic parameters from non-isothermal thermogravimetric analysis (tga) data," *Energy & Fuels*, vol. 24, no. 5, pp. 2841–2847, 2010.
[40] B. Li, G. Chen, H. Zhang, and C. Sheng, "Development of non-isothermal tga–dsc for kinetics analysis of low temperature coal oxidation prior to ignition," *Fuel*, vol. 118, pp. 385–391, 2014.
[41] M. Hupfer, R. Gtichter, and R. R. Ruegger, "Polyphosphate in lake sediments: 31p nmr spectroscopy as a tool for its identification," *Limnology and Oceanography*, vol. 40, no. 3, pp. 610–617, 1995.
[42] M. Crutchfield, C. Callis, R. Irani, and G. Roth, "Phosphorus nuclear magnetic resonance studies of ortho and condensed phosphates," *Inorganic Chemistry*, vol. 1, no. 4, pp. 813–817, 1962.
[43] J. Bates, "Fourier transform infrared spectroscopy," *Science*, vol. 191, no. 4222, pp. 31–37, 1976.
[44] D. Swinehart, "The beer-lambert law," *Journal of chemical education*, vol. 39, no. 7, p. 333, 1962.
[45] J. H. Lambert, *Photometria sive de mensura et gradibus luminis, colorum et umbrae*. Klett, 1760.
[46] A. Beer, "Determination of the absorption of red light in colored liquids," *Ann. Phys. Chem*, vol. 86, pp. 78–88, 1852.
[47] S. K. Upadhyay, *Chemical kinetics and reaction dynamics*. Springer Science & Business Media, 2007.
[48] J. Devore, *Applied statistics for engineers and scientists*. Belmont, CA: Thomson Brooks/Cole, 2005, isbn: 0-534-46719-9.

Appendix A: Purity Analysis results

A.1 ICP-OES results

ICP-OES analyses was done by XRD analytics, and the results are shown on the next page. As can be seen most impurities tested for are below the detection limit of 0.001wt.%, with magnesium, iron and aluminum being the most notable of the impurities found. The expected phosphorus mass fraction of phosphorus for a pure sample would have been 19.6%, while an actual fraction of 17.6% was found, this indicates a purity of roughly 90%.

ANALYTICAL REPORT:

To:	**XRD ANALYTICAL AND CONSULTING**	Date of Request 06.09.2018	UIS Analytical Services Analytical Chemistry Laboratories 4, 6 Tel: (012) 665 4291 Fax: (012) 665 4294
Attention:	**Sabine Verryn**		
Ref:			

Certificate of analysis: 23523

Lims ID	Sample ID	SiO2	Al2O3	Fe(tot)	Fe2O3	TiO2	CaO	MgO	Na2O	K2O	MnO	P	Ba	Cr	Cu	Ni	Sr	V	Zn	Moisture	LOI
		%	%	%	%	%	%	%	%	%	%	%	%	%	%	%	%	%	%	%	%
576752	**Urea/Phosphate/QU0002104**	<0.001	0.034	0.044	0.063	0.008	<0.001	0.130	<0.001	0.020	0.007	17.5	<0.001	0.002	0.001	<0.001	<0.001	<0.001	<0.001	0.28	79.1
576752 QC	**duplicate**	<0.001	0.030	0.039	0.056	0.008	<0.001	0.130	<0.001	0.011	0.007	17.7	<0.001	0.004	0.001	<0.001	<0.001	<0.001	<0.001	0.30	79.1
576752 QC	**triplicate**	<0.001	0.034	0.054	0.077	0.009	<0.001	0.130	<0.001	0.040	0.008	17.6	<0.001	0.003	<0.001	<0.001	<0.001	<0.001	<0.001	0.23	79.2

note: Analysis done on samples as received before drying

note: L.O.I. does not include moisture

		Chemical elements:	Si, Al, Fe, Ti, Ca, Mg, Na, K, Mn, P, Ba, Cr, Cu, Sr, V, Zn
		Instrument:	ICP-OES, LECO CS 230
		Method	Soil/Ore Samples by ICP-OES
Date:	29.10.2018	Date:	29.10.2018
Analysed by:	SS Nel	Authorised :	JJ Oberholzer

A.2 XRD analysis results

An XRD analysis was performed by using a back loading preparation method by XRD analytical, and the reported weight % valeus were estimated with the Rietveld method. The results reported by xrd analytical is a 100 % pure sample. but a weight detection limit of 0.5 - 3 wt.%, for any individual impurity, the conclusion is made that no single impurity is greater than 3 wt.%.

Dr Sabine Verryn

m: 083 548 0586
f: 086 565 7368
e: sabine.verryn@xrd.co.za

XRD Analytical and Consulting cc
75 Kafue Street, Lynnwood Glen,
0081, South Africa

CLIENT: NWU (Zandre)

DATE: 17 September 2018

SAMPLES: 1 Sample (Urea)

ANALYSIS: Qualitative and quantitative XRD

The material was prepared for XRD analysis using a back loading preparation method. It was analysed with a PANalytical Aeris diffractometer with PIXcel detector and fixed slits with Fe filtered Co-Kα radiation. The phases were identified using X'Pert Highscore plus software.

The relative phase amounts (weight %) were estimated using the Rietveld method.

Comment:

- In case the results do not correspond to results of other analytical techniques, please let me know for further fine tuning of XRD results.
- Mineral names may not reflect the actual compositions of minerals identified, but rather the mineral group.
- Due to crystallite size and preferred orientation effects, results may not be as accurate as shown in the table.
- Traces of additional phases may be present.
- Amorphous phases, if present, were not taken into consideration during quantification.

If you have any further queries, kindly contact me.

Dr. Sabine Verryn (Pr.Sci.Nat)

Samples will be stored for 3 months after which they will be discarded.

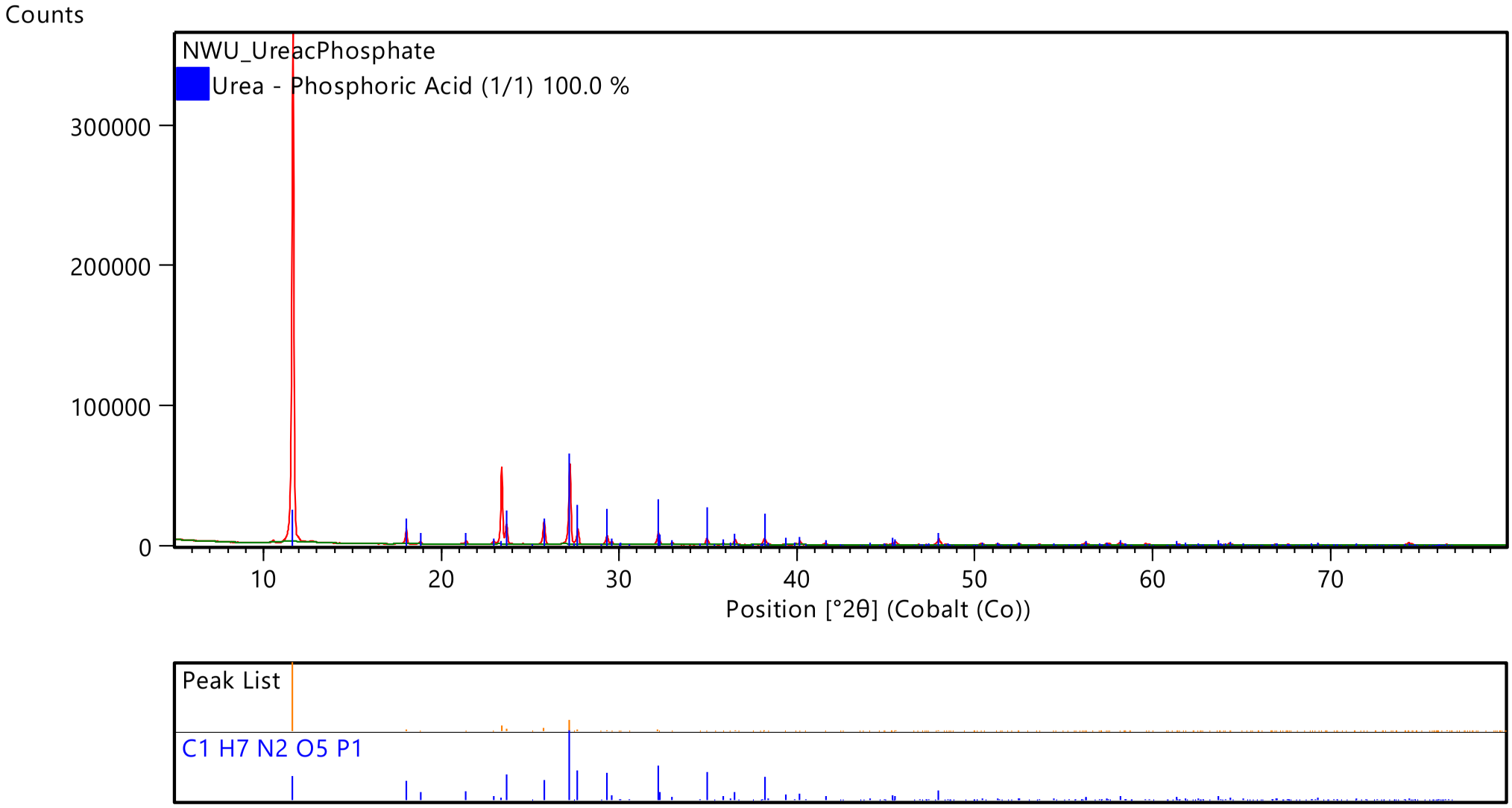

0 = n.d. – not detected above the detection limit of 0.5-3 weight per cent

Appendix B: FTIR Calibration

The FTIR signal is reported in absorbance, which is a unitless value which is a function of the fraction of infra-red light that does not pass through the sample. This relates to the concentration of non-infra-red transparent substances present in the sample. The absorbance can be used to quantify the concentration of a substance if the composition is known according to the beer-Lambert law [44]. The Beer-Lamber law is summarised by

$$A = \log_{10}\frac{I}{I_0} = \varepsilon l c \tag{B.1}$$

where

- A = absorbance
- I = light intensity
- ε = absorptivity constant of species ($Lcm^{-1}mol^{-1}$)
- l = length of the medium through which the light passes (cm)
- c = concentration of chemical species (mol/l)

When considering the experimental setup, the only infrared species present is expected to be CO_2, and the same analyser is continually used, meaning that the only variable in equation B.1 is the concentration passing through the analyser. Thus with rearrangement, you can get concentration (c) as a function of absorbance.

$$c = \frac{A}{\varepsilon l} mol/l \tag{B.2}$$

In order to calculate the total amount of CO_2 then, the concentration time value must be integrated to yield

$$m_{CO_2 t_f} = MW_{CO_2} \int_0^{t_f} \frac{A(t)}{\varepsilon l} dt \tag{B.3}$$

The constants can be lumped together into a single value (c_{FTIR}), which yields:

$$m_{CO_2 t_f} = c_{FTIR} \int_0^{t_f} A(t) dt \tag{B.4}$$

The decomposition of $CaCO_3$ according to the reaction

$$C_aCO_3 \rightarrow CaO_{(s)} + CO_{2(g)} \tag{B.5}$$

over the tamperature range of 600 – 700°C was used for calibrating the FTIR. With A being recorded on the FTIR, and $m_{CO_2 t_f}$ corresponding with the total mass loss measured

by the TGA. The value for c_{FTIR} is then calculated via a regression to minimise the total error between the left-hand side and right-hand side of equation B.4.

This regression was performed with each of the experimental runs, in order to improve accuracy, and as can be seen in Table B.1 fall within the uncertainty range calculated in Section 3.5, with the exception of 3 experiments.

The determined values for c_{FTIR} for each experiment conducted is shown in Table B.1. The calibration constant was optimised for each experimental run, to ensure accurate approximation of the mass of NH_3 produced for the parameter fit. These values were comparably close to the determined value for the calibration run. The first outlier value is with the increased mass loading sample, where the calibration constant is calculated to be significantly higher, this value is suspected to be higher due to the rate of CO_2 formation being too high to pass through the crucible lid unhindered. The same phenomenon is suspectded for the higher heating rates requiring a larger calibration constant to reconcile the mass loss with the FTIR signal. With the higher heating rates, the rate of CO_2 formation also increases, and reaches a flow rate too high to pass through the crucible lid unhindered, resulting in lower absorbance values recorded by the FTIR.

Table B.1: Summary of the values for c_{FTIR} for each experiment conducted

Run	c_{FTIR}
calibration	0.18
1K/m R2	0.17
1K/m R5	0.17
0.5K/m R2	0.17
2K/m	0.25
5K/m	0.34
1K/min 10mg	0.23

Appendix C: Mechanism derivation

C.1 Ammonium di-phosphate mechanism

The mechanism proposed in section 2.2.4 is summarised by the next 6 elementary steps for the production of ammonium di-phosphate:

$$2H_3PO_4 \rightarrow HO(PO_3H)_2H + H_2O \tag{C.1}$$
$$HO(PO_3H)_2H + H_2O \rightarrow 2H_3PO_4 \tag{C.2}$$
$$CO(NH_2)_2 \rightarrow NH_3 + HNCO \tag{C.3}$$
$$HNCO + H_2O \rightarrow NH_3 + CO_2 \tag{C.4}$$
$$HO(PO_3H)_2H + NH_3 \rightarrow HOPO_3NH_4PO_3H_2 \tag{C.5}$$
$$HOPO_3NH_4PO_3H_2 + NH_3 \rightarrow HO(PO_3NH_4)_2H \tag{C.6}$$

Where di-phosphate ($HO(PO_3H)_2H$), water(H_2O), ammonia(NH_3), cyanic acid (HNCO), and mono-ammonium di-phosphatev($HOPO_3NH_4PO_3H_2$) are proposed as reaction intermediates. The production of mono-ammonium di-phosphate as a reaction intermediate in the production of ammonium di-phosphates is expected as it requires two consecutive bimolecular reactions, rather than a single tri-molecular reaction, which is statistically much less likely [11], [28], [47].

Since these are elementary reactions by definition, the rate laws are directly proportional to the product of the first order concentrations of the reagents in each reaction. The rate equations for each of these elementary reaction steps are given by:

$$r_{C.1} = k_{C.1}[H_3PO_4]^2$$
$$r_{C.2} = k_{C.2}[HO(PO_3H)_2H][H_2O]$$
$$r_{C.3} = k_{C.3}[CO(NH_2)_2]$$
$$r_{C.4} = k_{C.4}[HNCO][H_2O]$$
$$r_{C.5} = k_{C.5}[HO(PO_3H)_2H][NH_3]$$
$$r_{C.6} = k_{C.6}[HOPO_3NH_4PO_3H_2][NH_3]$$

By using the pseudo steady state assumption on reaction intermediates, rate equations for each of the reaction intermediates can be derived and the system of equations can be solved to find the net rate law of the full reaction. The steady state assumption for the reaction intermediates, *Inter Alia* NH_3 , $HO[PO_3H]_2H$, HNCO, H_2O and

$HOPO_3NH_4PO_3H_2$ can then be calculated as:

$$\frac{d[NH_3]}{dt} = 0 = r_{C.3} - r_{C.4} - r_{C.5} - r_{C.6}$$
$$\frac{d[HO(PO_3H)_2H]}{dt} = 0 = r_{C.1} - r_{C.2} - r_{C.5}$$
$$\frac{d[HNCO]}{dt} = 0 = r_{C.3} - r_{C.4}$$
$$\frac{d[H_2O]}{dt} = 0 = r_{C.1} - r_{C.2} - r_{C.4}$$
$$\frac{d[HOPO_3NH_4PO_3H_2]}{dt} = 0 = r_{C.5} - r_{C.6}$$

which expands to:

$$\frac{d[NH_3]}{dt} = 0 = k_{C.3}[CO(NH_2)_2] - k_{C.4}[HNCO][H_2O] - k_{C.5}[HO(PO_3H)_2H][NH_3] - k_{C.6}[HOPO_3NH_4PO_3H_2][NH_3]$$
$$\frac{d[HO(PO_3H)_2H]}{dt} = 0 = k_{C.1}[H_3PO_4]^2 - k_{C.2}[HO(PO_3H)_2H][H_2O] - k_{C.5}[HO(PO_3H)_2H][NH_3]$$
$$\frac{d[HNCO]}{dt} = 0 = k_{C.3}[CO(NH_2)_2] - k_{C.4}[HNCO][H_2O]$$
$$\frac{d[H_2O]}{dt} = 0 = k_{C.1}[H_3PO_4]^2 - k_{C.2}[HO(PO_3H)_2H][H_2O] - k_{C.4}[HNCO][H_2O]$$
$$\frac{d[HOPO_3NH_4PO_3H_2]}{dt} = 0 = k_{C.5}[HO(PO_3H)_2H][NH_3] - k_{C.6}[HOPO_3NH_4PO_3H_2][NH_3]$$

Solving this set of equations was done using Matlab's symbolic solver, the code for which can be found in section C.3.

Using the solved set of equations, each step can be expressed in terms of chemical species that can be measured. The solution to these equations are summarised below:

$$[NH_3] = \frac{k_{C.3}[CO(NH_2)_2]}{k_{C.6}}$$
$$[HO(PO_3H)_2H] = \frac{k_{C.6}}{k_{C.5}}$$
$$[HNCO] = \frac{k_{C.2}k_{C.6}k_{C.3}[CO(NH_2)_2]}{k_{C.4}k_{C.5}(k_{C.1}[H_3PO_4]^2 - k_{C.3}[CO(NH_2)_2])}$$
$$[H_2O] = \frac{k_{C.5}(k_{C.1}[H_3PO_4]^2 - k_{C.3}[CO(NH_2)_2])}{k_{C.2}k_{C.6}}$$
$$[HOPO_3NH_4PO_3H_2] = 1$$

Re-substitution of these answers back into the rate equations of the reaction intermediates shows these solutions to be correct.

Rewriting $r_{C.1}$ - $r_{C.6}$ in terms of only the measurable variables, the equations become:

$$r_{C.1} = k_{C.1}[H_3PO_4]^2$$
$$r_{C.2} = k_{C.2}\frac{k_{C.6}}{k_{C.5}}\frac{k_{C.5}(-k_{C.3}[CO(NH_2)_2] + k_{C.1}[H_3PO_4]^2)}{k_{C.2}k_{C.6}}$$
$$r_{C.3} = k_{C.3}[CO(NH_2)_2]$$
$$r_{C.4} = k_{C.4}\frac{k_{C.2}k_{C.6}k_{C.3}[CO(NH_2)_2]}{k_{C.1}[H_3PO_4]^2 - k_{C.3}[CO(NH_2)_2]}\frac{k_{C.5}(-k_{C.3}[CO(NH_2)_2] + k_{C.1}[H_3PO_4]^2)}{k_{C.2}k_{C.6}}$$
$$r_{C.5} = k_{C.5}\frac{k_{C.6}}{k_{C.5}}\frac{k_{C.3}[CO(NH_2)_2]}{k_{C.6}}$$
$$r_{C.6} = k_{C.6}1\frac{k_{C.3}[CO(NH_2)_2]}{k_{C.6}}$$

since the multiplication of rate constants at the same temperature yields,

$$A_1e^{-\frac{E_{A1}}{RT}} \times A_2e^{-\frac{E_{A2}}{RT}} = A_1A_2e^{-\frac{E_{A1}}{RT}-\frac{E_{A2}}{RT}} = A_1A_2e^{-\frac{E_{A1}+E_{A2}}{RT}}$$

rate constants can be lumped together into a single reaction rate constant for the purpose of the parameter search. The equations required to perform a parameter search reduces to effectively the following 3 possibilities:

$$r_1 = k_1[H_3PO_4]^2$$
$$r_1 = k_1[H_3PO_4]^2 - k_2[CO(NH_2)_2]$$
$$r_1 = k_1[CO(NH_2)_2]$$

The rate-limiting step can be determined by the rate equation with the best ability to predict the mass loss measured by the TGA.

C.2 Ammonium tri-phosphate mechanism

For the second reaction, the reaction scheme is similar, but NH_3 is present in the gas phase, and thus reaction $r_{C.10}$ accounts for the formation of the measurable ammonia gas.

$$HO(PO_3NH_4)_2H + H_3PO_4 \rightarrow HO(PO_3NH4)_2HPO_3H + H_2O \quad (C.7)$$
$$HO(PO_3NH4)_2HPO_3H + H_2O \rightarrow HO(PO_3NH_4)_2H + H_3PO_4 \quad (C.8)$$
$$CO(NH_2)_2 \rightarrow NH_3 + HNCO$$
$$HNCO + H_2O \rightarrow NH_3 + CO_2$$
$$HO(PO_3NH4)_2HPO_3H + NH_3 \rightarrow HOPO_3NH_4PO_3H_2 \quad (C.9)$$
$$NH_{3(aq)} \rightarrow NH_{3(gas)} \quad (C.10)$$

The addition of di-amminium tri-phosphate ($HO(PO_3NH4)_2HPO_3H$) is suggested as another new reaction intermediate in addition to water(H_2O), ammonia(NH_3) and cyanic acid (HNCO) which is already proposed in the previous section. The elementary rate

laws for the new equations are:

$$\begin{aligned} r_{C.7} &= k_{C.7}[H_3PO_4][HO(PO_3NH_4)_2H] \\ r_{C.8} &= k_{C.8}[HO(PO_3NH4)_2HPO_3H][H_2O] \\ r_{C.9} &= k_{C.9}[HO(PO_3NH4)_2HPO_3H][NH_3] \\ r_{C.10} &= k_{C.10}[NH_{3(aq)}] \end{aligned}$$

The steady state assumption for the reaction intermediates $HO(PO_3NH4)_2HPO_3H$, HNCO, H_2O and $NH_{3(liq)}$ leads to the following set of equations to solve.

$$\begin{aligned} \frac{d[HO(PO_3NH4)_2HPO_3H]}{dt} &= 0 = r_{C.7} - r_{C.8} - r_{C.9} \\ \frac{d[HNCO]}{dt} &= 0 = r_{C.3} - r_{C.4} \\ \frac{d[H_2O]}{dt} &= 0 = r_{C.7} - r_{C.8} - r_{C.4} \\ \frac{d[NH_{3(liq)}]}{dt} &= 0 = r_{C.3} + r_{C.4} - r_{C.9} - r_{C.10} \end{aligned}$$

These equations once again expand to:

$$\begin{aligned} \frac{d[HO(PO_3NH4)_2HPO_3H]}{dt} &= 0 = k_{C.7}[H_3PO_4][HO(PO_3NH_4)_2H] - \\ &\quad k_{C.8}[HO(PO_3NH4)_2HPO_3H][H_2O] - \\ &\quad k_{C.9}[HO(PO_3NH4)_2HPO_3H][NH_3] \\ \frac{d[HNCO]}{dt} &= 0 = k_{C.3}[CO(NH_2)_2] - k_{C.4}[HNCO][H_2O] \\ \frac{d[H_2O]}{dt} &= 0 = k_{C.7}[H_3PO_4][HO(PO_3NH_4)_2H] - \\ &\quad k_{C.8}[HO(PO_3NH4)_2HPO_3H][H_2O] - k_{C.4}[HNCO][H_2O] \\ \frac{d[NH_{3(liq)}]}{dt} &= 0 = k_{C.3}[CO(NH_2)_2] + k_{C.4}[HNCO][H_2O] - \\ &\quad k_{C.9}[HO(PO_3NH4)_2HPO_3H][NH_3] - k_{C.10}[NH_{3(aq)}] \end{aligned}$$

Solving this set of equations was done using Matlab's symbolic solver, the code for which can be found in section C.3. The reaction intermediates, expressed as functions of measurable variables is expressed as:

$$\begin{aligned} [HO(PO_3NH4)_2HPO_3H] &= \frac{k_{C.10}}{k_{C.9}} \\ [NH_3] &= \frac{k_{C.3}[CO(NH_2)_2]}{k_{C.10}} \\ [HNCO] &= \frac{k_{C.8}k_{C.10}k_{C.3}[CO(NH_2)_2]}{k_{C.4}k_{C.9}(k_{C.7}[H_3PO_4][HO(PO_3NH_4)_2H] - k_{C.3}[CO(NH_2)_2])} \\ [H_2O] &= \frac{k_{C.9}(k_{C.7}[H_3PO_4][HO(PO_3NH_4)_2H] - k_{C.3}[CO(NH_2)_2])}{k_{C.8}k_{C.10}} \end{aligned}$$

The validity of these solutions have been verified with re-substitution into the rate equations of the reaction intermediates. The expressions for the reaction intermediates in

terms of measurable variables can then be substituted into the various rate equations and tested for the determination of a rate-limiting step. These rate equations, once expanded, become:

$$r_{C.7} = k_{C.7}[H_3PO_4][HO(PO_3NH_4)_2H]$$
$$r_{C.8} = k_{C.8}\frac{k_{C.10}}{k_{C.9}}\frac{k_{C.9}(k_{C.7}[H_3PO_4][HO(PO_3NH_4)_2H] - k_{C.3}[CO(NH_2)_2])}{k_{C.8}k_{C.10}}$$
$$r_{C.3} = k_{C.3}[CO(NH_2)_2]$$
$$r_{C.4} = k_{C.4}\frac{k_{C.8}k_{C.10}k_{C.3}[CO(NH_2)_2]}{k_{C.4}k_{C.9}(k_{C.7}[H_3PO_4][HO(PO_3NH_4)_2H] - k_{C.3}[CO(NH_2)_2])}$$
$$\frac{k_{C.9}(k_{C.7}[H_3PO_4][HO(PO_3NH_4)_2H] - k_{C.3}[CO(NH_2)_2])}{k_{C.8}k_{C.10}}$$
$$r_{C.9} = k_{C.9}\frac{k_{C.10}}{k_{C.9}}\frac{k_{C.3}[CO(NH_2)_2]}{k_{C.10}}$$
$$r_{C.10} = k_{C.10}\frac{k_{C.3}[CO(NH_2)_2]}{k_{C.10}}$$

Once again, the rate constants can be lumped together, and the equations can be simplified to yield these three effective reaction rate equations:

$$r_2 = k_3[H_3PO_4][HO(PO_3NH_4)_2H]$$
$$r_2 = k_3[H_3PO_4][HO(PO_3NH_4)_2H] - k_4[CO(NH_2)_2]$$
$$r_2 = k_3[CO(NH_2)_2]$$

Where the rate limiting reaction should be able to best describe the mass loss observed within the TGA.

C.3 Matlab Code for solution to pseudo steady state equations

```
syms k1 k2 k3 k4 k5 k6 k7 k8 k9 k10 PA U ADP DP A CA W MADP
   DADP DATP

r1(k1, k3, k4, k2, k5, k6, k7, k8, k9, PA, U, ADP, DP, A, CA,
    W, MADP, DADP, DATP) = k1*PA^2;
r2(k1, k3, k4, k2, k5, k6, k7, k8, k9, PA, U, ADP, DP, A, CA,
    W, MADP, DADP, DATP) = k2*DP*W;
r3(k1, k3, k4, k2, k5, k6, k7, k8, k9, PA, U, ADP, DP, A, CA,
    W, MADP, DADP, DATP) = k3*U;
r4(k1, k3, k4, k2, k5, k6, k7, k8, k9, PA, U, ADP, DP, A, CA,
    W, MADP, DADP, DATP) = k4*CA*W;
r5(k1, k3, k4, k2, k5, k6, k7, k8, k9, PA, U, ADP, DP, A, CA,
    W, MADP, DADP, DATP) = k5*DP*A;
r6(k1, k3, k4, k2, k5, k6, k7, k8, k9, PA, U, ADP, DP, A, CA,
    W, MADP, DADP, DATP) = k6*MADP*A;
```

```
r7(k1, k3, k4, k2, k5, k6, k7, k8, k9, PA, U, ADP, DP, A, CA,
    W, MADP, DADP, DATP) = k7*ADP*PA;
r8(k1, k3, k4, k2, k5, k6, k7, k8, k9, PA, U, ADP, DP, A, CA,
    W, MADP, DADP, DATP) = k8*DATP*W;
r9(k1, k3, k4, k2, k5, k6, k7, k8, k9, PA, U, ADP, DP, A, CA,
    W, MADP, DADP, DATP) = k9*DATP*A;
r10(k1, k3, k4, k2, k5, k6, k7, k8, k9, PA, U, ADP, DP, A, CA
   , W, MADP, DADP, DATP) = k10*A;

% Equation sets
% r1:       2PA = DP + W
% r2:    DP + W = 2PA
% r3:         U = A + CA
% r4:    CA + W = A +CO2
% r5:    DP + A = MADP
% r6: MADP + A = ADP
dAdt = r3 + r4 -r5 -r6;
dDPdt = r1-r5-r2;
dCAdt = r3-r4;
dWdt = r1-r4-r2;
dMADPdt = r5-r6;

dndt = [dAdt ; dDPdt; dCAdt ; dWdt; dMADPdt];
N = solve(dndt,DP, A,CA, W, MADP);
display(N.A(1));
display(N.DP(1));
display(N.MADP(1));
display(N.W(1));
display(N.CA(1));
% Equation sets
% r7: ADP + PA = DATP + W
% r8: DATP + W = ADP + PA
% r3:         U = A + CA
% r4:    CA + W = A +CO2
% r9: DATP + A = ATP
% r10: A(liq) = A(Gas)
dAdt = r3 + r4 - r9 - r10;
dCAdt = r3-r4;
dWdt = r7- r8 - r4;
dDATPdt = r7 -r9 - r8;
dndt = [ dAdt ; dCAdt ; dWdt; dDATPdt];
N = solve(dndt, A, CA, W, DATP);
display('Reaction 2');
display(N.DATP(1));
display(N.A(1));
display(N.CA);
display(N.W);
```

Appendix D: Matlab Code

The program in Matlab was wirtten using an object oriented philosophy, and each function was written in its own file. The raw TGA data was saved as matlab variable under the file name TGAdata.mat.

D.1 Derive

The code below was executed to perform a regression on the experimental data. Code for the various functions being called is shown in subsequent sections.

```
clear all
[~, Fractions, SolverOptions, A, Ea,DataSets, ~, isolate] =
   Options;
%initialising variables
ydata = [];
xdata = [];
if isolate == true
    A = A(1);
    Ea = Ea(1);
end
%initial guess values loaded from the function Options
AEa = [A ; Ea];
%combining all the experimental data into one array for the
   regression
for k=1:DataSets
    [Reaction] = DataLoad(k);%Reaction = [temp, time, xu, xp,
        xADP, xATP, xCO2, xNH3, m];
    xdata = [xdata ; Reaction(:,2)];
    Reaction(:,1:2) = [];
    Reaction(:,8) = [];
    %if data is represented as fractions, raw mass data is
       not modeled.
    if Fractions == false
        Reaction(:,7) = [];
    end
    ydata = [ydata ; Reaction];
end
%non linear solver used to find rate constants
```

```
if numel(A) == 1
    kinParms = lsqcurvefit(@(AEa,xdata)integrated(AEa,xdata),
       AEa,xdata,ydata,[-inf,0],[],SolverOptions);
    A(1) = kinParms(1);
    Ea(1) = kinParms(2);
elseif numel(A) == 2
    kinParms = lsqcurvefit(@(AEa,xdata)integrated(AEa,xdata),
       AEa,xdata,ydata,[-inf,-inf,0,0],[],SolverOptions);
    A(1) = kinParms(1);
    Ea(1) = kinParms(2);
    A(2) = kinParms(3);
    Ea(2) = kinParms(4);
elseif numel(A) == 3
    kinParms = lsqcurvefit(@(AEa,xdata)integrated(AEa,xdata),
       AEa,xdata,ydata,[-inf,-inf,-inf,0,0,0],[],
       SolverOptions);
    A(1) = kinParms(1);
    Ea(1) = kinParms(2);
    A(2) = kinParms(3);
    Ea(2) = kinParms(4);
    A(3) = kinParms(5);
    Ea(3) = kinParms(6);
elseif numel(A) == 4
    kinParms = lsqcurvefit(@(AEa,xdata)integrated(AEa,xdata),
       AEa,xdata,ydata,[-inf,-inf,-inf,-inf,0,0,0,0],[],
       SolverOptions);
    A(1) = kinParms(1);
    Ea(1) = kinParms(2);
    A(2) = kinParms(3);
    Ea(2) = kinParms(4);
    A(3) = kinParms(5);
    Ea(3) = kinParms(6);
    A(4) = kinParms(7);
    Ea(4) = kinParms(8);
end
AEa = [A ; Ea];
%save the kinetic parameters found with the regression
save('FittedParms.mat','AEa');
%Goodness of fit determination
for k=1:DataSets
    [~, ~, ~, name{k,1}] = DataLoad(k);  %cell array with
       data set names
    [Rsq(k,1), RMSE(k,1)] = GoF(kinParms,k); %array with R
       quare and rootmean squared values
end
Rsqt = mean(Rsq);
RMSEt = mean(RMSE);
name{k+1,1} = 'Average fit';
Rsq = [Rsq ; Rsqt];
```

```
RMSE = [RMSE ; RMSEt];
RMSE = round(RMSE,5);
FitT = table(name,Rsq,RMSE);

%displaying the rate constants with accompanying fit.
%RateLaw = strcat( {'k1 = '}, num2str(exp(A(1)),3), {' exp
   (-'},num2str(Ea(1),3),'/RT)',{' and k2(T) = '}, num2str(
   exp(A(2)),3),{' exp(-'},num2str(Ea(2),3),'/RT)');
%disp(RateLaw{1});
disp(FitT);
```

D.2 Model display

This program was executed separately to graphically inspect the quality of fit for the regressed model, on both the data used for regression and additional experimental runs. The various user created functions being called in this program is shown in subsequent sections.

```
load('FittedParms.mat');
%Options
ShowHRcomp = true; %to graphically compare the various
   heating rates
[~, ~, ~, ~, ~,DataSets, SaveExcel] = Options;
%plot a graph showing the quality of fit with experimental
   data

for k=1:17
    if SaveExcel == true
        [Rsq, RMSE] = GoF(AEa,k);
        WriteToExcel(k,AEa)
    else
        graphs(k,AEa)
    end
end

%to show the comparisson of different heating rates
if SaveExcel == false
    if ShowHRcomp == true
        figure
        hold on
        for k=1:9
            HRcomparisson(k,AEa)
        end
        hold off
    end
end
```

```
    %Table displaying the R squared and RMSE for
       quantification of goodness of
    %fit
    for k=1:17
        [~, ~, ~, name{k,1}] = DataLoad(k);
        [Rsq(k,1), RMSE(k,1)] = GoF(AEa,k);
    end
    Rsqt = mean(Rsq);
    RMSEt = mean(RMSE);
    name{k+1,1} = 'z';
    Rsq(k+1) = Rsqt;
    RMSE(k+1) = RMSEt;
    RMSE = round(RMSE,5);
    FitT = table(name,Rsq,RMSE);
    FitT = sortrows(FitT);
    FitT{end,1} = {'Average fit'};
    A(1) = AEa(1);
    Ea(1) = AEa(2);
     A(2) = AEa(3);
     Ea(2) = AEa(4);
     RateLaw = strcat( {'k1 = '}, num2str(exp(A(1)),3), {'
        exp(-'},num2str(Ea(1),3),'/RT)',{' and k2(T) = '},
        num2str(exp(A(2)),3),{' exp(-'},num2str(Ea(2),3),'/RT
        )');
if SaveExcel == false
    disp(RateLaw{1});
    disp(FitT);
else
    warning('off','MATLAB:xlswrite:AddSheet')
    writetable(FitT,'Kinetics.xlsx','Range','A3','Sheet','
       General');
end
```

D.3 Options

Some options and constants passed to various functions was stored in its own function for ease of passing and globally changing them.

```
function [MWn, Fractions, SolverOptions, A, Ea, DataSets,
   SaveExcel, isolate] = Options
    %Options
    %Solver options to supress output
    SolverOptions = optimoptions('lsqcurvefit','Display','off
       ');
    %Should calculations be done based on mole fractions?
    Fractions = false;
    %Number of datasets
```

```
    DataSets = 13;
    %true exports the data to excel
    SaveExcel = false;
    %isolate first reaction for solo regression
    isolate = false;

    MWurea = 60.05564;%g/mol
    MWphos = 97.995182;%g/mol
    MWADP = 212.036204;%g/mol
    MWCO2 = 44.0098;%g/mol
    MWATP = 309.046666;%g/mol
    MWNH3 = 17.03056;%g/mol

    MWn = [MWurea, MWphos, MWADP, MWCO2, MWATP, MWNH3];

    %initial guess values
    A = [38.965453173849850,58.459919722258260];
    Ea = [1.504226226628036e+02,2.081055215622347e+02];
%      A =
   [38.339037018221330,67.286416303263800,2.722664803493316];
%      Ea = [1.395406599243680e+02,2.415710118585192e
   +02,2.394434711811365e+02];
end
```

D.4 Data load

The raw TGA data couples with integrated FTIR data was stored in a Matlab variable (.mat) file. This function retrieved the raw data from the stored variable and performed various calculations on the data such as to isolate reaction data, perform a complete mole balance and some constants for the experimental run, such as heating rate, sample mass and the name of the experimental run.

```
function [Reaction, ExtraParms, TGAdata, name] = DataLoad(
   TGAn)
%Raw TGA data exported as matlab variables into the file
   TGAdata
load('TGAdata')
%Loading variables
if TGAn == 1 %1K/min R2
    TGA = TGA1;
    name = '1 K per min R2';
elseif TGAn == 2 %1K/min 10mg
    TGA = TGA2;
    name = '1 K per min 10mg';
elseif TGAn== 3 %0.5K/min 8Jun
    TGA = TGA3;
    name = '0.5 K per min R2';
```

```
elseif TGAn == 4 %0.5K/min 7Jun
    TGA = TGA4;
    name = '0.5 K per min R1';
elseif TGAn == 5 %1K/min 7Jun
    TGA = TGA5;
    name = '1 K per min R5';
elseif TGAn == 6 %2K/min 6Jun
    TGA = TGA6;
    name = '2 K per min R1';
elseif TGAn == 7 %5K/min 5Jun
    TGA = TGA7;
    name = '5 K per min R1';
elseif TGAn == 8 %3 K per min 1Aug
    TGA = TGA8;
    name = '3 K per min R1';
elseif TGAn == 9 %4 K per min 1Aug
    TGA = TGA9;
    name = '4 K per min R1';
elseif TGAn == 10 %isothermal 122°C 30 min
    TGA = TGA10;
    name = 'isothermal 122°C R1';
elseif TGAn == 12 %isothermal 122°C 60min
    TGA = TGA11;
    name = 'isothermal 122°C R2';
elseif TGAn == 11
    TGA = TGA12;
    name = 'isothermal 119°C R1';
elseif TGAn == 13
    TGA = TGA13;
    name = 'isothermal 125°C R1';
elseif TGAn == 14
    TGA = TGA14;
    name = 'isothermal 130°C R1';
elseif TGAn == 15
    TGA = TGA15;
    name = 'isothermal 130°C R2';
elseif TGAn == 16
    TGA = TGA16;
    name = '1 K per min R1';
elseif TGAn == 17
    TGA = TGA17;
    name = '1 K per min R4';
end
%seperating variables from the full array
temp = (TGA(1:end,1));
temp = temp + 273.15;
time = (TGA(1:end,2));
DSC = (TGA(1:end,3));
mfrac = (TGA(1:end,7));
```

```
CO2 = (TGA(1:end,6));
m = (TGA(1:end,4));
%NH3 calculated as difference between CO2 and liquid mass
NH3 = CO2 - m;

%export variable of raw TGA data
TGAdata = [temp, time, DSC, m, CO2, NH3];

%sample mass determination
%sample mass is not in the stored data

Mass = -m(end)/(1-mfrac(end));
m = Mass + m;
CO2 = -CO2;

%Search for Reaction Starting point
dDSC = diff(DSC);
f1 = find(dDSC == max(dDSC)); %dDSC/dt is a max just as
   melting finishes
m = m(f1:end); %cutting off all mass data prior to melting
f =  find(m == max(m)); %max mass after melting achieved
m = m(f(end)+1:end); %reaction starts as soon as mass starts
   decreasing
f = f(end)+ f1; %final cut off point for all other data sets

%cutting off non-reaction data on remaining data sets

temp = temp(f:end);
time = time(f:end);
time = time - time(1);
CO2 = CO2(f:end);
NH3 = NH3(f:end);
DSC = DSC(f:end);
CO2 = smooth(CO2);
NH3 = smooth(NH3);

Mass = m(1); %initial mass taken as mass export value to
   compesate for possible mass loss due to water

if min(NH3) >= 0 %shift CO2 graph down if needed
    CO2 = CO2 - min(NH3);
    NH3 = NH3 - min(NH3);
end

%required options and constants called from options function
[MWn, Fractions, ~, ~, ~, ~, ~, isolate] = Options;
MWurea = MWn(:,1);
MWphos = MWn(:,2);
MWADP = MWn(:,3);
```

```
MWCO2 = MWn(:,4);
MWATP = MWn(:,5);
MWNH3 = MWn(:,6);

%Extent of reactions from balanced equation
if max(NH3) <= 0.01 %if non signifficant amount of NH3
   produced assume only first reaction
    E2 = 0.* NH3;
else
    E2 = NH3./MWNH3;
end
E1 = 2*(CO2./MWCO2 - E2);

%equimolar feed, thus np0 = nu0
n0 = Mass/(MWphos + MWurea);
%mole balance
nu = n0 - 0.5*E1 - E2;
np = n0 - E1 - E2;
nADP = 0.5*E1 - E2;
nATP = E2;
nCO2 = 0.5*E1 + E2;
nNH3 = E2;

% cutting off reaction data where chain length > 3
%if mole balance yields negative amounts of ADP, the
   assumption of only ATP
%forming fails
f = find(nADP >= 0);
f = f(end);
if f ~= numel(nADP)
    nu = nu(1:f);
    np = np(1:f);
    nADP = nADP(1:f);
    nATP = nATP(1:f);
    nCO2 = nCO2(1:f);
    nNH3 = nNH3(1:f);
    time = time(1:f);
    temp = temp(1:f);
    m = m(1:f);
    DSC = DSC(1:f);
end
if isolate == true
    f = find(NH3 <= 0.01);
    f = f(end);
    temp = temp(1:f);
    time = time(1:f);
    nu = nu(1:f);
    np = np(1:f);
    nADP = nADP(1:f);
```

```
    nATP = nATP(1:f);
    nCO2 = nCO2(1:f);
    nNH3 = nNH3(1:f);
    m = m(1:f);
    DSC = DSC(1:f);
end
%Calculating mole balance based on molar amounts or mole
   fractions
if Fractions == true
    nliq = nu + np + nADP + nATP;
    xu = nu./nliq;
    xp = np./nliq;
    xADP = nADP./nliq;
    xATP = nATP./nliq;
    xCO2 = nCO2./nliq;
    xNH3 = nNH3./nliq;
    Reaction = [temp, time, xu, xp, xADP, xATP, xCO2, xNH3, m
       , DSC];
else
    Reaction = [temp, time, nu, np, nADP, nATP, nCO2, nNH3, m
       , DSC];
end

%calculation of ode parameters
HReq = polyfit(time,temp,1);%calculation of heating rate
if HReq(1) >= 0.4 %seperation between isothermal and non
   isothermal data
    HR = HReq(1);
    Ti = temp(1);
else
    HR = 0;
    Ti = HReq(2)+2; %offset in isothermal data
end
%extra parameters found from the raw data
ExtraParms = [Mass, Ti, HR, time(1), time(end)];
```

D.5 Integrated

This function returned the integrated set of differential equations as laid out in Chapter 4

```
function [y, x] = integrated(AEa,xdata,HR)

[MWn, Fractions, ~, ~, ~, DataSets] = Options;

A = AEa(1);
Ea = AEa(2);
```

```
if numel(AEa) > 2
    A(2) = AEa(3);
    Ea(2) = AEa(4);
    if numel(AEa) > 4
        A(3) = AEa(5);
        Ea(3) = AEa(6);
        if numel(AEa) > 6
            A(4) = AEa(7);
            Ea(4) = AEa(8);
        end
    end
end
%Arrhenius factor represented as exponential value to keep in
    the same
%range as Activaition energy for improved solver performance
A = exp(A);

MWurea = MWn(:,1);
MWphos = MWn(:,2);

%if xdata has a single data point, this function predicts the
    output,
%otherwise ode paremeters are obtained from experimental data
    .
if numel(xdata) == 1 %output for prediction
    if xdata <=  100
        [time, ExtraParms] = DataLoad(xdata);
        time = time(:,2);
        Mass = ExtraParms(1);
        t0 = ExtraParms(4);
        tf = ExtraParms(5);
    else
        if HR < 1
            Ti = 116 + 273.15;
            tf = ((135 + 273.15)-Ti)/HR;
        else
            Ti = 120 + 273.15;
            tf = ((140 + 273.15)-Ti)/HR;
        end
        Mass = 1;
        t0 = 0;
        ExtraParms = [Mass, Ti, HR];
    end
    dataspan = [t0 tf];
    pi = Mass/(MWphos + MWurea);
    ui = Mass/(MWphos + MWurea);
    ADPi = 0;
    ATPi = 0;
    CO2i = 0;
```

```
    NH3i=0;
    %building of initial values array for ode solver
    if Fractions == true
        mi = Mass;
        StartConditions = [pi, ui, ADPi, ATPi, CO2i, NH3i, mi
           ];
    else
        StartConditions = [pi, ui, ADPi, ATPi, CO2i, NH3i];
    end

    %ode solver
    [t,yi] = ode45(@(t,N)dNdt(t,N,A,Ea,ExtraParms),dataspan,
       StartConditions);
    if Fractions == true
        %converting molar amounts to mol fractions
        liquid = yi(:,1)+yi(:,2)+yi(:,3)+yi(:,4);
        yi(:,1:6) = yi(:,1:6)./liquid;
    end
    yt = yi;
else %output for regression
    yt = [];
    for k=1:DataSets
        [time, ExtraParms] = DataLoad(k);
        %loading of experimental data
        time = time(:,2);
        Mass = ExtraParms(1);
        t0 = ExtraParms(4);
        tf = ExtraParms(5);
        dataspan = [t0 tf];

        %building of initial value array

        pi = Mass/(MWphos + MWurea);
        ui = Mass/(MWphos + MWurea);
        ADPi = 0;
        ATPi = 0;
        CO2i = 0;
        NH3i=0;
        if Fractions == true
            mi = Mass;
            StartConditions = [pi, ui, ADPi, ATPi, CO2i, NH3i
               , mi];
        else
            StartConditions = [pi, ui, ADPi, ATPi, CO2i, NH3i
               ];
        end
        %ode solver
        [t,yi] = ode113(@(t,N)dNdt(t,N,A,Ea,ExtraParms),
           dataspan,StartConditions);
```

```
        if Fractions == true
            %converting molar amounts to mol fractions
            liquid = yi(:,1)+yi(:,2)+yi(:,3)+yi(:,4);
            yi(:,1:6) = yi(:,1:6)./liquid;
        end
        %splining to get the matricies to match, as the ode
           solver does not
        %produce the same output size as the experimental
           data, lsqcurvefit
        %requires function output to be the same size for
           least squares
        %calculation, thus splining for smooth interpolation
           between
        %points.
        ycol1 = spline(t,yi(:,1),time);
        ycol2 = spline(t,yi(:,2),time);
        ycol3 = spline(t,yi(:,3),time);
        ycol4 = spline(t,yi(:,4),time);
        ycol5 = spline(t,yi(:,5),time);
        ycol6 = spline(t,yi(:,6),time);
        %if data is read as fractions, mass is also
           calculated for model
        %fit
        if Fractions == true
            ycol7 = spline(t,yi(:,7),time);
            yi = [ycol1, ycol2, ycol3, ycol4, ycol5, ycol6,
               ycol7];
        else
            yi = [ycol1, ycol2, ycol3, ycol4, ycol5, ycol6];
        end
        yt = [yt ; yi];
    end
end
%export of the final arrays calculated by the ode solvers
y = yt;
x = t;
end
```

D.6 dNdt

The function to be integrated is defined in the function dNdt, listing the set of auxiliary equations and ordinary differential equations as shown in 4.

```
function N = dNdt(t,N,A,Ea,ExtraParms)
Mass = ExtraParms(1);
Ti = ExtraParms(2);
HR = ExtraParms(3);
```

```
[MWn, Fractions, ~, ~, ~, ~, ~, isolate] = Options;
%Initial values passed from parent function
Nu = N(1);
Np = N(2);
NADP = N(3);
NATP = N(4);
NCO2 = N(5);
NNH3 = N(6);
if Fractions == true
    m = N(7);
end
%constants required for conversions
MWu = MWn(:,1);
MWp = MWn(:,2);
MWADP = MWn(:,3);
MWCO2 = MWn(:,4);
MWATP = MWn(:,5);
MWNH3 = MWn(:,6);
R = 8.314; %J/mol K
rho = 1770;%g/cm3
%equations
T = Ti + HR*t;
k1 = A(1)*exp(-Ea(1)*1000/(R*T)); %min-1
if Fractions == false
    m = Nu*MWu + Np*MWp + NADP*MWADP + NATP*MWATP;
end
if numel(A) == 1
    k2 = 0;
    k3 = 0;
    k4 = 0;
elseif numel(A) == 2
    k2 = A(2)*exp(-Ea(2)*1000/(R*T)); %min-1
    k3 = 0;
    k4 = 0;
elseif numel(A) == 3
    k2 = A(2)*exp(-Ea(2)*1000/(R*T)); %min-1
    k3 = A(3)*exp(-Ea(3)*1000/(R*T)); %min-1;
    k4 = 0;
elseif numel(A) == 4
    k2 = A(2)*exp(-Ea(2)*1000/(R*T)); %min-1
    k3 = A(3)*exp(-Ea(3)*1000/(R*T)); %min-1;
    k4 = A(4)*exp(-Ea(4)*1000/(R*T)); %min-1;
end

%initial values
m0 = Mass;
V0 = m0/rho;
V = V0*m/m0;
Cp = Np/V;
```

```
Cu = Nu/V;
CADP = NADP/V;
CATP = NATP/V;
%force 0 values if solver jumps over asimptote
if Cp <= 0
    Cp = 0;
end
if CADP <=0
    CADP = 0;
end
if Cu <= 0
    Cu = 0;
end
%r1 possibilities
r1 = k1*Cu;
%r1 = k1*Cp^2-k2*Cu;
%r1 = k1*Cp^2;

%r2 possibilities
r2 = k2*CADP*Cp;
%r2 = k2*CADP*Cp - k3*Cu;
%r2 = k2*Cu;
if isolate == true
    r2 = 0;
end
%rate equations
rU = -0.5*r1-r2;
rP = -r1-r2;
rADP = 0.5*r1-r2;
rATP = r2;
rCO2 = 0.5*r1+r2;
rNH3 = r2;
%output ODE's
if Fractions == true
    N = [rU*V; rP*V; rADP*V; rATP*V; rCO2*V; rNH3*V; (rU*V*
       MWu + rP*V*MWp + rADP*V*MWADP + rATP*V*MWATP) ];%
       output = [Nu, Np, NADP, NATP, NCO2, NNH3, m];
else
    N = [rU*V; rP*V; rADP*V; rATP*V; rCO2*V; rNH3*V];
end
```

D.7 Quality of Fit

This function quantified the quality of fit of the model on experimental data, based on the R^2 and RMSE values.

```
function [Rsq, RMSE] = GoF(AEa,k)
```

```
%loading of relavent options and constants
[MWn, Fractions] = Options;
[y, t] = integrated(AEa,k);
%y = [xu, xp, xADP, xATP, xCO2, xNH3, m];
[Reaction] = DataLoad(k);
%Reaction = [temp, time, xu, xp, xADP, xATP, xCO2, xNH3, m];
   output format

%R squared calculation
ydata = Reaction(:,9);
if Fractions == true
    yCalc = y(:,7);
else
    MWu = MWn(:,1);
    MWp = MWn(:,2);
    MWADP = MWn(:,3);
    MWCO2 = MWn(:,4);
    MWATP = MWn(:,5);
    MWNH3 = MWn(:,6);
    Nu = y(:,1);
    Np = y(:,2);
    NADP = y(:,3);
    NATP = y(:,4);
    yCalc = Nu*MWu + Np*MWp + NADP*MWADP + NATP*MWATP;
end
yCalc = spline(t,yCalc,Reaction(:,2));

Rsq = 1 - sum((ydata - yCalc).^2)/sum((ydata - mean(ydata))
   .^2);
%root mean squared calculation
RMSE = sqrt(1/numel(ydata)*sum((yCalc-ydata).^2));
```

D.8 Graphing

This function was called to plot the experimental data and model predictions on the same graphs, in order to visually inspect the quality of fit.

```
function graphs(k,AEa,HR)
    %loading of relavent options and constants
    [MWn, Fractions] = Options;
    LegendFontSize = 10;

    if k <= 99 %k< 99 plots modeled data on experimental data
        else only model
        [y, x] = integrated(AEa,k);
        %y = [xu, xp, xADP, xATP, xCO2, xNH3, m]; output
           format
```

```
%loading of experimental data
[Reaction, HR, ~, name] = DataLoad(k);
HR = HR(3);
temp = Reaction(:,1) - 273.15;
time = Reaction(:,2);
tempm = spline(Reaction(:,2),temp,x);
timem = spline(Reaction(:,2),time,x);
Reaction(:,1) = [];
%Reaction = [temp, time, xu, xp, xADP, xATP, xCO2,
   xNH3, m];
%TGAdata = [temp, time, DSC, m, CO2, NH3];
%ExtraParms = [Mass, Ti, HR, time(1), time(end)];
figure('Name',name,'units','normalized','
   outerposition',[0 0 1 1]);

%top graph (mole balance)
subplot(2,1,1)

if HR == 0 %isothermal data has time on ex axis
    plot(timem,y(:,1:6),'-o',time,Reaction(:,2:7),'--
       ');
    xlabel('Time (min)');
    xlim([time(1) time(end)]);
else %non isothermal data shows temperature on x axis
    plot(tempm,y(:,1:6),'-o',temp,Reaction(:,2:7),'--
       ');
    xlabel('Temp (°C)');
    xlim([temp(1) temp(end)]);
end

%labeling based on fractions or olar amounts
if Fractions == true
    ylabel('liquid mole fraction');
else
    ylabel('Mole (mmole)');
end
title('Pyrolysis of urea phosphate model fit')
set(gca,'FontSize',18)
legend({'Urea model','Phosphoric Acid model','ADP
   model','ATP model','CO2 model','NH3 model','Urea
   exp','Phosphoric Acid exp','ADP exp','ATP exp','
   CO2 exp','NH3 exp'},'FontSize',LegendFontSize);
legend('Location','eastoutside')
%bottom graph (overall mass balance)
subplot(2,1,2)
if Fractions == true
    m = y(:,7);
else
```

```
            MWu = MWn(:,1);
            MWp = MWn(:,2);
            MWADP = MWn(:,3);
            MWCO2 = MWn(:,4);
            MWATP = MWn(:,5);
            MWNH3 = MWn(:,6);
            Nu = y(:,1);
            Np = y(:,2);
            NADP = y(:,3);
            NATP = y(:,4);
            m = Nu*MWu + Np*MWp + NADP*MWADP + NATP*MWATP;
        end
        plot(x,m,'-o',Reaction(:,1),Reaction(:,8),'--');
        xlabel('time (min)');
        ylabel('mass (mg)');
        xlim([x(1) x(end)]);
        legend({'mass model','mass exp'},'FontSize',
           LegendFontSize);
        legend('Location','eastoutside')
        set(gca,'FontSize',18)
    else %only modeled data
        [y, x] = integrated(AEa,k,HR);
        %y = [xu, xp, xADP, xATP, xCO2, xNH3, m];
        temp = (120) + x*HR;
        figure('Name',strcat(num2str(HR),'K/min prediction'),
           'units','normalized','outerposition',[0 0 1 1]);

        %top graph (mole balance)
        subplot(2,1,1)

        plot(temp,y(:,1:6),'-o');

        xlabel('Temp (°C)');
        xlim([temp(1) temp(end)]);
        if Fractions == true
            ylabel('liquid mole fraction');
        else
            ylabel('Mole (mmole)');
        end
        set(gca,'FontSize',18)
        legend({'Urea','Phosphoric Acid','ADP','ATP','CO2','
           NH3'},'FontSize',LegendFontSize);
        legend('Location','eastoutside')
        %bottom graph (mass balance)
        subplot(2,1,2)
        if Fractions == true
            m = y(:,7);
        else
            MWu = MWn(:,1);
```

```
            MWp = MWn(:,2);
            MWADP = MWn(:,3);
            MWCO2 = MWn(:,4);
            MWATP = MWn(:,5);
            MWNH3 = MWn(:,6);
            Nu = y(:,1);
            Np = y(:,2);
            NADP = y(:,3);
            NATP = y(:,4);
            m = Nu*MWu + Np*MWp + NADP*MWADP + NATP*MWATP;
        end
        plot(x,m,'-o');
        xlabel('time (min)');
        ylabel('mass (mg)');
        xlim([x(1) x(end)]);

        title('Pyrolysis of urea phosphate model')
        set(gca,'FontSize',18)
        legend({'mass model'},'FontSize',LegendFontSize);
        legend('Location','eastoutside')
    end
end
```

D.9 Graph export

This function exported the raw TGA data, calculated mole balance and predicted model data in vector format, for the purpose of creating the graphs shown in Appendix E.

```
load('FittedParms.mat');
warning('off','all');
[MWn, Fractions] = Options;

MWu = MWn(:,1);
MWp = MWn(:,2);
MWADP = MWn(:,3);
MWCO2 = MWn(:,4);
MWATP = MWn(:,5);
MWNH3 = MWn(:,6);

widthsquish = 75;
for k=1:17
[Reaction,Parms,TGA,Name] = DataLoad(k);
mass = Parms(1);
HR = Parms(3);
%TGAdata = [temp, time, DSC, m, CO2, NH3];
Name = Name(find(~isspace(Name)));
Name(Name=='.') = [];
```

```
Name(Name=='°') = [];
Name = strrep(Name,'Kpermin','kpm_');
%%%%%%%%%%%%%%%%%%%%%%
% TGA plot
%%%%%%%%%%%%%%%%%%%%%%
time = TGA(:,2);
temp = TGA(:,1)-273.15;
temp(temp>140) = 140;
m = TGA(:,4);
DSC = TGA(:,3);
CO2 = TGA(:,5);

CO2 = CO2./mass;
m = m./mass;
if HR == 0
    plot(time,m,time,CO2);
    xlabel('Time (min)')
else
    if k <= 15
        plot(temp,m,temp,CO2);
    else
        plot(temp,m);
    end
    xlabel('Temperature')
end

%set(gcf,'OuterPosition', get(gcf,'OuterPosition') + [0 0 0 -
   widthsquish])
set(gcf,'units','centimeters','OuterPosition', [0 0 16 10]);
ylabel('Mass loss dmm0')

A = ylim;
if ~isempty(strfind(Name,'kpm'))
    axislimits = xlim;
    axislimits(1) = 0.5*(axislimits(2) - axislimits(1))+
       axislimits(1);
    xlim(axislimits)
    Anew = ylim;
    if Anew(2) ~= A(2)
        ylim(A);
    end
end
%move x axis to origin on graph
set(gca,'XAxisLocation','origin')
%values for y axis alignment
minA = -A(1);
maxA = A(2);
%plot DSC on seperate y axis
yyaxis right
```

```
set(gca,'YColor','black') %black axis color
if HR == 0
    plot(time,DSC)
else
    plot(temp,DSC)
end
%y axis alignment with origin
B = ylim;
minB = -B(1);
maxB = B(2);
x = minA*maxB/(minB*(maxA+minA)-minA*minB);
ylim([x*-minB maxB]);

ylabel('DSC (\muV)')

%legend
legendentries = {'total massspace';'CO2space';'DSC'};
legend(legendentries,'Location','southoutside','Orientation',
   'horizontal')
legend('boxoff')

%Display grid lines, as grey (not transparent)
grid on
set(gca, 'GridAlpha', 1)
set(gca, 'GridColor', [0.8 0.8 0.8])

%export as vector pdf
print(strcat(Name,'_TGA'),'-dpdf')
movefile(strcat(Name,'_TGA','.pdf'), 'graphs')
close

%%%%%%%%%%%%%%%%%%%%%%
% DSC plot
%%%%%%%%%%%%%%%%%%%%%%
time = TGA(:,2);
temp = TGA(:,1)-273.15;
temp(temp>140) = 140;
m = TGA(:,4);
DSC = TGA(:,3);
CO2 = TGA(:,5);

CO2 = CO2./mass;
m = m./mass;
if HR == 0
    plot(time,m,time,CO2);
    xlabel('Time (min)')
else
    if k <= 15
        plot(temp,m,temp,CO2);
```

```
    else
        plot(temp,m);
    end
    xlabel('Temperature')
end

%set(gcf,'OuterPosition', get(gcf,'OuterPosition') + [0 0 0 -
   widthsquish])
set(gcf,'units','centimeters','OuterPosition', [0 0 16 10]);
ylabel('Mass loss dmm0')

A = ylim;
A(2) = 0;
if ~isempty(strfind(Name,'kpm'))
    axislimits = xlim;
    axislimits(1) = 0.5*(axislimits(2) - axislimits(1))+
       axislimits(1);
    xlim(axislimits)
    Anew = ylim;
    if Anew(2) ~= A(2)
        ylim(A);
    end
end
%move x axis to origin on graph
set(gca,'XAxisLocation','origin')
%values for y axis alignment
minA = -A(1);
maxA = A(2);

%legend
legendentries = {'total massspace';'CO2space'};
legend(legendentries,'Location','southoutside','Orientation',
   'horizontal')
legend('boxoff')

%Display grid lines, as grey (not transparent)
grid on
set(gca, 'GridAlpha', 1)
set(gca, 'GridColor', [0.8 0.8 0.8])

%export as vector pdf
print(strcat(Name,'_DSC'),'-dpdf')
movefile(strcat(Name,'_DSC','.pdf'), 'graphs')
close

%%%%%%%%%%%%%%%%%%%%%%
% Gas Balance plots
%%%%%%%%%%%%%%%%%%%%%%
[y, x] = integrated(AEa,k);
```

```
temp = Reaction(:,1) - 273.15;
time = Reaction(:,2);
CO2 = Reaction(:,7) * MWCO2;
tempm = spline(Reaction(:,2),temp,x);
temp = spline(time,temp,x);
CO2 = spline(time,CO2,x);
time = x;
if HR == 0 %isothermal data has time on x axis
    plot(time,CO2,'x')
    hold on
    plot(x,y(:,5)*MWCO2,'-');
    xlabel('Time (min)');
    xlim([time(1) time(end)]);
else %non isothermal data shows temperature on x axis
    plot(temp,CO2,'x');
    hold on
    plot(tempm,y(:,5)*MWCO2,'-');
    xlabel('Temperature');
    xlim([120 140]);
end
A = ylim;
A(1) = 0;
ylim(A)
if Fractions == true
    ylabel('liquid mole fraction');
else
    ylabel('Mass CO2 (mg)');
end
%legend
legendentries = {'CO2 modeledspace','CO2 raw'};
legend(legendentries,'Location','southoutside','Orientation',
   'horizontal')
legend('boxoff')

%Display grid lines, as grey (not transparent)
grid on
set(gca, 'GridAlpha', 1)
set(gca, 'GridColor', [0.8 0.8 0.8])
%set(gcf,'OuterPosition', get(gcf,'OuterPosition') + [0 0 0 -
   widthsquish])
set(gcf,'units','centimeters','OuterPosition', [0 0 16 11]);
%set(gca,'OuterPosition', get(gca,'OuterPosition') + [0 0.05
   0 0])
%export as vector pdf
print(strcat(Name,'_GB'),'-dpdf')
movefile(strcat(Name,'_GB','.pdf'), 'graphs')
close
```

```
%%%%%%%%%%%%%%%%%%%%%%
% Mass correllation
%%%%%%%%%%%%%%%%%%%%%%
Reaction(:,1) = [];
if Fractions == true
    m = y(:,7);
else
    Nu = y(:,1);
    Np = y(:,2);
    NADP = y(:,3);
    NATP = y(:,4);
    m = Nu*MWu + Np*MWp + NADP*MWADP + NATP*MWATP;
end
mexp = -(Reaction(:,8) - m(1))/m(1);
mexp = spline(Reaction(:,1),mexp,x);
m = -(m - m(1))/m(1);
err = 0.085*mexp;
errorbar(x,mexp,err,'x');
hold on
plot(x,m,'-')
xlabel('Time (min)');
ylabel('Normalised Mass loss mm0');
set(gca, 'Ydir', 'reverse')
xlim([x(1) x(end)]);
legendentries = {'mass experimentalspace','mass model'};
legend(legendentries,'Location','southoutside','Orientation',
   'horizontal')
legend('boxoff')
%Display grid lines, as grey (not transparent)
grid on
set(gca, 'GridAlpha', 1)
set(gca, 'GridColor', [0.8 0.8 0.8])
%set(gcf,'OuterPosition', get(gcf,'OuterPosition') + [0 0 0 -
   widthsquish])
set(gcf,'units','centimeters','OuterPosition', [0 0 16 11]);
%export as vector pdf
print(strcat(Name,'_Mass'),'-dpdf')
movefile(strcat(Name,'_Mass','.pdf'), 'graphs')
close
end

%%%%%%%%%%%%%%%%%%%%%%%%%%%%%%%%
%       Experimental data T      %
%%%%%%%%%%%%%%%%%%%%%%%%%%%%%%%%
figure
legendentries = {};
legendindex = 1;
SeqNumber = 1;
while SeqNumber < 7
```

```
    Sequence = {'0.5 Kpm', '1 Kpm', '2 Kpm', '3 Kpm', '4 Kpm'
       , '5 Kpm', 'end'};
    for k=1:17
        hold on
        [Reaction,Mass,TGA,Name] = DataLoad(k);
        Mass = Mass(1);
        %Reaction = [temp, time, nu, np, nADP, nATP, nCO2,
           nNH3, m, DSC];
        nonisothermalmarker = strfind(Name,'K per min');
        Name = strrep(Name,'10mg','R3');
        Name = strrep(Name,'K per min','Kpm');
        Rnr = strfind(Name,'R')-2;
        Name = Name(1:Rnr);
        if strcmp(Name, Sequence{SeqNumber}) == 1
            SeqNumber = SeqNumber + 1 ;
            if ~isempty(nonisothermalmarker)
                if ~any(strcmp(legendentries,Name))
                    x = Reaction(:,1) -273.15; %convert from
                       K to °C
                    y = Reaction(:,9)./ Mass; %convert to
                       normalised mass
                    plot(x,y);
                    legendentries{legendindex} = strcat(Name,
                       'space');
                    legendindex = legendindex + 1;
                end
            end
        end
    end
end
ylabel('Normalised mass mm0')
xlabel('Temperature')
ylim([0.8 1])
xlim([120 140]);
legend(legendentries,'Location','southoutside','Orientation',
   'horizontal')
legend('boxoff')

%Display grid lines, as grey (not transparent)
grid on
set(gca, 'GridAlpha', 1)
set(gca, 'GridColor', [0.8 0.8 0.8])
%set(gcf,'OuterPosition', get(gcf,'OuterPosition') + [0 0 120
    -50])
set(gcf,'units','centimeters','OuterPosition', [0 0 16 11]);
%export as vector pdf
print('Experimental','-dpdf','-bestfit')
movefile(strcat('Experimental','.pdf'), 'graphs')
close
```

```
%%%%%%%%%%%%%%%%%%%%%%%%%%%%%%%%%%
%     Experimental data time      %
%%%%%%%%%%%%%%%%%%%%%%%%%%%%%%%%%%
figure
legendentries = {};
legendindex = 1;
SeqNumber = 1;
while SeqNumber < 7
    Sequence = {'0.5 Kpm', '1 Kpm', '2 Kpm', '3 Kpm', '4 Kpm'
       , '5 Kpm', 'end'};
    for k=1:17
        hold on
        [Reaction,Mass,TGA,Name] = DataLoad(k);
        Mass = Mass(1);
        %Reaction = [temp, time, nu, np, nADP, nATP, nCO2,
           nNH3, m, DSC];
        nonisothermalmarker = strfind(Name,'K per min');
        Name = strrep(Name,'10mg','R3');
        Name = strrep(Name,'K per min','Kpm');
        Rnr = strfind(Name,'R')-2;
        Name = Name(1:Rnr);
        if strcmp(Name, Sequence{SeqNumber}) == 1
            SeqNumber = SeqNumber + 1 ;
            if ~isempty(nonisothermalmarker)
                if ~any(strcmp(legendentries,Name))
                    x = Reaction(:,2); %convert from K to °C
                    y = Reaction(:,9)./ Mass; %convert to
                       normalised mass
                    plot(x,y);
                    legendentries{legendindex} = strcat(Name,
                       'space');
                    legendindex = legendindex + 1;
                end
            end
        end
    end
end
ylabel('Normalised mass mm0')
xlabel('Time (min)')
ylim([0.8 1])
xlim([0 45]);
legend(legendentries,'Location','southoutside','Orientation',
   'horizontal')
legend('boxoff')

%Display grid lines, as grey (not transparent)
grid on
set(gca, 'GridAlpha', 1)
```

```
set(gca, 'GridColor', [0.8 0.8 0.8])
%set(gcf,'OuterPosition', get(gcf,'OuterPosition') + [0 0 120
    -50])
set(gcf,'units','centimeters','OuterPosition', [0 0 16 11]);
%export as vector pdf
print('Experimentaltime','-dpdf','-bestfit')
movefile(strcat('Experimentaltime','.pdf'), 'graphs')
close

%%%%%%%%%%%%%%%%%%%%%%%%%%%%%%%%%%%%%%%%%%%%%%%%%%%%%%%%
%     isothermal Experimental data time     %
%%%%%%%%%%%%%%%%%%%%%%%%%%%%%%%%%%%%%%%%%%%%%%%%%%%%%%%%
figure
legendentries = {};
legendindex = 1;
SeqNumber = 1;
while SeqNumber < 5
    Sequence = {'119C', '122C', '125C', '130C','end'};
    for k=1:17
        hold on
        [Reaction,Mass,TGA,Name] = DataLoad(k);
        Mass = Mass(1);
        %Reaction = [temp, time, nu, np, nADP, nATP, nCO2,
           nNH3, m, DSC];
        isothermalmarker = strfind(Name,'isothermal');
        Name = strrep(Name,'isothermal ','');
        Name = strrep(Name,'°','');
        Rnr = strfind(Name,'R')-2;
        Name = Name(1:Rnr);
        if strcmp(Name, Sequence{SeqNumber}) == 1
            SeqNumber = SeqNumber + 1 ;
            if ~isempty(isothermalmarker)
                if ~any(strcmp(legendentries,Name))
                    x = Reaction(:,2);
                    y = Reaction(:,9)./ Mass; %convert to
                       normalised mass
                    plot(x,y);
                    legendentries{legendindex} = strcat(Name,
                       'space');;
                    legendindex = legendindex + 1;
                end
            end
        end
    end
end
ylabel('Normalised mass mm0')
xlabel('Time (min)')
ylim([0.7 1])
xlim([0 60]);
```

```
legend(legendentries,'Location','southoutside','Orientation',
    'horizontal')
legend('boxoff')

%Display grid lines, as grey (not transparent)
grid on
set(gca, 'GridAlpha', 1)
set(gca, 'GridColor', [0.8 0.8 0.8])
%set(gcf,'OuterPosition', get(gcf,'OuterPosition') + [0 0 120
    -50])
set(gcf,'units','centimeters','OuterPosition', [0 0 16 11]);
%export as vector pdf
print('Experimentalisothermal','-dpdf','-bestfit')
movefile(strcat('Experimentalisothermal','.pdf'), 'graphs')
close

%%%%%%%%%%%%%%%%%%%%%%%%%%%%%%%%%%%%
%    Experimental & model fit    %
%%%%%%%%%%%%%%%%%%%%%%%%%%%%%%%%%%%%
figure
legendentries = {};
legendindex = 1;
SeqNumber = 1;
while SeqNumber < 7
    Sequence = {'0.5 Kpm', '1 Kpm', '2 Kpm', '3 Kpm', '4 Kpm'
        , '5 Kpm', 'end'};
    for k=1:17
        hold on
        [Reaction,Mass,TGA,Name] = DataLoad(k);
        Mass = Mass(1);
        %Reaction = [temp, time, nu, np, nADP, nATP, nCO2,
            nNH3, m, DSC];
        nonisothermalmarker = strfind(Name,'K per min');
        Name = strrep(Name,'10mg','R3');
        Name = strrep(Name,'K per min','Kpm');
        Rnr = strfind(Name,'R')-2;
        Name = Name(1:Rnr);
        if strcmp(Name, Sequence{SeqNumber}) == 1
            SeqNumber = SeqNumber + 1 ;
            if ~isempty(nonisothermalmarker)
                if ~any(strcmp(legendentries,Name))
                    x = Reaction(:,1) -273.15; %convert from
                        K to °C
                    y = Reaction(:,9)./ Mass; %convert to
                        normalised mass
                    plot(x,y);
                    legendentries{legendindex} = strcat(Name,
                        'space');
                    legendindex = legendindex + 1;
```

```
                end
            end
        end
    end
end
for HR = 0:5
    if HR == 0
        [y,x] = integrated(AEa,101,0.5);%model prediction for
            mass loss
    else
        [y,x] = integrated(AEa,101,HR);%model prediction for
           mass loss
    end
    if HR == 0
        x = 116 + 0.5 * x;
    else
        x = 120 + HR * x;
    end
    if Fractions == true
        y = y(:,7);
    else
        MWu = MWn(:,1);
        MWp = MWn(:,2);
        MWADP = MWn(:,3);
        MWCO2 = MWn(:,4);
        MWATP = MWn(:,5);
        MWNH3 = MWn(:,6);
        Nu = y(:,1);
        Np = y(:,2);
        NADP = y(:,3);
        NATP = y(:,4);
        y = Nu*MWu + Np*MWp + NADP*MWADP + NATP*MWATP;
    end
    err = 0.085*(y-y(1)); %normalised error
    errorbar(x,y,err,'x','color','black');
end
Name = 'Model';
legendentries{legendindex} = Name;
ylabel('Normalised mass mm0')
xlabel('Temperature')
ylim([0.8 1])
xlim([120 140]);
legend(legendentries,'Location','eastoutside','Orientation','
   vertical')
legend('boxoff')

%Display grid lines, as grey (not transparent)
grid on
set(gca, 'GridAlpha', 1)
```

```
set(gca, 'GridColor', [0.8 0.8 0.8])
%set(gcf,'OuterPosition', get(gcf,'OuterPosition') + [0 0 120
    -50])
set(gcf,'units','centimeters','OuterPosition', [0 0 16 11]);
%export as vector pdf
print('Modelfit','-dpdf','-bestfit')
movefile(strcat('Modelfit','.pdf'), 'graphs')
close

%%%%%%%%%%%%%%%%%%%%%%%%%%%%%%%%%%
%  Experimental & model fit CO2  %
%%%%%%%%%%%%%%%%%%%%%%%%%%%%%%%%%%
figure
legendentries = {};
legendindex = 1;
SeqNumber = 1;
while SeqNumber < 7
    Sequence = {'0.5 Kpm', '1 Kpm', '2 Kpm', '3 Kpm', '4 Kpm'
       , '5 Kpm', 'end'};
    for k=1:17
        hold on
        [Reaction,Mass,TGA,Name] = DataLoad(k);
        Mass = Mass(1);
        %Reaction = [temp, time, nu, np, nADP, nATP, nCO2,
           nNH3, m, DSC];
        nonisothermalmarker = strfind(Name,'K per min');
        Name = strrep(Name,'10mg','R3');
        Name = strrep(Name,'K per min','Kpm');
        Rnr = strfind(Name,'R')-2;
        Name = Name(1:Rnr);
        if strcmp(Name, Sequence{SeqNumber}) == 1
            SeqNumber = SeqNumber + 1 ;
            if ~isempty(nonisothermalmarker)
                if ~any(strcmp(legendentries,Name))
                    x = Reaction(:,1) -273.15; %convert from
                       K to °C
                    y = -Reaction(:,7)*MWCO2./ Mass + 1; %
                       convert to normalised mass
                    y = 1- y;
                    plot(x,y);
                    legendentries{legendindex} = strcat(Name,
                       'space');
                    legendindex = legendindex + 1;
                end
            end
        end
    end
end
for HR = 0:5
```

```
    if HR == 0
        [y,x] = integrated(AEa,101,0.5);%model prediction for
            mass loss
    else
        [y,x] = integrated(AEa,101,HR);%model prediction for
           mass loss
    end
    if HR == 0
        x = 116 + 0.5 * x;
    else
        x = 120 + HR * x;
    end
    if Fractions == true
        y = y(:,7);
    else
        MWCO2 = MWn(:,4);
        NCO2 = y(:,5);
        y = -NCO2*MWCO2 + 1;
    end
    err = 0.085*(y-y(1)); %normalised error
    y = 1-y;
    errorbar(x,y,err,'x','color','black');
end
Name = 'Model';
legendentries{legendindex} = Name;
ylabel('Normalised mass dmm0')
xlabel('Temperature')
ylim([0 0.2])
xlim([120 140]);
legend(legendentries,'Location','eastoutside','Orientation','
   vertical')
legend('boxoff')

%Display grid lines, as grey (not transparent)
grid on
set(gca, 'GridAlpha', 1)
set(gca, 'GridColor', [0.8 0.8 0.8])
%set(gcf,'OuterPosition', get(gcf,'OuterPosition') + [0 0 120
    -50])
set(gcf,'units','centimeters','OuterPosition', [0 0 16 11]);
%export as vector pdf
print('ModelfitCarbon','-dpdf','-bestfit')
movefile(strcat('ModelfitCarbon','.pdf'), 'graphs')
close

%%%%%%%%%%%%%%%%%%%%%%%%%%%%%%%%%%%%%%%%%%%%%%%%%%%%
%     isothermal Experimental data time     %
%%%%%%%%%%%%%%%%%%%%%%%%%%%%%%%%%%%%%%%%%%%%%%%%%%%%
figure
```

```
legendentries = {};
legendindex = 1;
SeqNumber = 1;
while SeqNumber < 5
    Sequence = {'119C', '122C', '125C', '130C','end'};
    for k=1:17
        hold on
        [Reaction,Mass,TGA,Name] = DataLoad(k);
        Mass = Mass(1);
        %Reaction = [temp, time, nu, np, nADP, nATP, nCO2,
           nNH3, m, DSC];
        isothermalmarker = strfind(Name,'isothermal');
        Name = strrep(Name,'isothermal ','');
        Name = strrep(Name,'°','');
        Rnr = strfind(Name,'R')-2;
        Name = Name(1:Rnr);
        if strcmp(Name, Sequence{SeqNumber}) == 1
            SeqNumber = SeqNumber + 1 ;
            if ~isempty(isothermalmarker)
                if ~any(strcmp(legendentries,Name))
                    x = Reaction(:,2);
                    y = Reaction(:,9)./ Mass; %convert to
                       normalised mass
                    plot(x,y);
                    legendentries{legendindex} = strcat(Name,
                       'space');
                    legendindex = legendindex + 1;
                end
            end
        end
    end
end
for k=1:4
    switch k
        case 1
            T = 119;
            TGAn = 11;
        case 2
            T = 122;
            TGAn = 12;
        case 3
            T = 125;
            TGAn =  13;
        case 4
            T = 130;
            TGAn = 14;
    end
    [~,Mass] = DataLoad(TGAn);
    Mass = Mass(1);
```

```
    [y,x] = integrated(AEa,TGAn);%model prediction for mass
       loss
    if Fractions == true
        y = y(:,7);
    else
        MWu = MWn(:,1);
        MWp = MWn(:,2);
        MWADP = MWn(:,3);
        MWCO2 = MWn(:,4);
        MWATP = MWn(:,5);
        MWNH3 = MWn(:,6);
        Nu = y(:,1);
        Np = y(:,2);
        NADP = y(:,3);
        NATP = y(:,4);
        y = Nu*MWu + Np*MWp + NADP*MWADP + NATP*MWATP;
        y = y./Mass;
    end
    f = find(y <= 0.8);
    if ~isempty(f)
        f = f(1);
        y = y(1:f);
        x = x(1:f);
    end
    err = 0.085*(y-y(1)); %normalised error
    errorbar(x,y,err,'x','color','black');
end
legendentries{legendindex} = 'Model';
ylabel('Normalised mass mm0')
xlabel('Time (min)')
ylim([0.8 1])
xlim([0 60]);

legend(legendentries,'Location','southoutside','Orientation',
   'horizontal')
legend('boxoff')

%Display grid lines, as grey (not transparent)
grid on
set(gca, 'GridAlpha', 1)
set(gca, 'GridColor', [0.8 0.8 0.8])
%set(gcf,'OuterPosition', get(gcf,'OuterPosition') + [0 0 120
    -50])
set(gcf,'units','centimeters','OuterPosition', [0 0 16 11]);
%export as vector pdf
print('Modelfitisothermal','-dpdf','-bestfit')
movefile(strcat('Modelfitisothermal','.pdf'), 'graphs')
close
```

```
%%%%%%%%%%%%%%%%%%%%%%%%%%%%%%%%%%
% repeats and experimental error %
%%%%%%%%%%%%%%%%%%%%%%%%%%%%%%%%%%
figure
legendentries = {};
legendindex = 1;
repcounter = 1;
datapoints = 35;
yaverage = zeros(datapoints,1);
xaverage = transpose(120:(140-120)/(datapoints -1):140);
while repcounter < 6
    for k =1:17
        hold on
        [Reaction,Mass,TGA,Name] = DataLoad(k);
        Mass = Mass(1);
        %Reaction = [temp, time, nu, np, nADP, nATP, nCO2,
           nNH3, m, DSC];
        Repeat = strfind(Name,'1 K per min');
        Name = strrep(Name,'10mg','R3');
        Name = strrep(Name,'1 K per min','');
        repeatnr = strfind(Name,'R') + 1;
        if ~isempty(Repeat)
            if Name(repeatnr) == string(repcounter)
                repcounter = repcounter + 1;
                x = Reaction(:,1) -273.15; %convert from K to
                    °C
                y = Reaction(:,9)./ Mass; %convert to
                   normalised mass
                plot(x,y);
                legendentries{legendindex} = strcat(Name,'
                   space');
                legendindex = legendindex + 1;
                k = 17;
                yaverage = yaverage + y(1:numel(y)/(
                   datapoints):end);
            end
        end
    end
end
yaverage = yaverage ./ 5;
err = 0.085*(yaverage-yaverage(1)); %normalised error
errorbar(xaverage,yaverage,err,'x','color','black');
ylabel('Normalised mass mm0')
xlabel('Temperature')
ylim([0.8 1])
xlim([120 140]);
legendentries{legendindex} = 'average';
legend(legendentries,'Location','southoutside','Orientation',
   'horizontal')
```

```
legend('boxoff')

%Display grid lines, as grey (not transparent)
grid on
set(gca, 'GridAlpha', 1)
set(gca, 'GridColor', [0.8 0.8 0.8])
%set(gcf,'OuterPosition', get(gcf,'OuterPosition') + [0 0 120
    -50])
set(gcf,'units','centimeters','OuterPosition', [0 0 16 11]);
%export as vector pdf
print('Repeatability','-dpdf','-bestfit')
movefile(strcat('Repeatability','.pdf'), 'graphs')
close

%%%%%%%%%%%%%%%%%%%%%%%%%%%%%%%%%%%%
%     Rate equations compare     %
%%%%%%%%%%%%%%%%%%%%%%%%%%%%%%%%%%%%
figure
legendentries = {};
legendindex = 1;
repcounter = 1;
[DSC] = DataLoad(1);
temp = DSC(:,1);
temp = temp -273.15;
DSC = DSC(:,10);
HR = 1;
[y,x] = integrated(AEa,101,HR);%model prediction for mass
   loss
x = 120 + x;
T = x + 273.15;
MWu = MWn(:,1);
MWp = MWn(:,2);
MWADP = MWn(:,3);
MWCO2 = MWn(:,4);
MWATP = MWn(:,5);
MWNH3 = MWn(:,6);
Nu = y(:,1);
Np = y(:,2);
NADP = y(:,3);
NATP = y(:,4);
m = Nu*MWu + Np*MWp + NADP*MWADP + NATP*MWATP;
A = AEa(1);
Ea = AEa(2);
if numel(AEa) > 2
    A(2) = AEa(3);
    Ea(2) = AEa(4);
    if numel(AEa) > 4
        A(3) = AEa(5);
        Ea(3) = AEa(6);
```

```
        if numel(AEa) > 6
            A(4) = AEa(7);
            Ea(4) = AEa(8);
        end
    end
end
R = 8.314; %J/mol K
rho = 1770;%g/cm3
m0 = 1;
V0 = m0/rho;
V = V0*m/m0;
Cp = Np./V;
Cu = Nu./V;
CADP = NADP./V;
A = exp(A);
k1 = A(1)*exp(-Ea(1)*1000./(R*T)); %min-1
k2 = A(2)*exp(-Ea(2)*1000./(R*T)); %min-1
r1 = k1.*Cu;
r2 = k2.*CADP.*Cp;
plot(x,r1,x,r2);
ylabel('Rate mol/L min')
xlabel('Temperature')
xlim([120 140]);
%plot DSC on seperate y axis
A = ylim;
minA = -A(1);
maxA = A(2);
ylim([-maxA maxA])
yyaxis right
set(gca,'YColor','black') %black axis color
plot(temp,DSC)
%y axis alignment with origin
B = ylim;
minB = -B(1);
maxB = B(2);
ylim([-maxB maxB]);

ylabel('DSC (\muV)')

legendentries = {'reaction 1space', 'reaction 2space', 'DSC'
   };
legend(legendentries,'Location','southoutside','Orientation',
   'horizontal')
legend('boxoff')

%Display grid lines, as grey (not transparent)
grid on
set(gca, 'GridAlpha', 1)
set(gca, 'GridColor', [0.8 0.8 0.8])
```

```
%set(gcf,'OuterPosition', get(gcf,'OuterPosition') + [0 0 120
    -50])
set(gcf,'units','centimeters','OuterPosition', [0 0 16 11]);
%export as vector pdf
print('Ratecomp','-dpdf','-bestfit')
movefile(strcat('Ratecomp','.pdf'), 'graphs')
close

%Convert pdf with inkscape
cd graphs
system('ConvertToEps.bat');
cd ..
```

Inkscape was used to convert the generated pdf files into eps file format for LaTeXintegration, this was done via a .bat file executed from within matlab in the code above.

```
@Echo off
del /s *-eps-converted-to.*
set "inkscapePath=C:\Program Files\Inkscape\inkscape.exe"
set /a count=0

echo This script allows you to convert all files in this
   folder from one file type to another.

set sourceType=pdf
set outputType=eps
set dpi=96

:: Running through all files found with the defined ending
for %%i in (.\*.%sourceType%) do (
    set /a count=count+1
    echo %%i to %%~ni.%outputType%
    "%inkscapePath%" --without-gui --file="%%i" --export-%
       outputType%="%%~ni.%outputType%" --export-area-
       drawing --export-dpi=%dpi% --export-latex
    powershell -Command "(gc %%~ni.%outputType%_tex) -
       replace 'unitlength]{', 'unitlength]{graphs/' | Out-
       File %%~ni.%outputType%_tex -encoding UTF8"
    powershell -Command "(gc %%~ni.%outputType%_tex) -
       replace 'Temperature', 'Temp ($^\circ C$)' | Out-
       File %%~ni.%outputType%_tex -encoding UTF8"
powershell -Command "(gc %%~ni.%outputType%_tex) -replace '
   dmm0', '$\frac {\Delta m}{m_0}$' | Out-File %%~ni.%
   outputType%_tex -encoding UTF8"
    powershell -Command "(gc %%~ni.%outputType%_tex) -
       replace 'mm0', '$\frac {m}{m_0}$' | Out-File %%~ni.%
       outputType%_tex -encoding UTF8"
    powershell -Command "(gc %%~ni.%outputType%_tex) -
       replace 'space', '' | Out-File %%~ni.%outputType%
       _tex -encoding UTF8"
```

```
        powershell -Command "(gc %%~ni.%outputType%_tex) -
           replace 'CO2', '$CO_2$' | Out-File %%~ni.%outputType
           %_tex -encoding UTF8"
    )

    echo %count% file(s) converted from %sourceType% to %
       outputType%!
```

Appendix E: Experimental data

The raw data, with model predicted values are shown below, for all experiments conducted on the TGA.

E.1 TGA Data

The raw TGA output combined with the integrated FTIR data (when applicable), as an FTIR analysis was not run on every experiment.

5 repeats were performed on a heating rate of 1 K/min, Although FTIR data is only available for 3 of the 5 runs. 1 of the runs was performed with a sample mass of 10 mg, to ensure that the mass did not affect the results obtained.

E.1.1 0.5 K/min

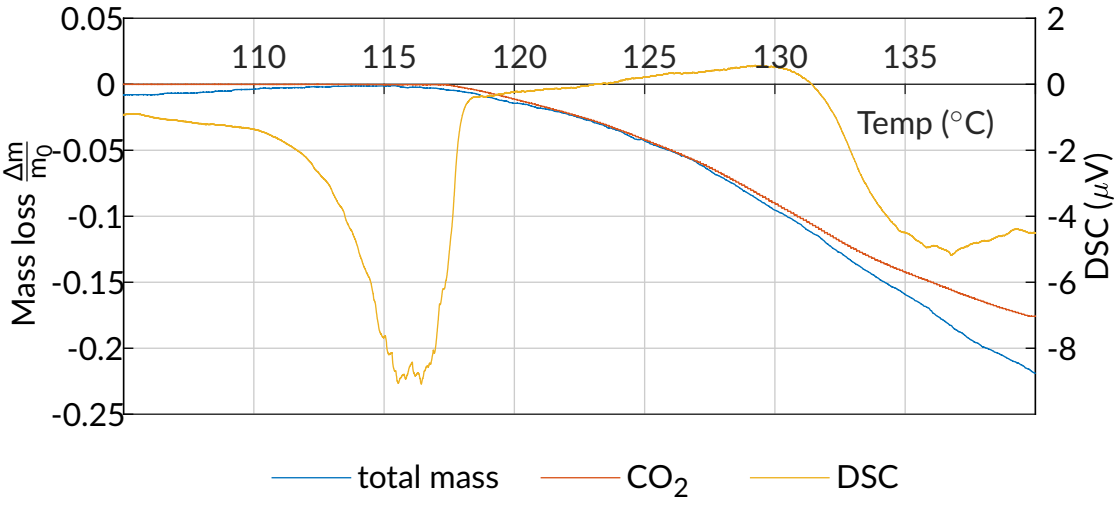

Figure E.1: Mass loss and thermal effects of the pyrolysis of urea phosphate at a constant heating rate of 0.5 K/min run # 1

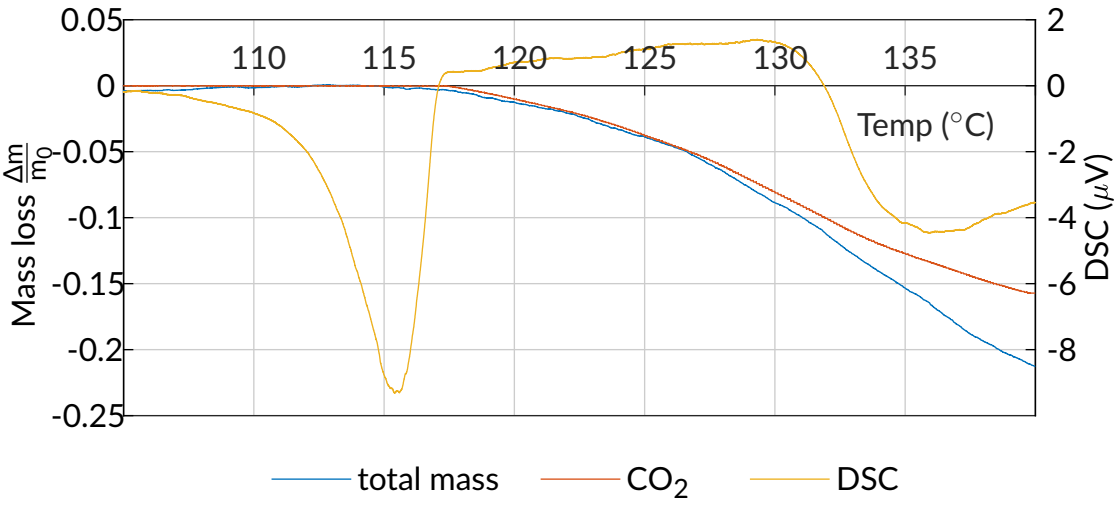

Figure E.2: Mass loss and thermal effects of the pyrolysis of urea phosphate at a constant heating rate of 0.5 K/min run # 2

E.1.2 1 K/min

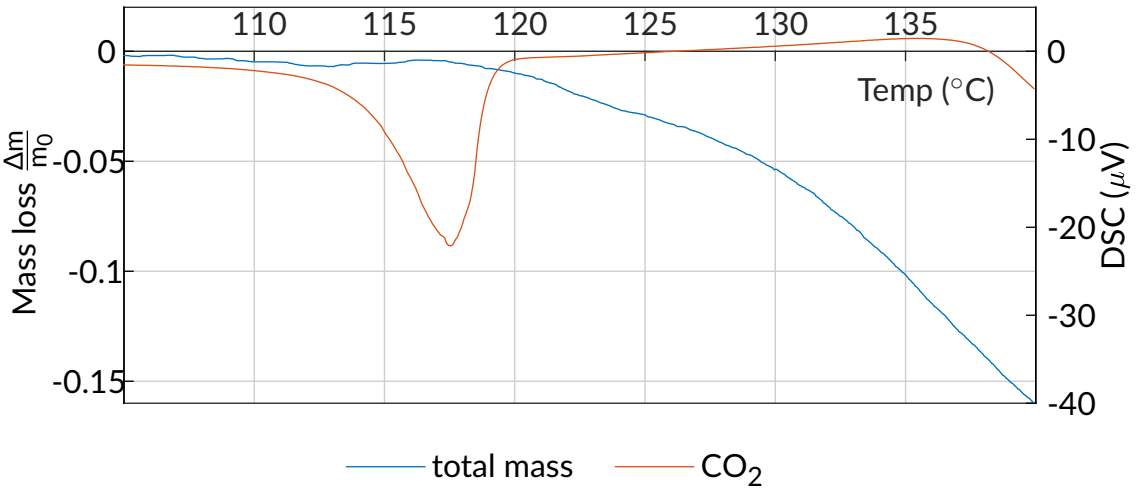

Figure E.3: Mass loss and thermal effects of the pyrolysis of urea phosphate at a constant heating rate of 1 K/min run # 1

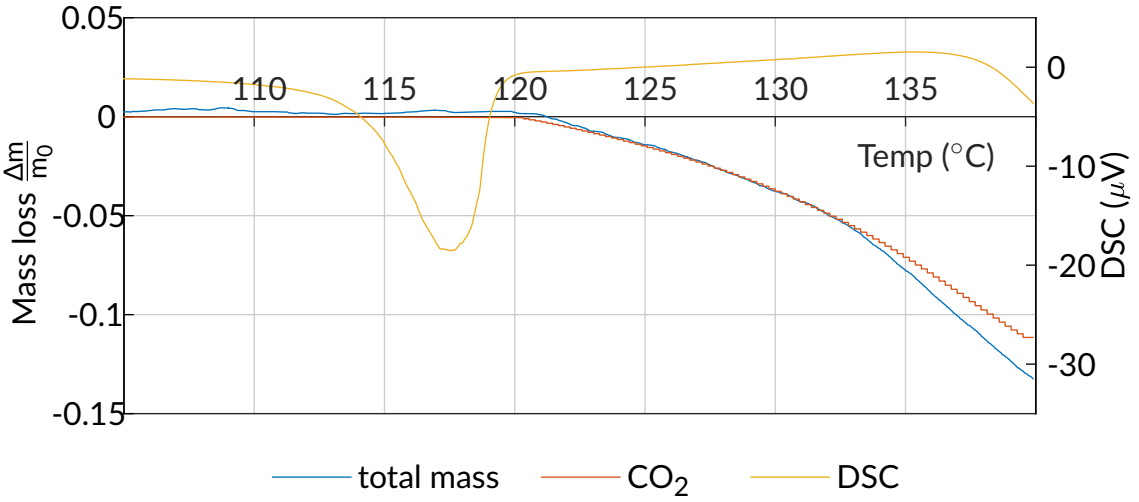

Figure E.4: Mass loss and thermal effects of the pyrolysis of urea phosphate at a constant heating rate of 1 K/min run # 2

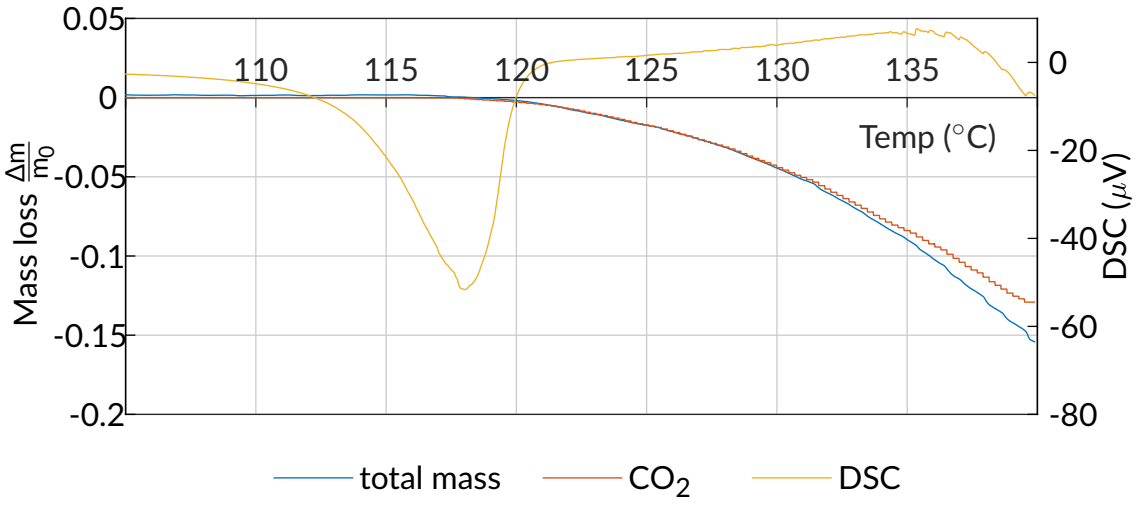

Figure E.5: Mass loss and thermal effects of the pyrolysis of urea phosphate at a constant heating rate of 1 K/min run # 3 (10mg)

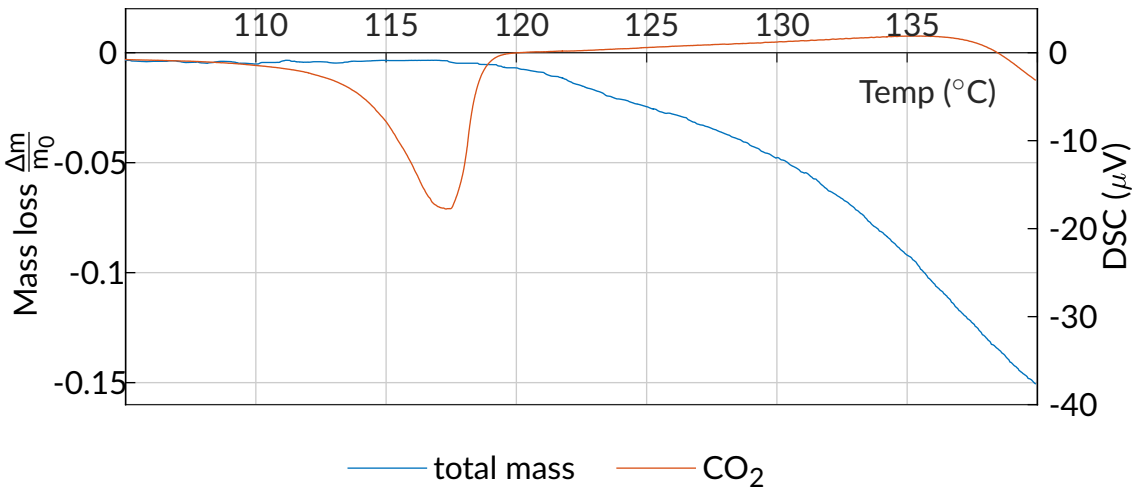

Figure E.6: Mass loss and thermal effects of the pyrolysis of urea phosphate at a constant heating rate of 1 K/min run # 4

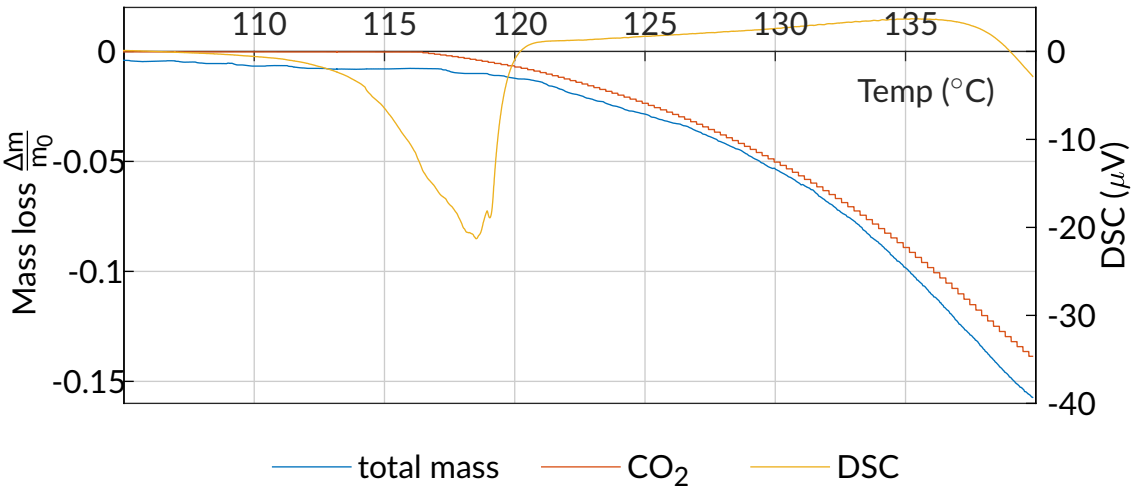

Figure E.7: Mass loss and thermal effects of the pyrolysis of urea phosphate at a constant heating rate of 1 K/min run # 5

E.1.3 2 K/min

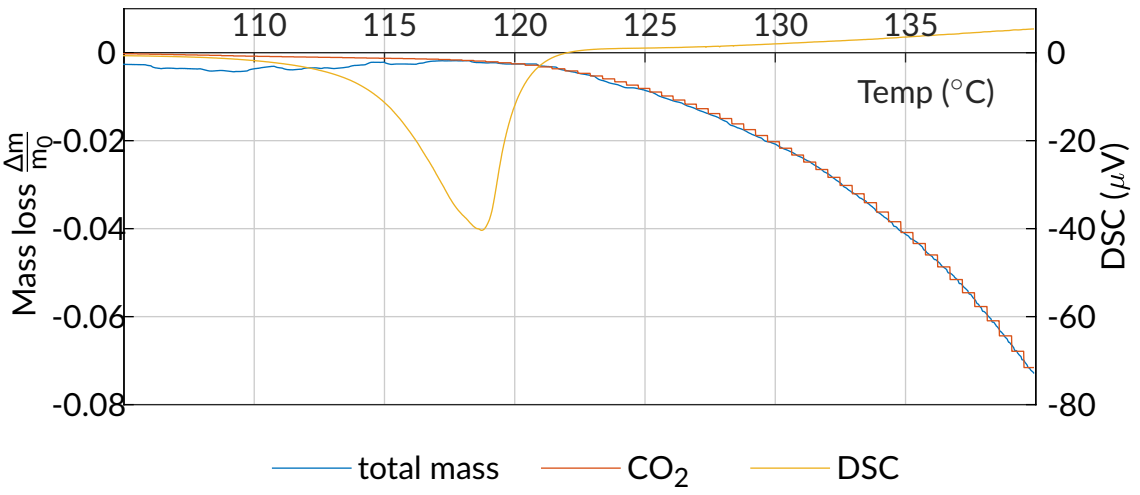

Figure E.8: Mass loss and thermal effects of the pyrolysis of urea phosphate at a constant heating rate of 2 K/min run # 1

E.1.4 3 K/min

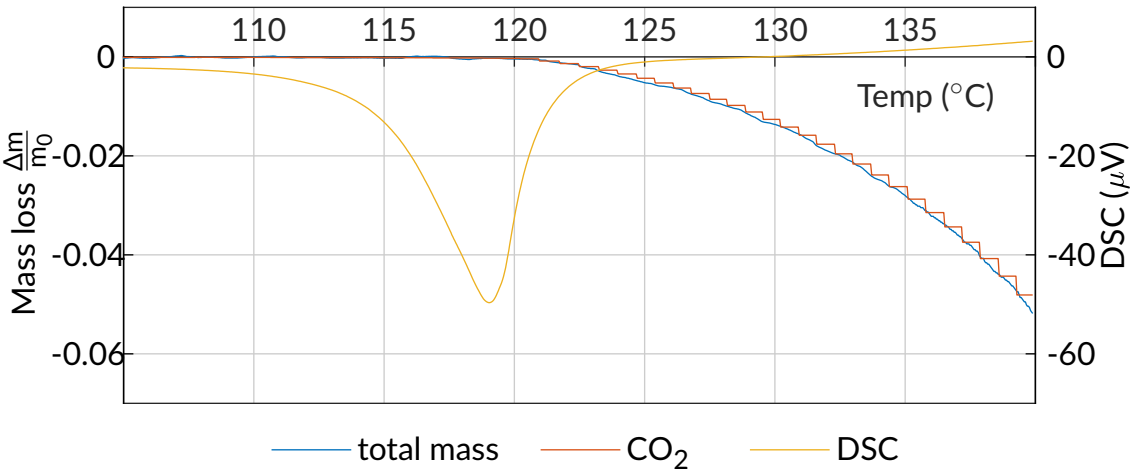

Figure E.9: Mass loss and thermal effects of the pyrolysis of urea phosphate at a constant heating rate of 3 K/min run # 1

E.1.5 4 K/min

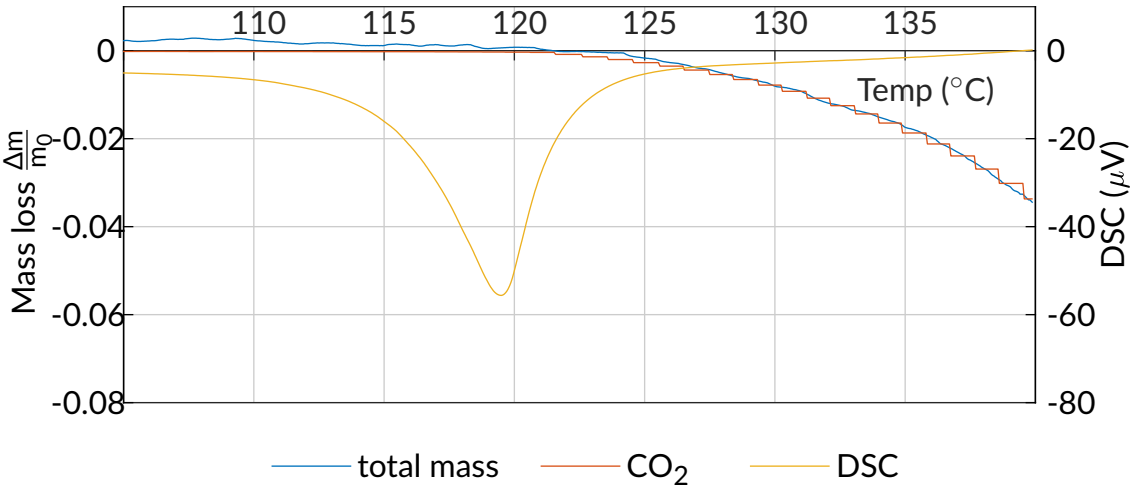

Figure E.10: Mass loss and thermal effects of the pyrolysis of urea phosphate at a constant heating rate of 4 K/min run # 1

E.1.6 5 K/min

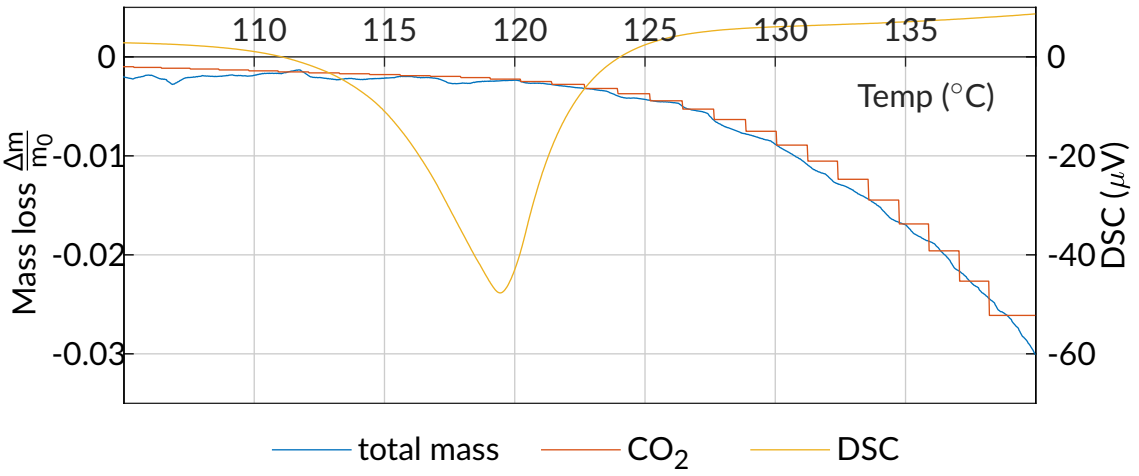

Figure E.11: Mass loss and thermal effects of the pyrolysis of urea phosphate at a constant heating rate of 5 K/min run # 1

E.1.7 Isothermal, 119 °C

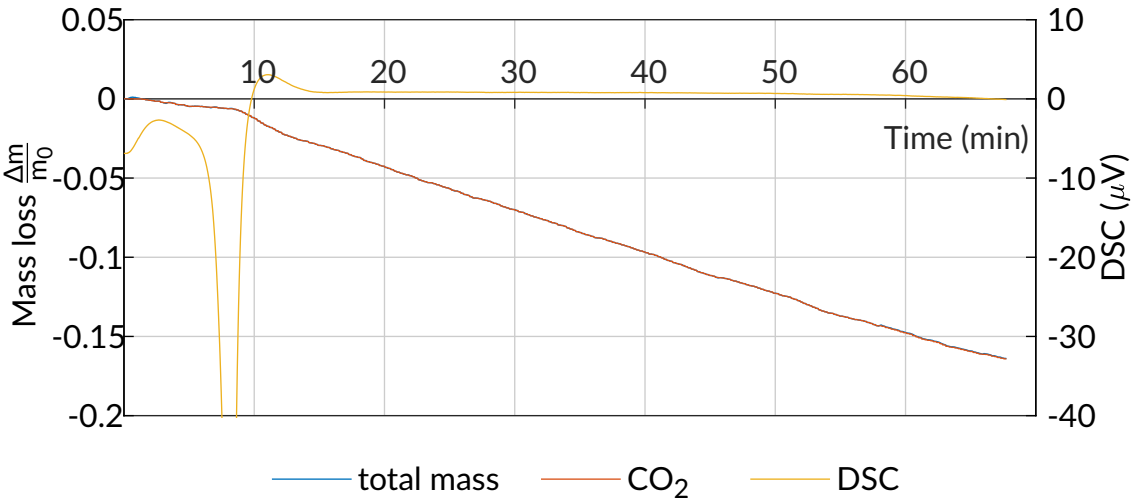

Figure E.12: Mass loss and thermal effects of the pyrolysis of urea phosphate at a constant temperature of 119 °C run # 1

E.1.8 Isothermal, 122 °C

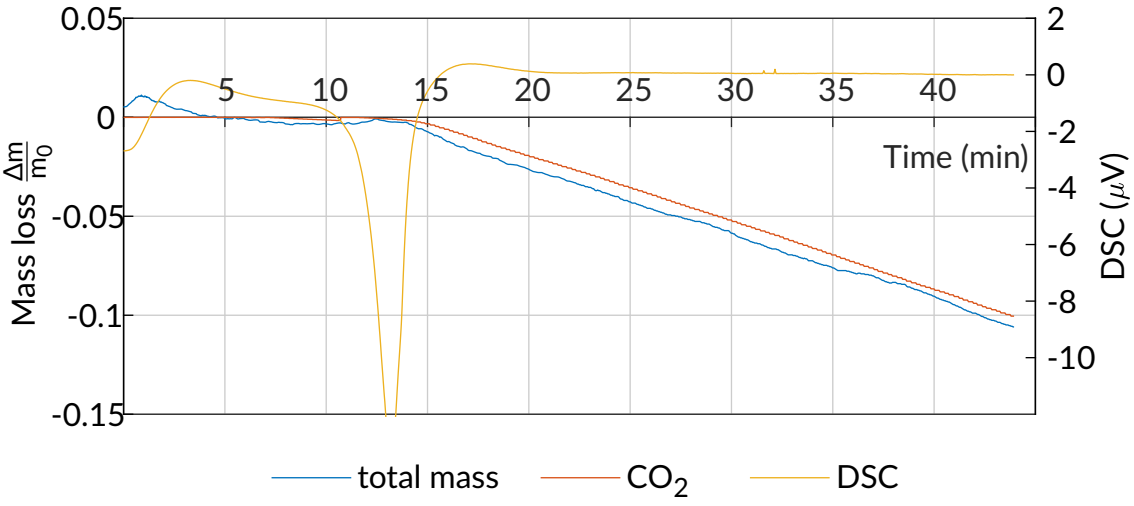

Figure E.13: Mass loss and thermal effects of the pyrolysis of urea phosphate at a constant temperature of 122 °C run # 1

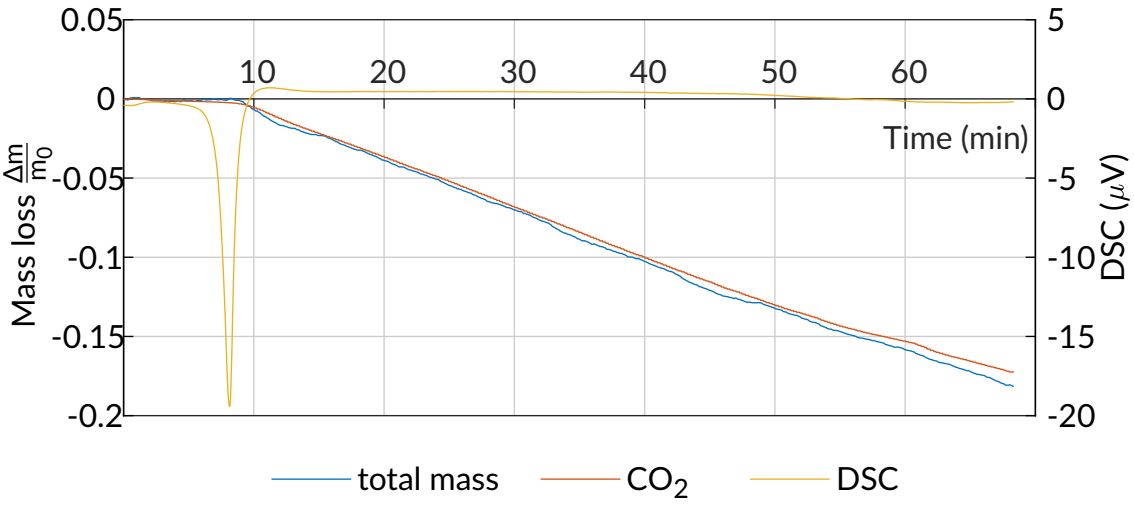

Figure E.14: Mass loss and thermal effects of the pyrolysis of urea phosphate at a constant temperature of 122 °C run # 2

E.1.9 Isothermal, 125 °C

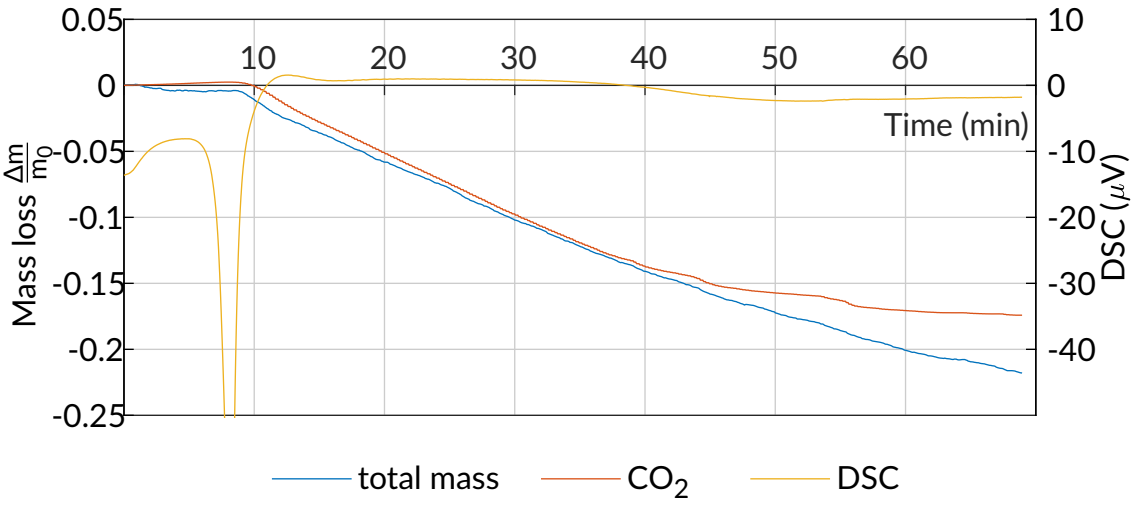

Figure E.15: Mass loss and thermal effects of the pyrolysis of urea phosphate at a constant temperature of 125 °C run # 1

E.1.10 Isothermal 130 °C

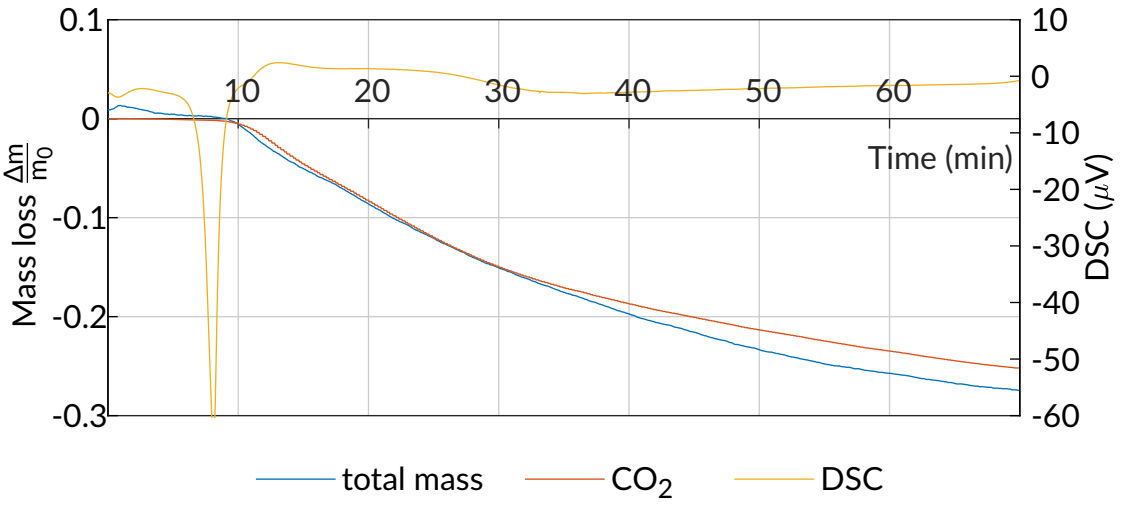

Figure E.16: Mass loss and thermal effects of the pyrolysis of urea phosphate at a constant temperature of 130 °C run # 1

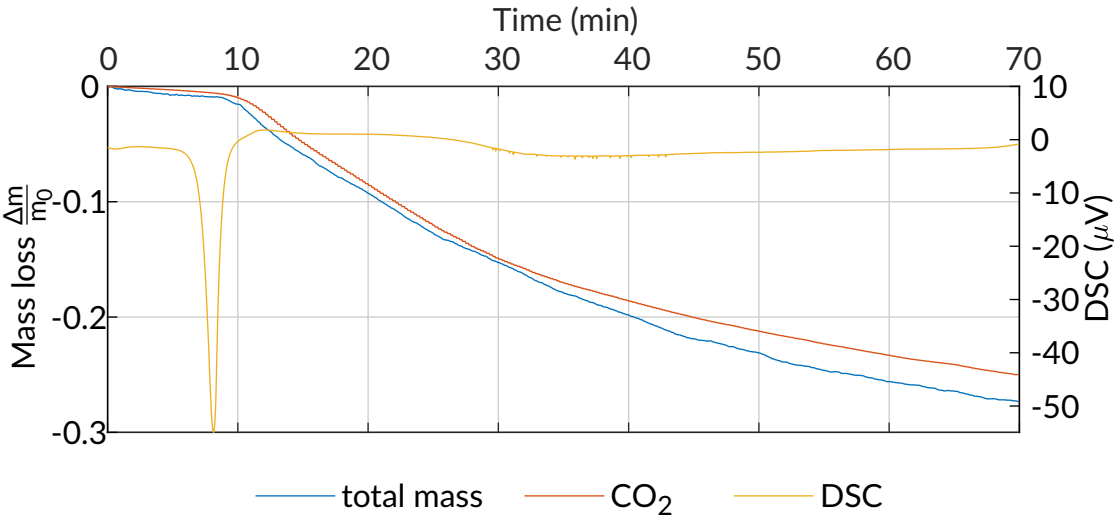

Figure E.17: Mass loss and thermal effects of the pyrolysis of urea phosphate at a constant temperature of 130 °C run # 2

E.2 Mass balances

E.2.1 0.5 K/min

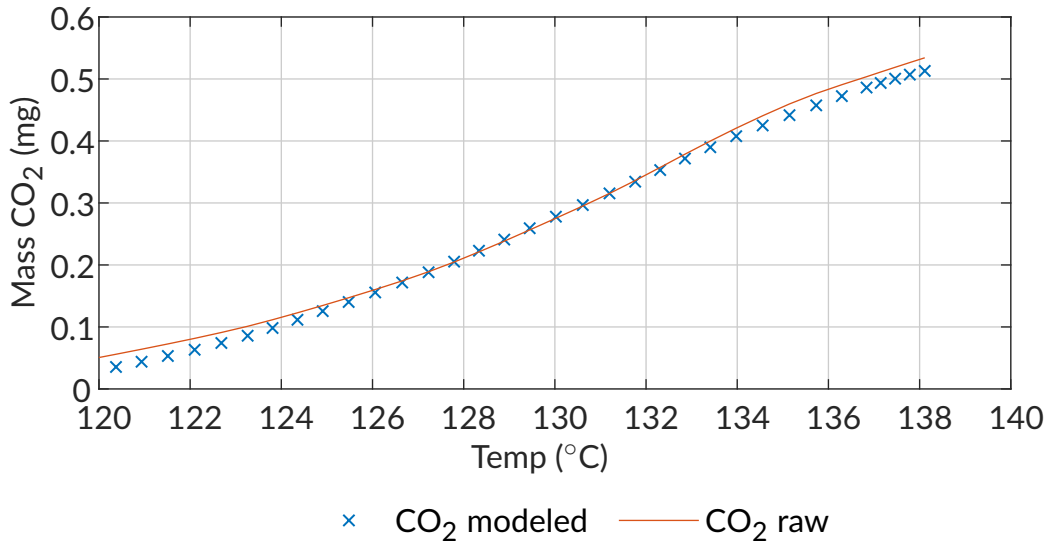

Figure E.18: Mass CO_2 produced during the pyrolysis of urea phosphate at a constant heating rate of 0.5 K/min run # 1

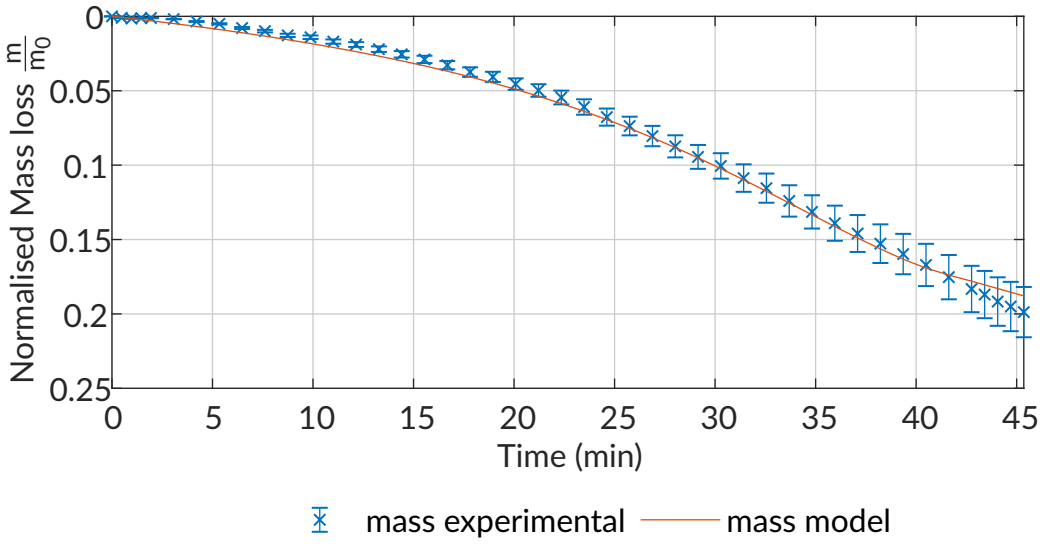

Figure E.19: Mass loss of predicted and experimental measurements as a constant heating rate of 0.5 K/min run # 1

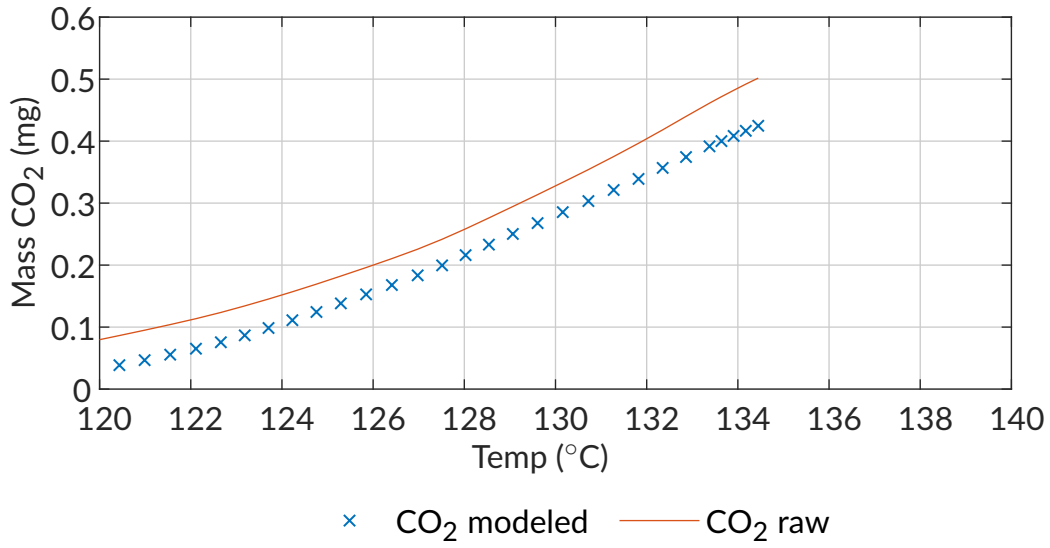

Figure E.20: Mass CO_2 produced during the pyrolysis of urea phosphate at a constant heating rate of 0.5 K/min run # 2

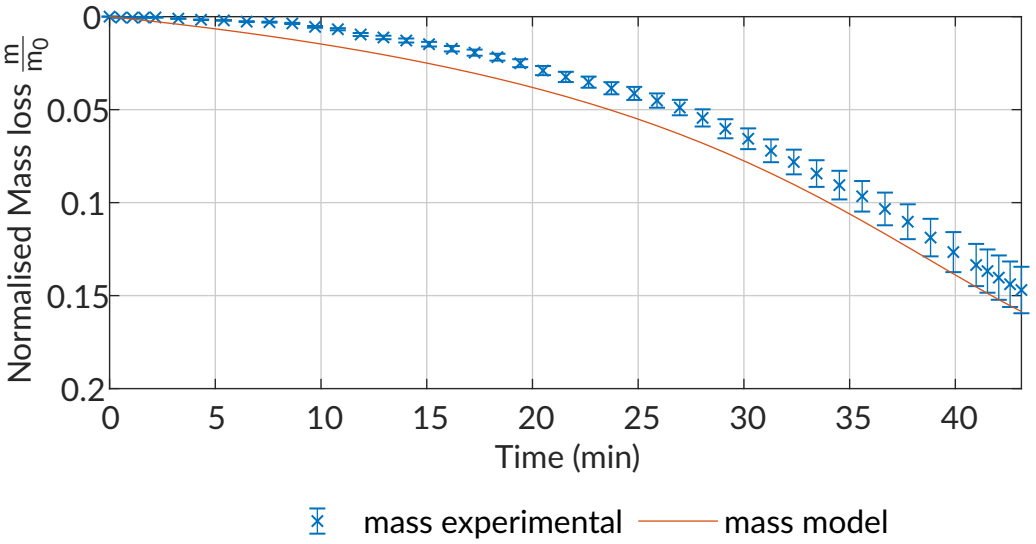

Figure E.21: Mass loss of predicted and experimental measurements as a constant heating rate of 0.5 K/min run # 2

E.2.2 1 K/min

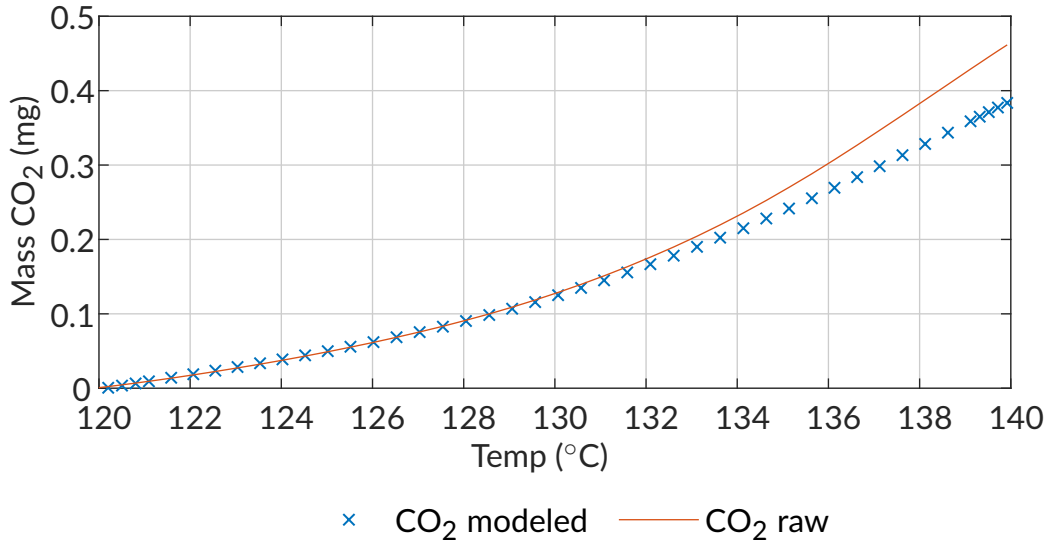

Figure E.22: Mass CO_2 produced during the pyrolysis of urea phosphate at a constant heating rate of 1 K/min run # 2

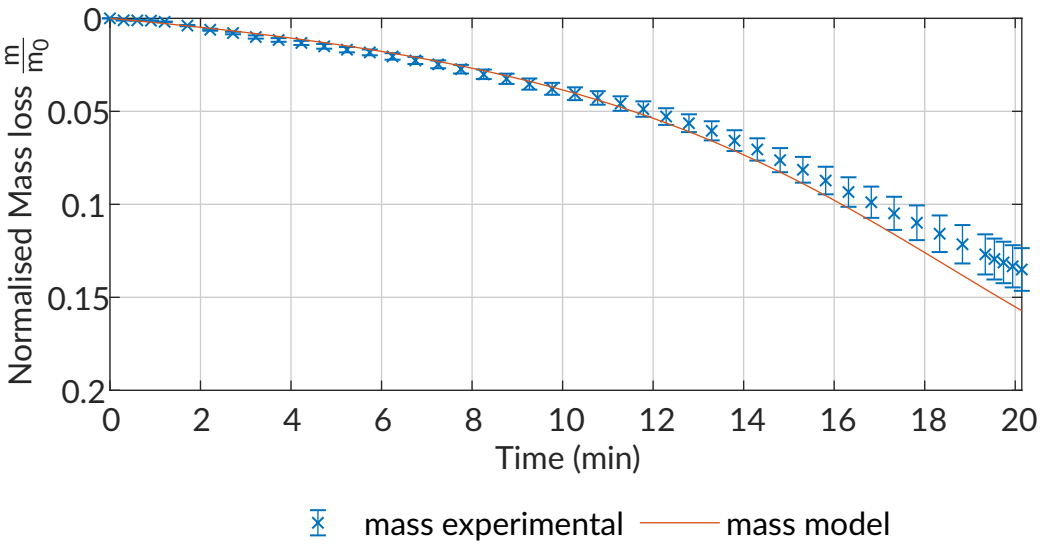

Figure E.23: Mass loss of predicted and experimental measurements as a constant heating rate of 1 K/min run # 2

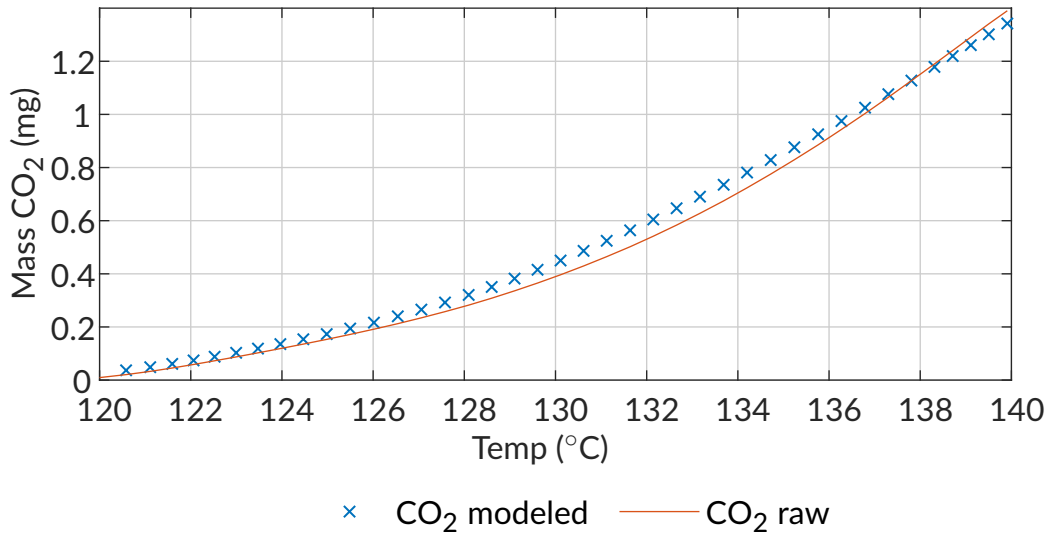

Figure E.24: Mass CO_2 produced during the pyrolysis of urea phosphate at a constant heating rate of 1 K/min run # 3

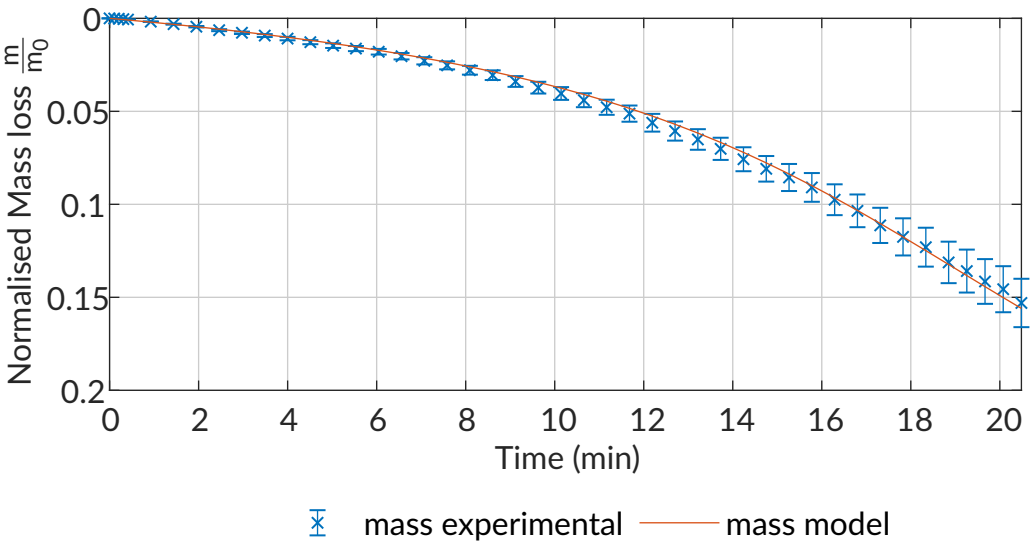

Figure E.25: Mass loss of predicted and experimental measurements as a constant heating rate of 1 K/min run # 3

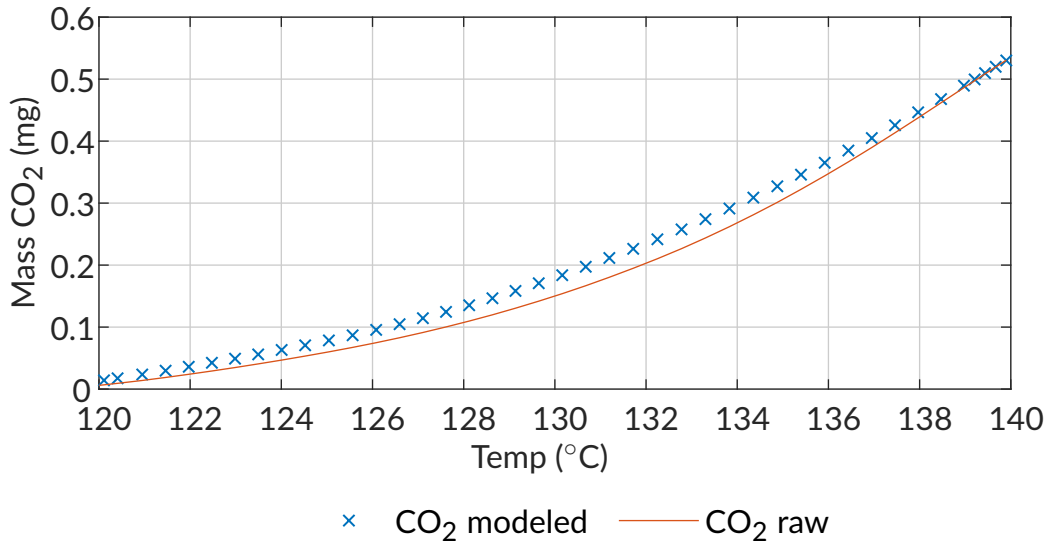

Figure E.26: Mass CO_2 produced during the pyrolysis of urea phosphate at a constant heating rate of 1 K/min run # 5

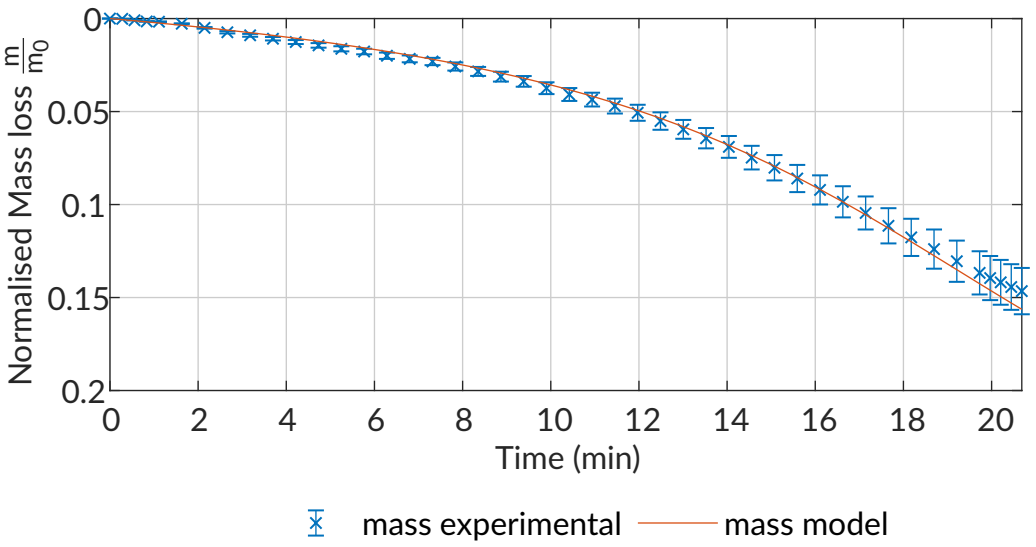

Figure E.27: Mass loss of predicted and experimental measurements as a constant heating rate of 1 K/min run # 5

E.2.3 2 K/min

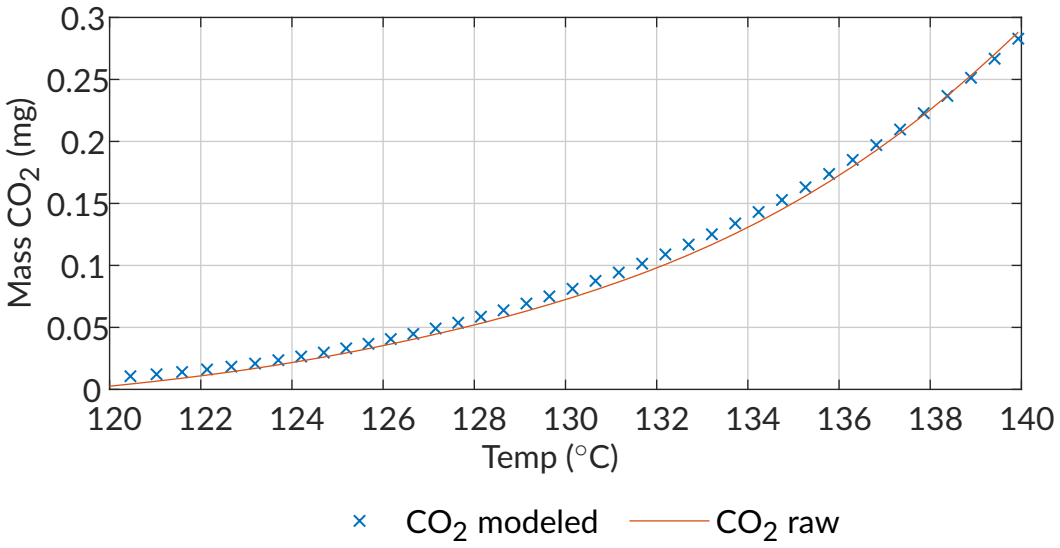

Figure E.28: Mass CO_2 produced during the pyrolysis of urea phosphate at a constant heating rate of 2 K/min run # 1

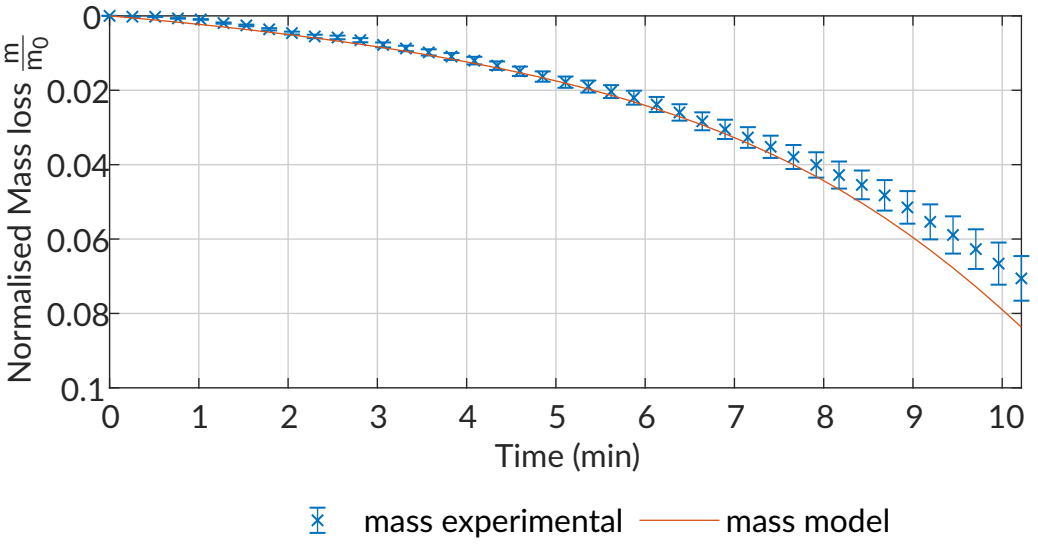

Figure E.29: Mass loss of predicted and experimental measurements as a constant heating rate of 2 K/min run # 1

E.2.4 3 K/min

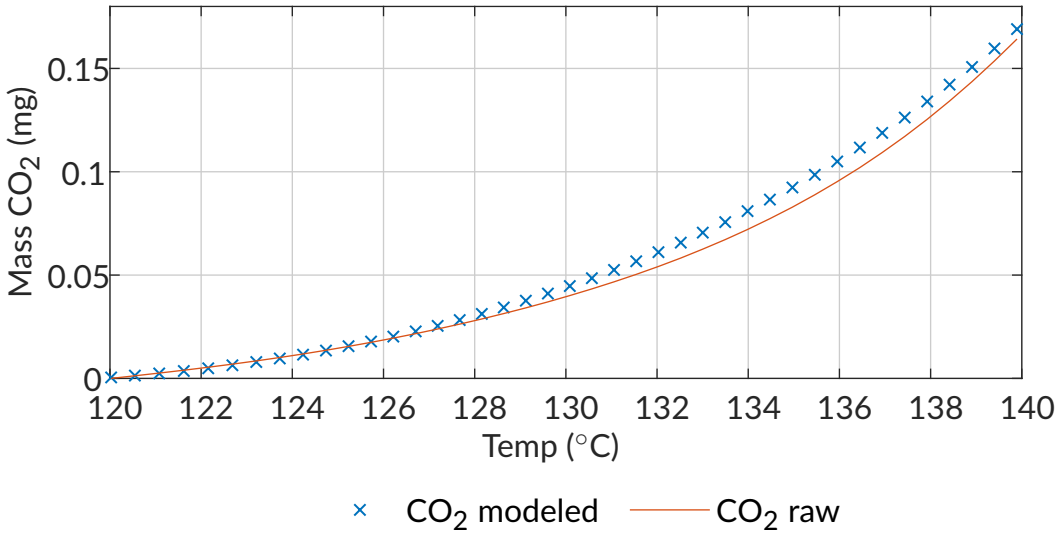

Figure E.30: Mass CO_2 produced during the pyrolysis of urea phosphate at a constant heating rate of 3 K/min run # 1

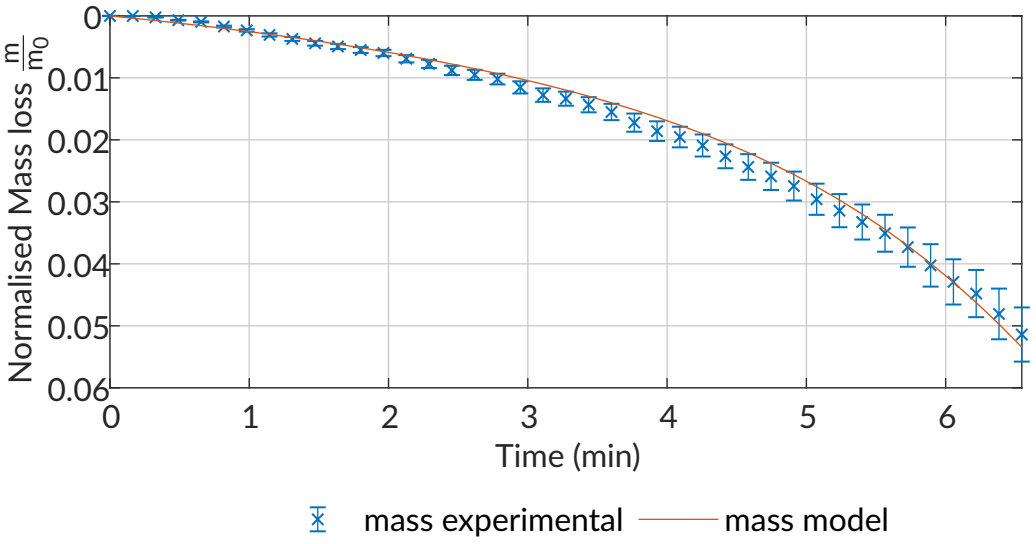

Figure E.31: Mass loss of predicted and experimental measurements as a constant heating rate of 3 K/min run # 1

E.2.5 4 K/min

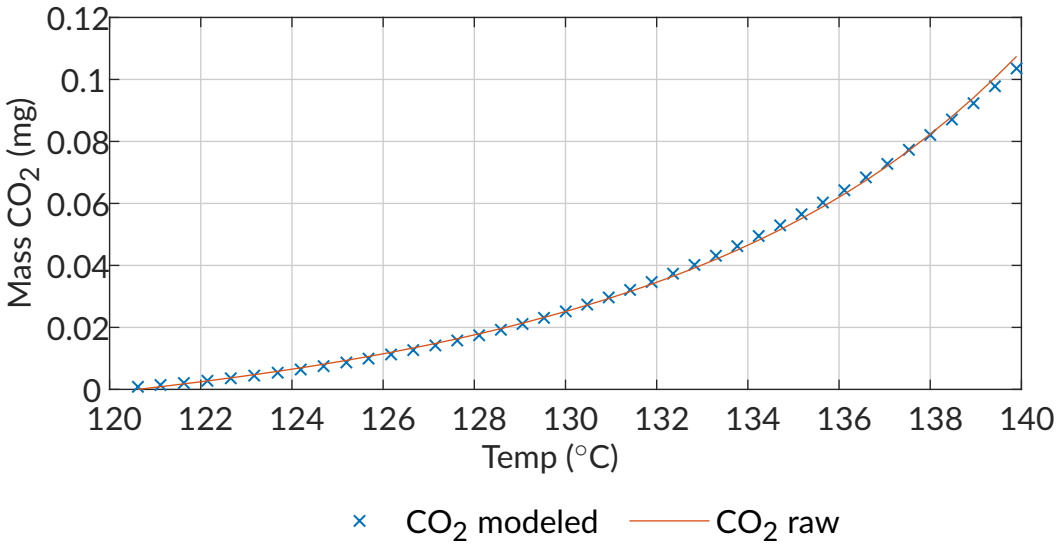

Figure E.32: Mass CO_2 produced during the pyrolysis of urea phosphate at a constant heating rate of 4 K/min run # 1

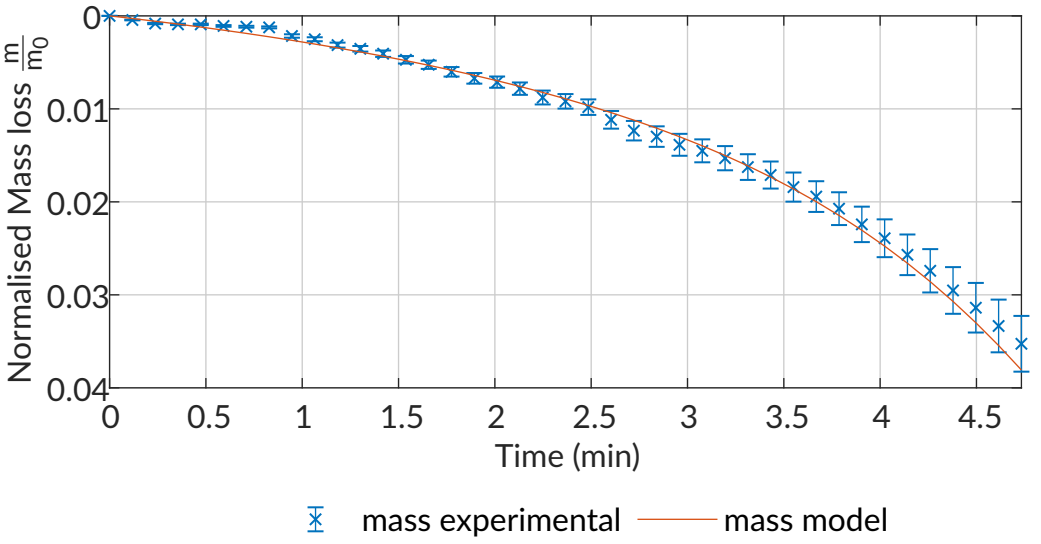

Figure E.33: Mass loss of predicted and experimental measurements as a constant heating rate of 4 K/min run # 1

E.2.6 5 K/min

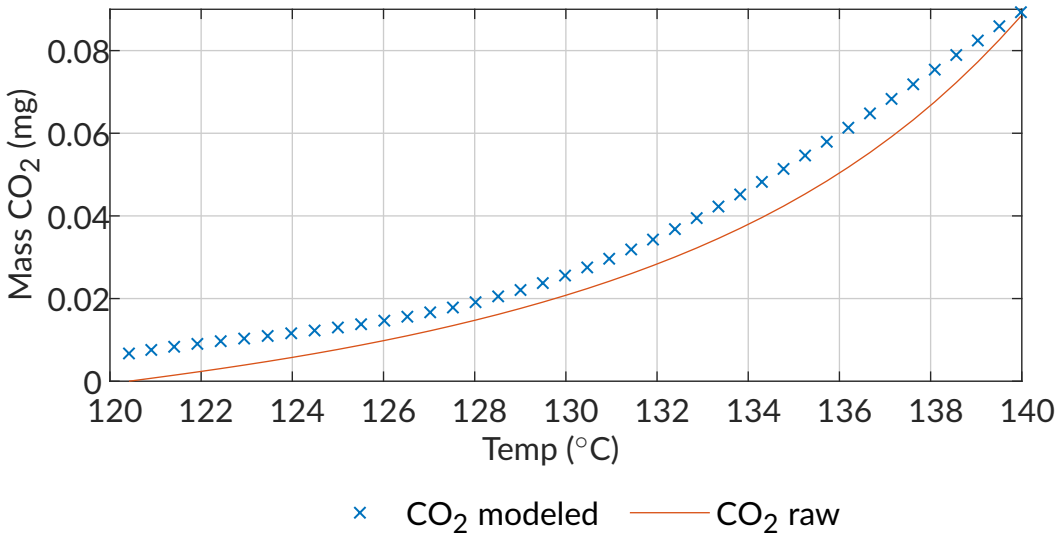

Figure E.34: Mass CO_2 produced during the pyrolysis of urea phosphate at a constant heating rate of 5 K/min run # 1

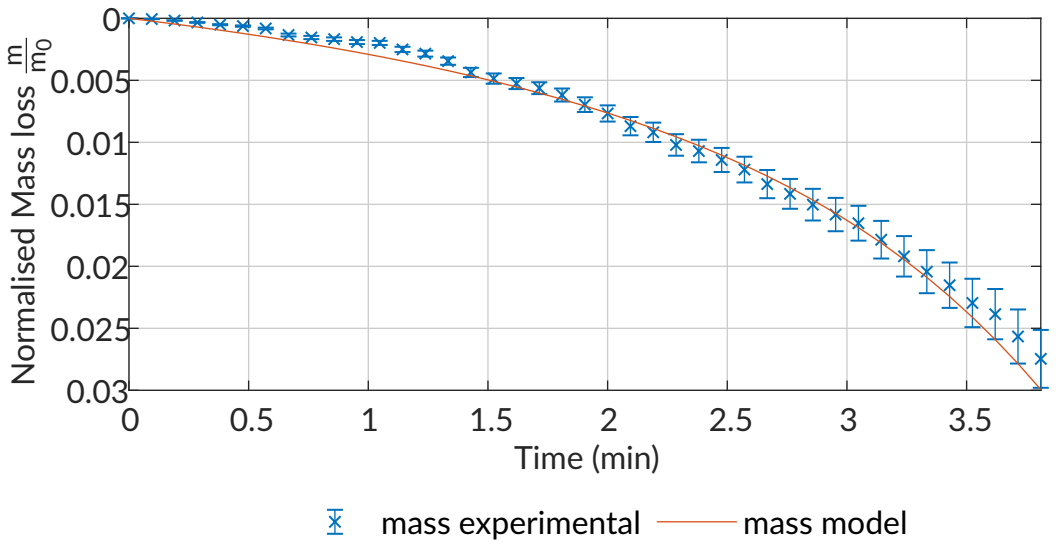

Figure E.35: Mass loss of predicted and experimental measurements as a constant heating rate of 5 K/min run # 1

E.2.7 Isothermal 119 °C

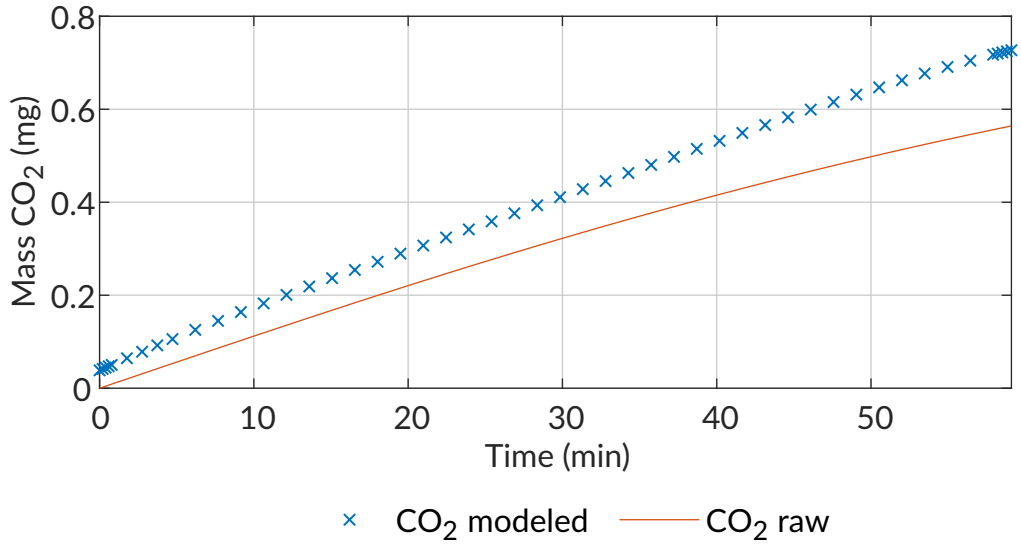

Figure E.36: Mass CO_2 produced during the pyrolysis of urea phosphate at a constant temperature of 119 °C run # 1

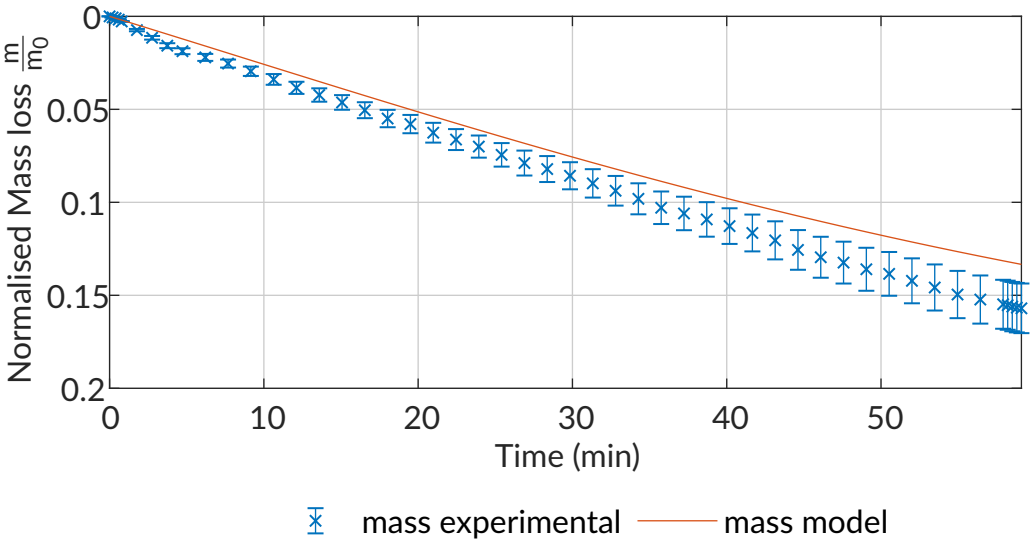

Figure E.37: Mass loss of predicted and experimental measurements as a constant temperature of 119 °C run # 1

E.2.8 Isothermal 122 °C

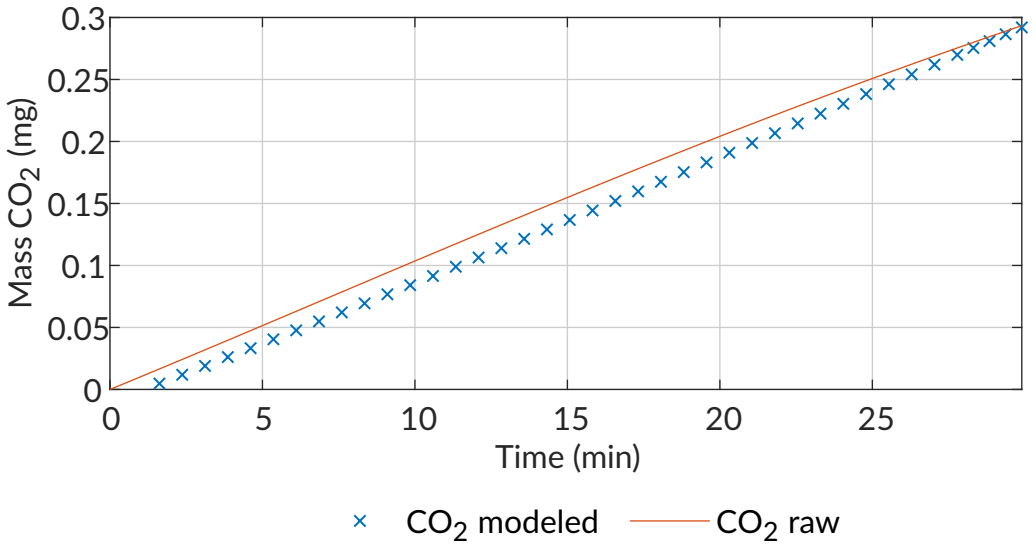

Figure E.38: Mass CO_2 produced during the pyrolysis of urea phosphate at a constant temperature of 122 °C run # 1

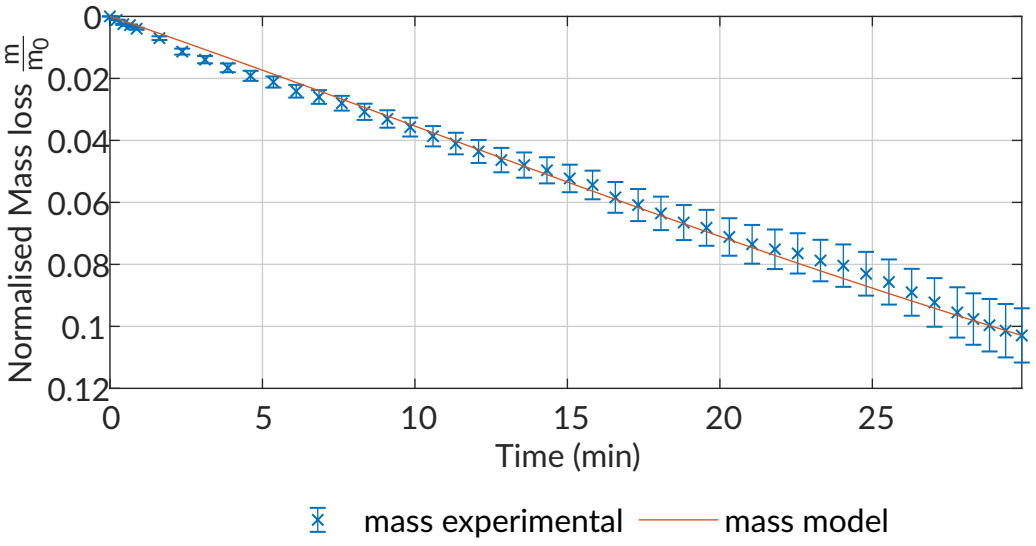

Figure E.39: Mass loss of predicted and experimental measurements as a constant temperature of 122 °C run # 1

A repeat of 122 °C was done, one, with a total time of 30 mins, and one with a total time of 60 minutes, in order to investigate correlation with NMR.

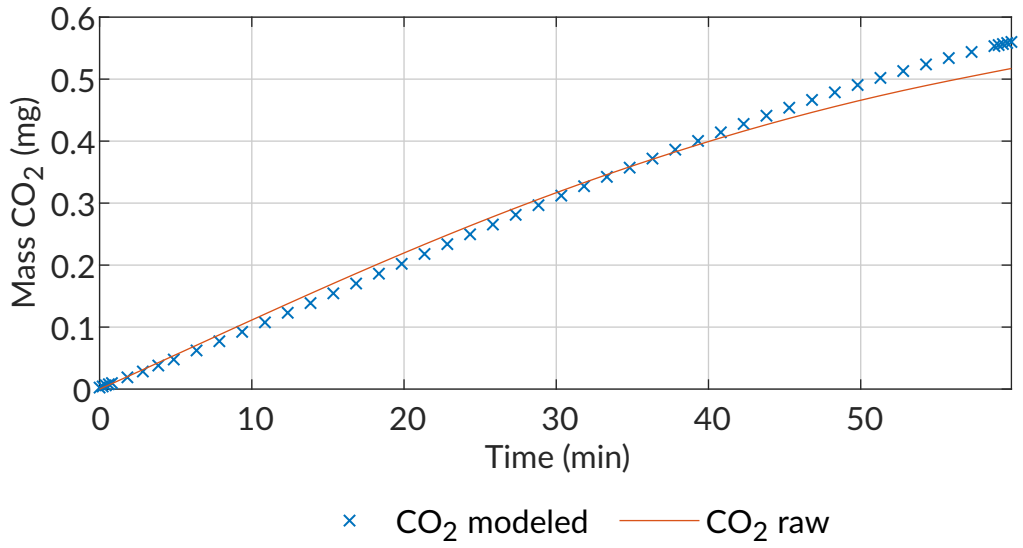

Figure E.40: Mass CO_2 produced during the pyrolysis of urea phosphate at a constant temperature of 122 °C run # 2

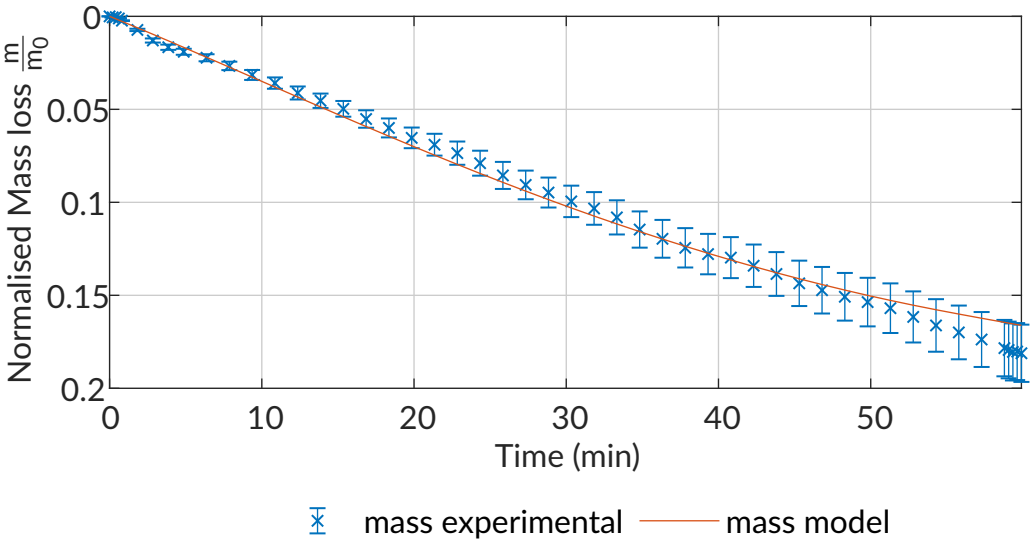

Figure E.41: Mass loss of predicted and experimental measurements as a constant temperature of 122 °C run # 2

E.2.9 Isothermal 125 °C

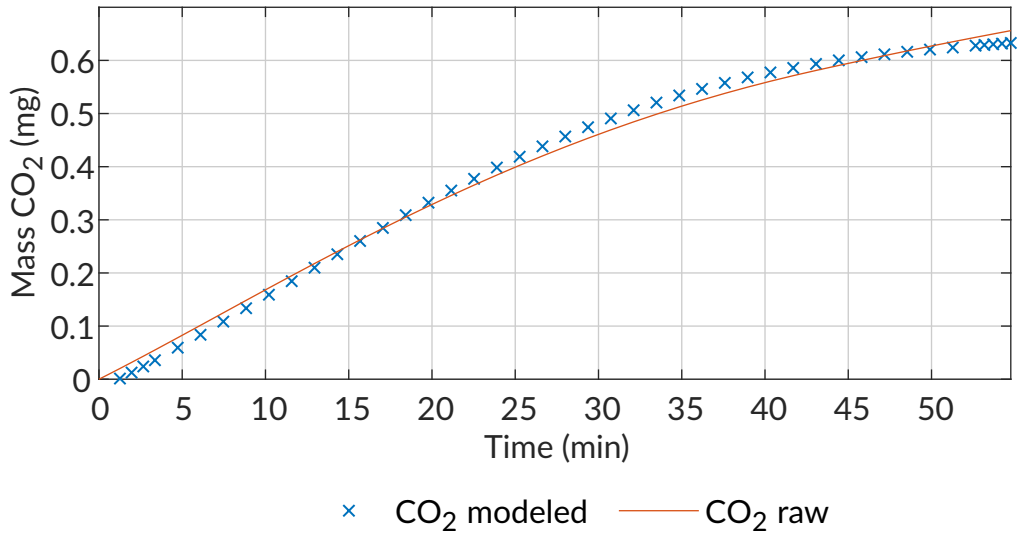

Figure E.42: Mass CO_2 produced during the pyrolysis of urea phosphate at a constant temperature of 122 °C run # 1

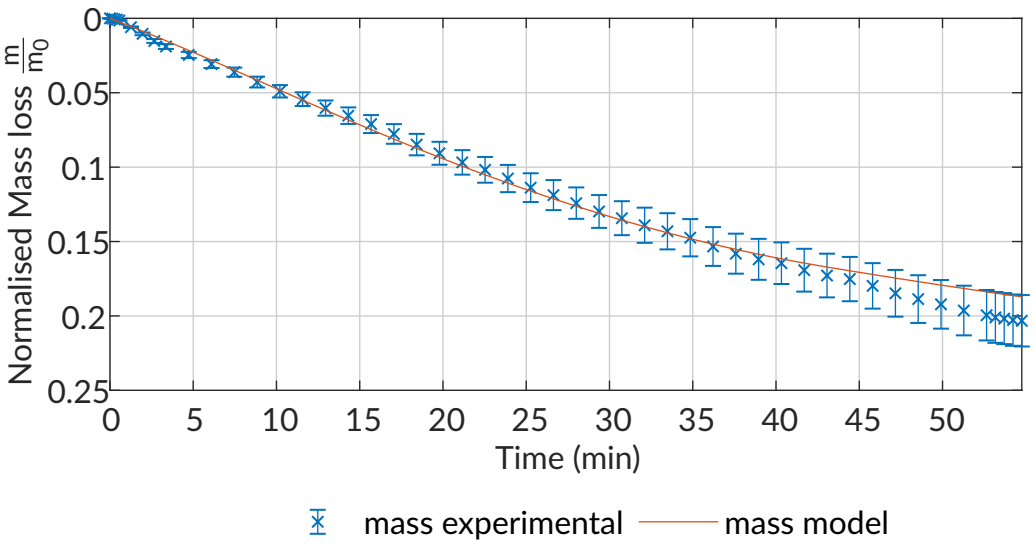

Figure E.43: Mass loss of predicted and experimental measurements as a constant temperature of 125 °C run # 1

E.2.10 Isothermal 130 °C

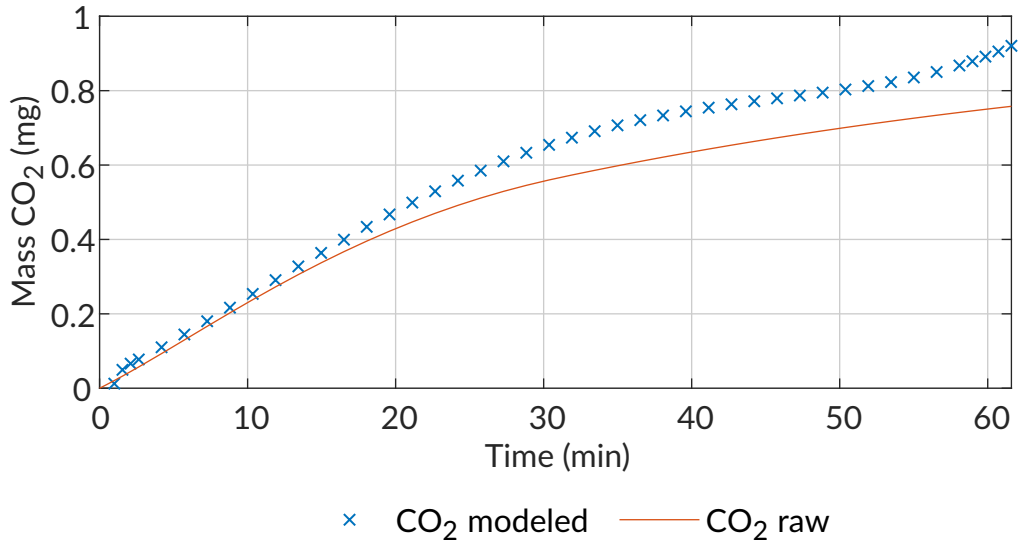

Figure E.44: Mass CO_2 produced during the pyrolysis of urea phosphate at a constant temperature of 130 °C run # 1

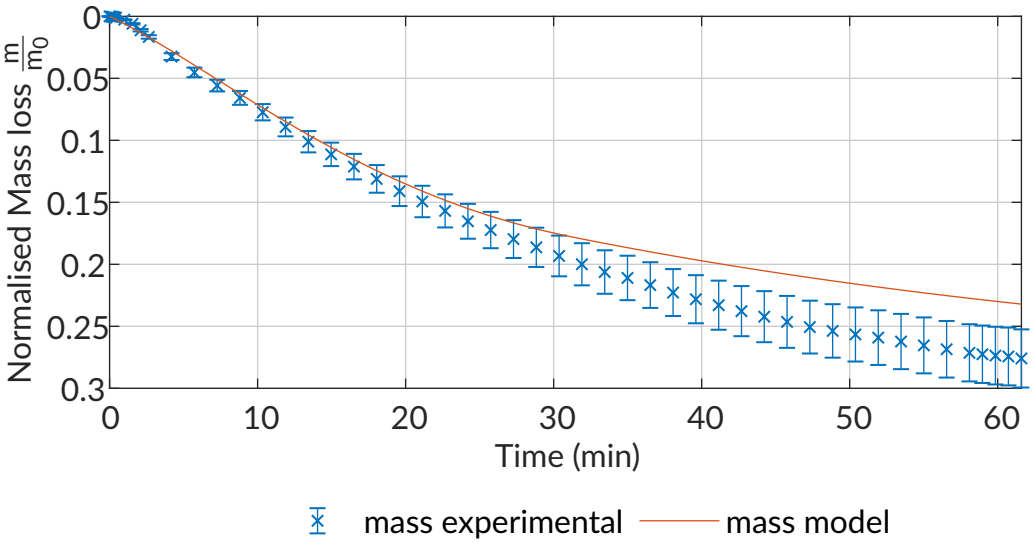

Figure E.45: Mass loss of predicted and experimental measurements as a constant temperature of 130 °C run # 1

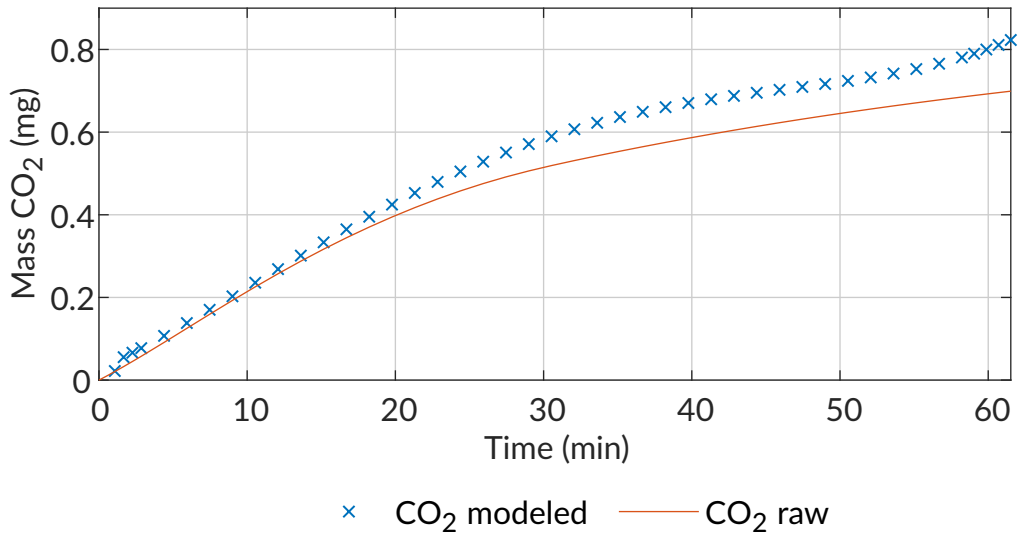

Figure E.46: Mass CO_2 produced during the pyrolysis of urea phosphate at a constant temperature of 130 °C run # 2

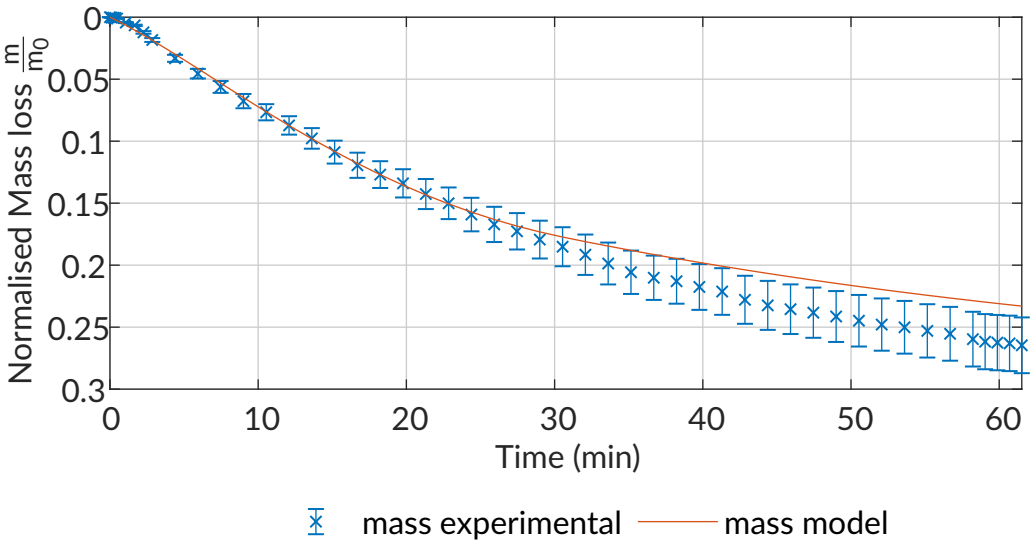

Figure E.47: Mass loss of predicted and experimental measurements as a constant temperature of 130 °C run # 2

E.3 FTIR data

The FTIR connected to the is shown graphically here. As can be seen in all these graphs, a single peak is observed at the wave number range that corresponds with a C = O bond. This is evidence that the only gas produced during the TGA run is CO_2, and can be corellated to the total . As stated in section 4.1, with this assumption, the exact

amount of CO_2 can be calculated with the Beer-Lambert Law, by means of integration if this curve at a set wave number, (2360cm⁻1) for CO_2.

E.3.1 Calibration run

The regressed Beer-Lambert constant fir the calibration run was 0.18.

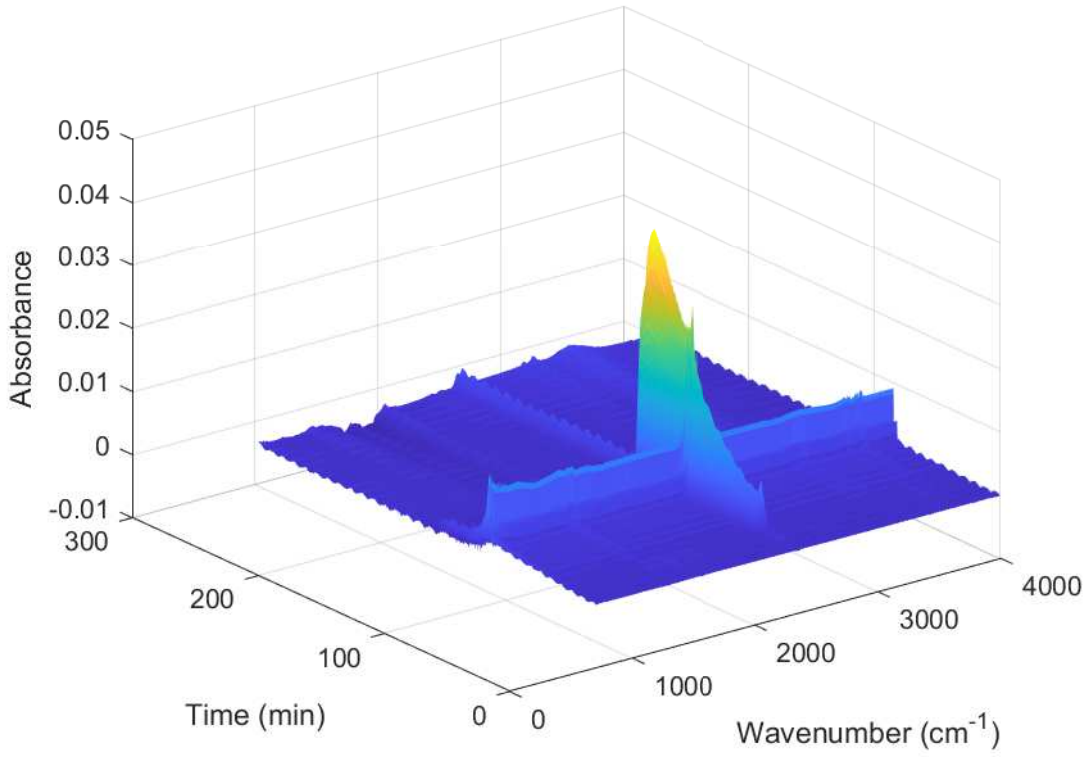

Figure E.48: CO_2 Calibration run FTIR feed

E.3.2 0.5 K/min

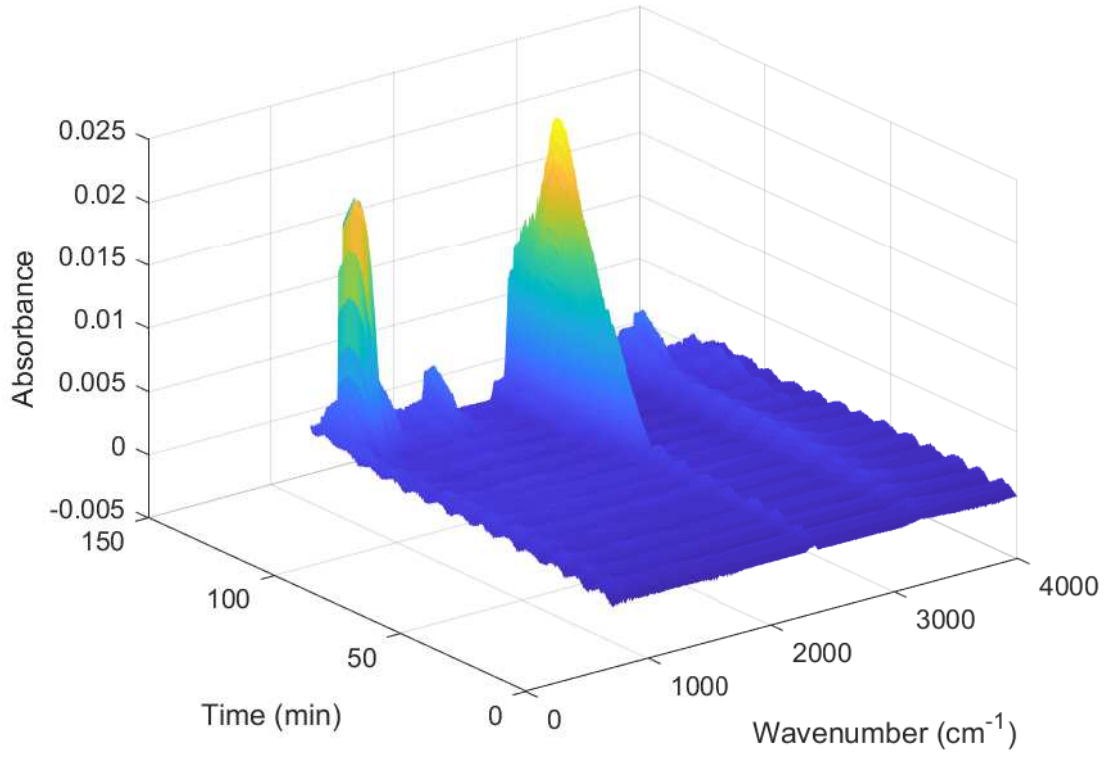

Figure E.49: 0.5 K/min run # 1 FTIR feed

E.3.3 1 K/min

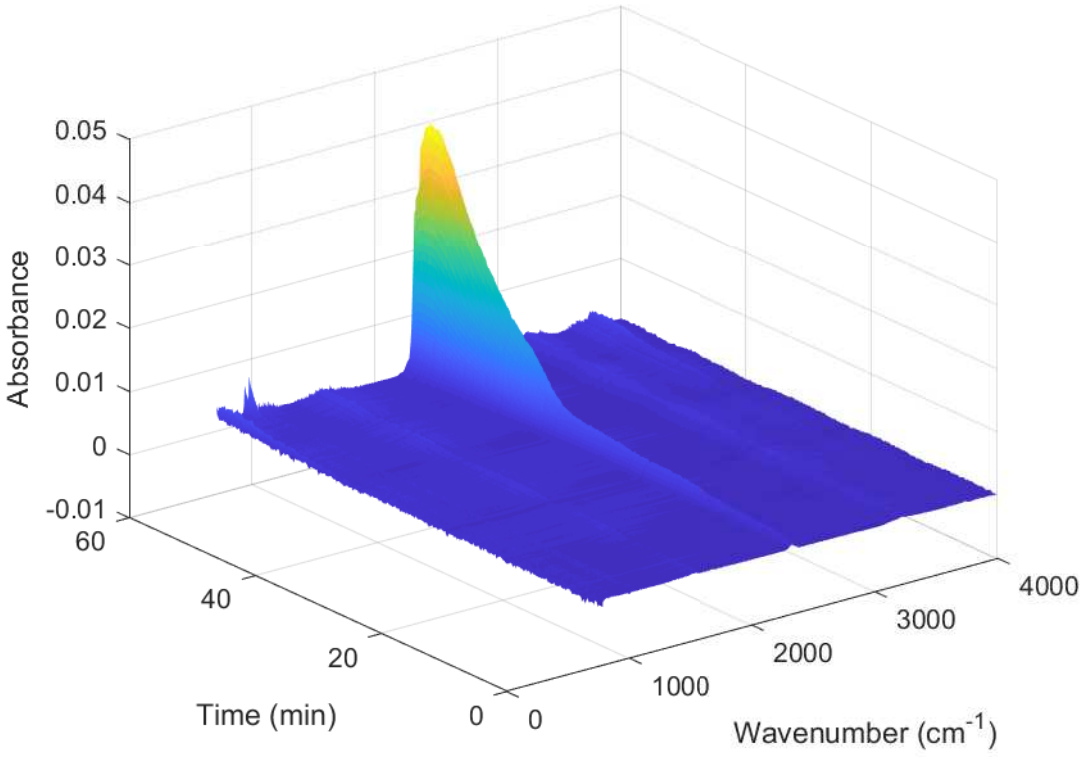

Figure E.50: 1 K/min run # 2 FTIR feed

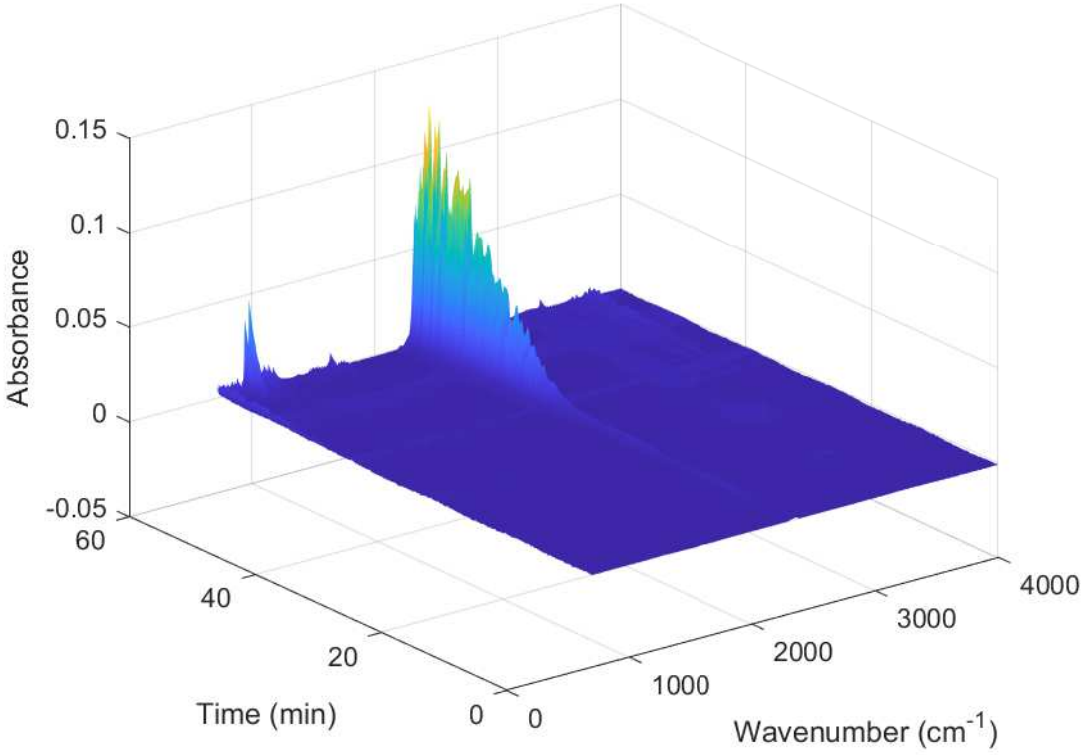

Figure E.51: 1 K/min run # 3 (10 mg) FTIR feed

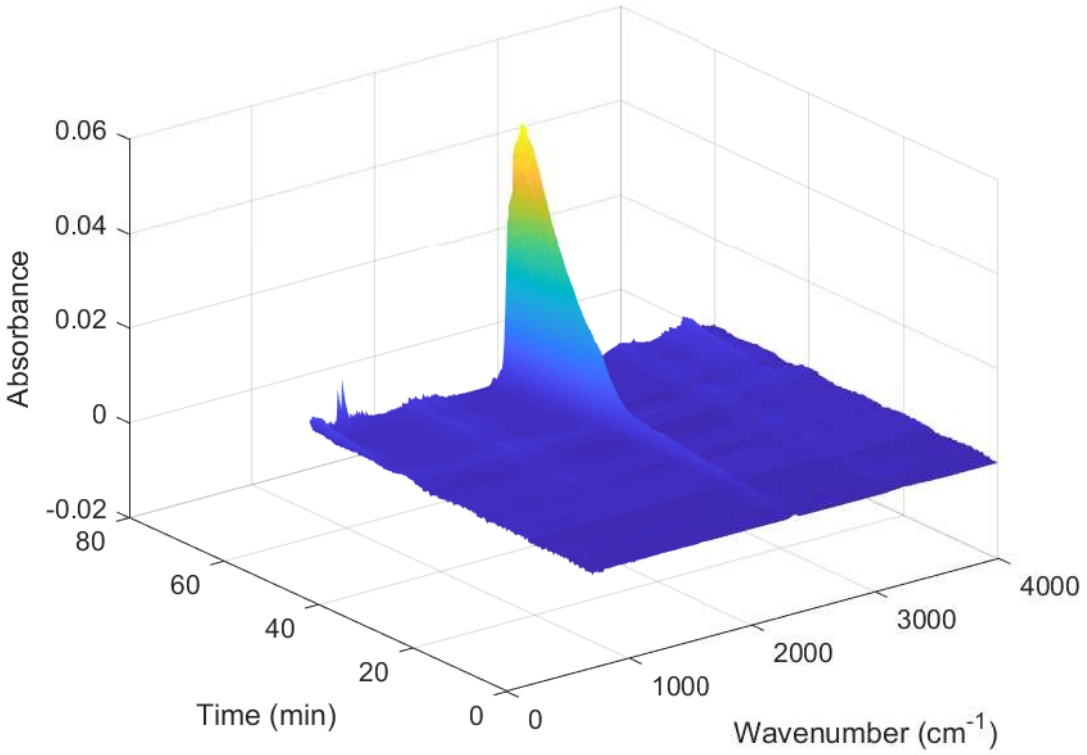

Figure E.52: 1 K/min run # 5 FTIR feed

E.3.4 2 K/min

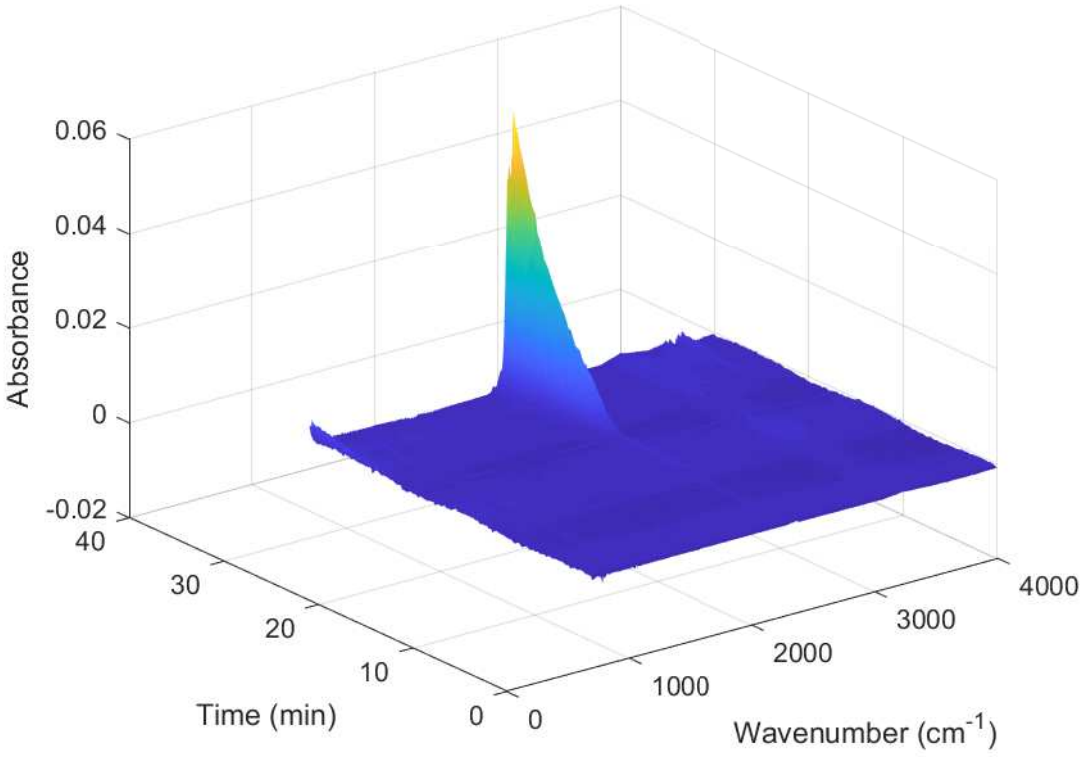

Figure E.53: 2 K/min run # 1 FTIR feed

E.3.5 3 K/min

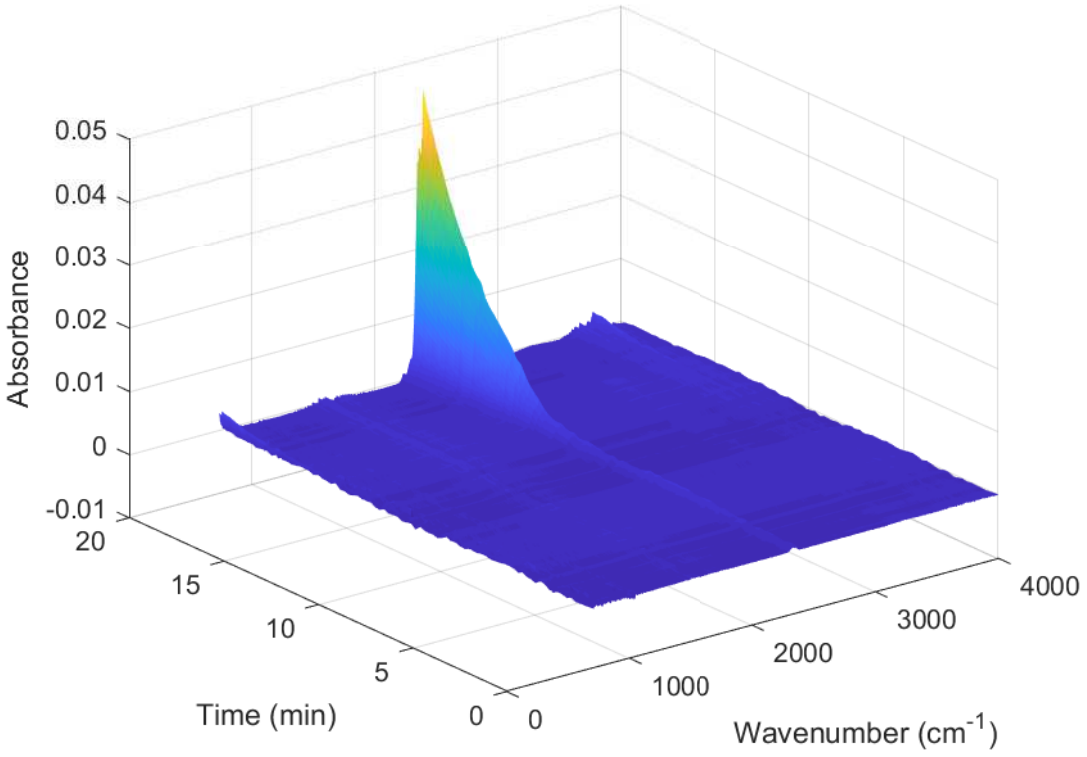

Figure E.54: 3 K/min run # 1 FTIR feed

E.3.6 4 K/min

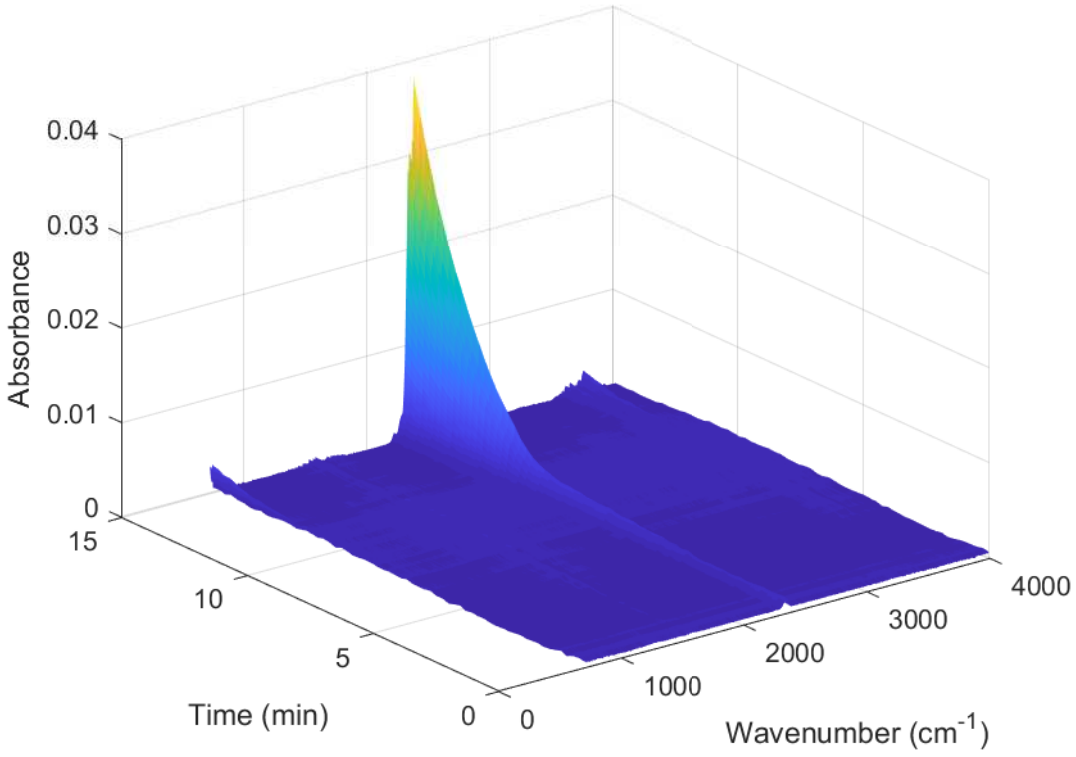

Figure E.55: 4 K/min run # 1 FTIR feed

E.3.7 5 K/min

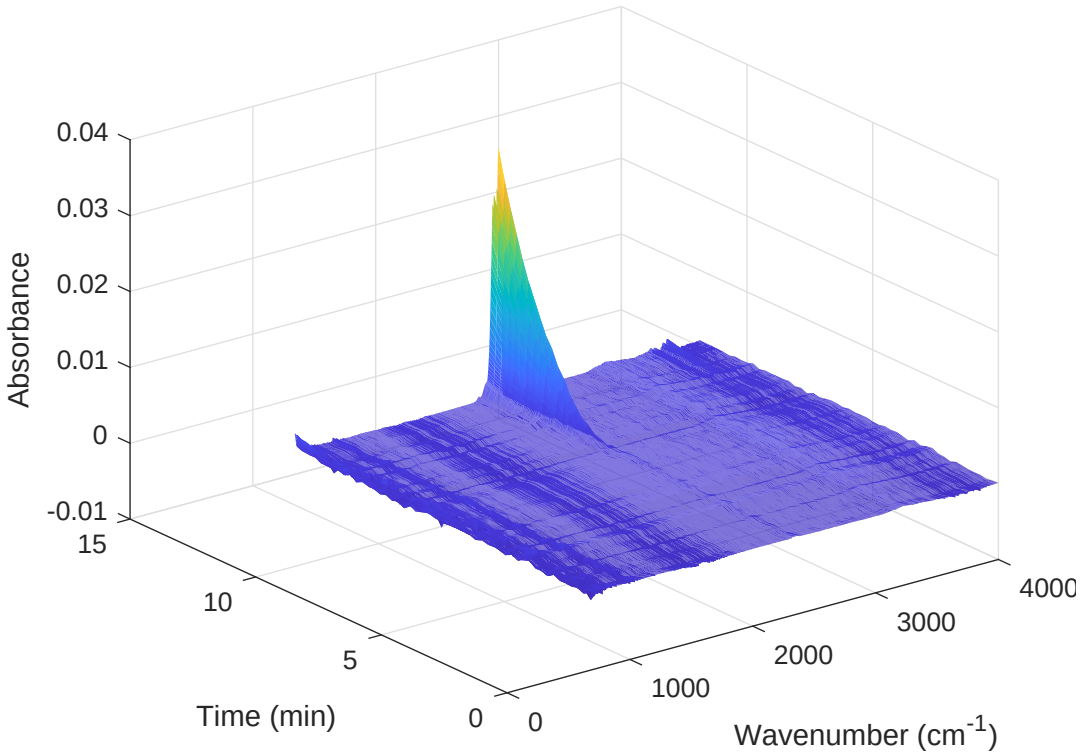

Figure E.56: 5 K/min run # 1 FTIR feed

E.3.8 130 °C isothermal

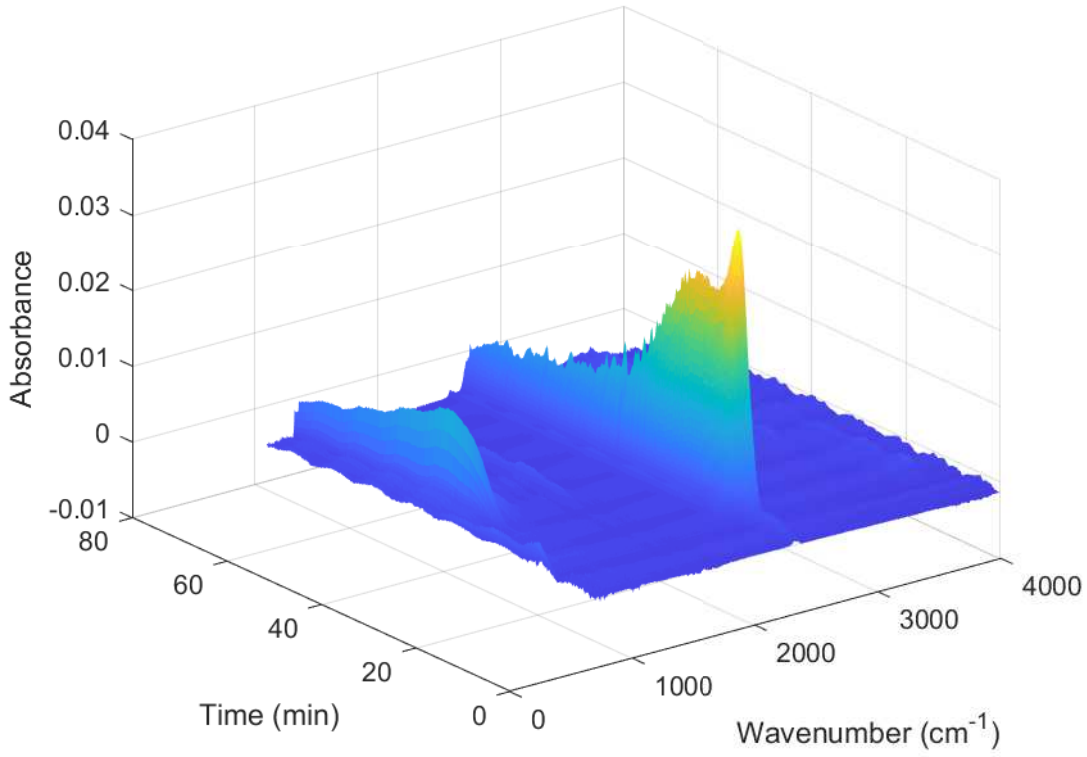

Figure E.57: 130 °C isothermal run # 1 FTIR feed

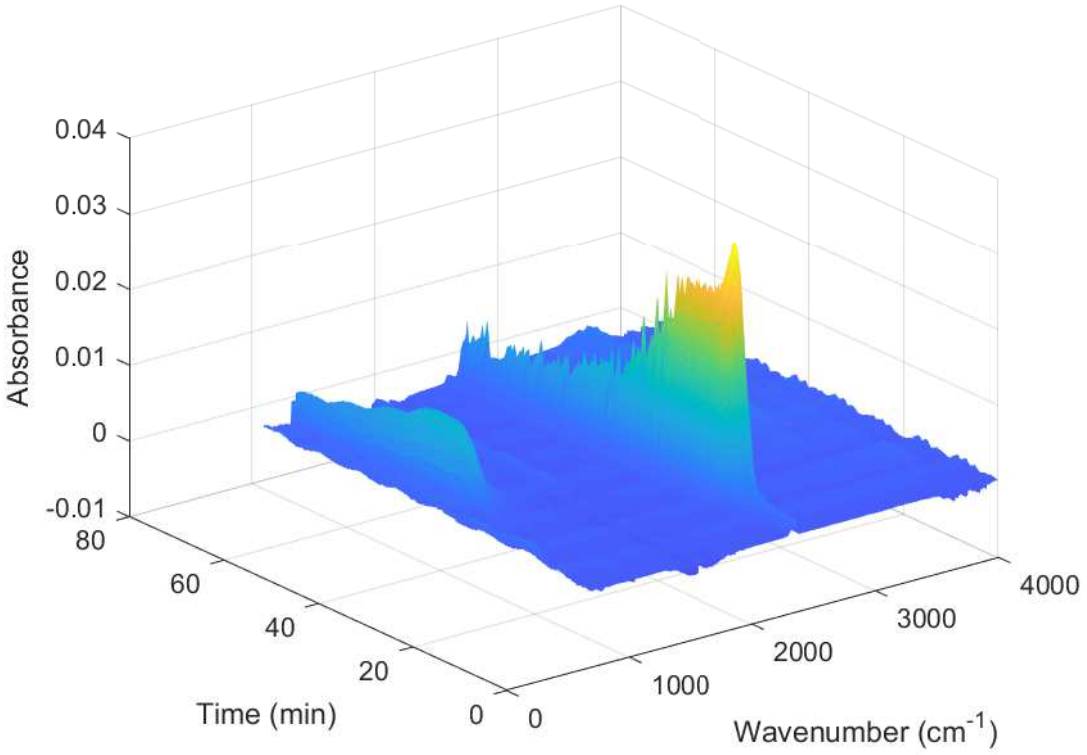

Figure E.58: 130 °C isothermal run # 2 FTIR feed

E.4 NMR results

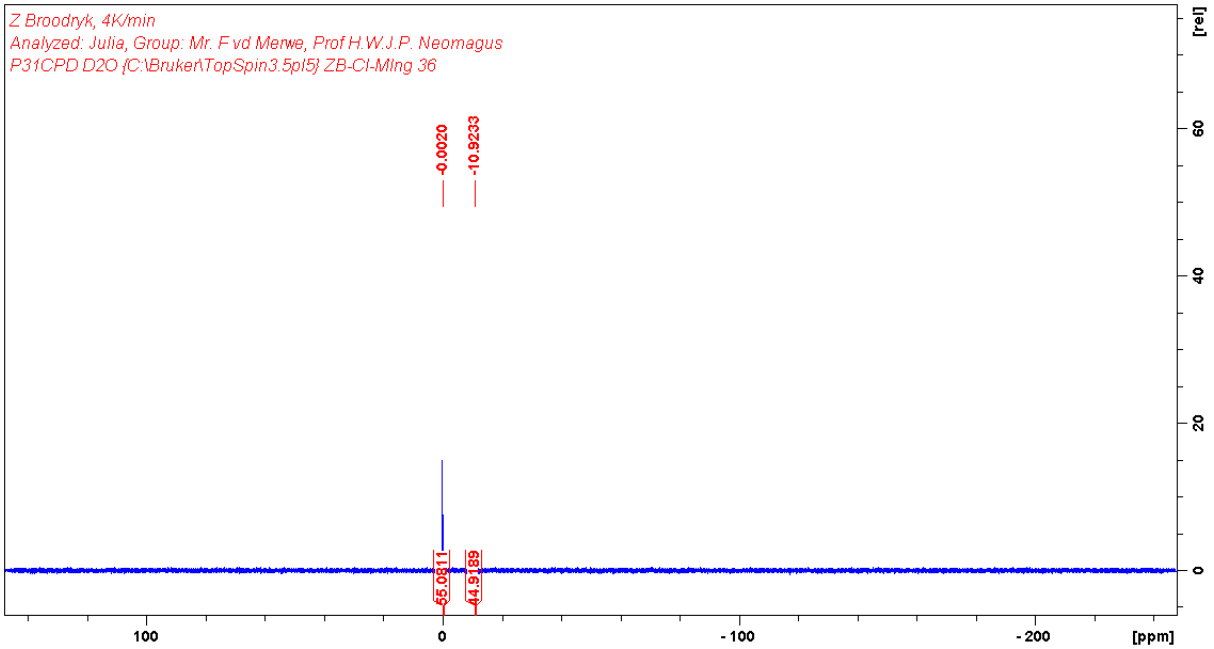

Figure E.59: NMR spectrum of the 122 °C isothermal 30 min sample

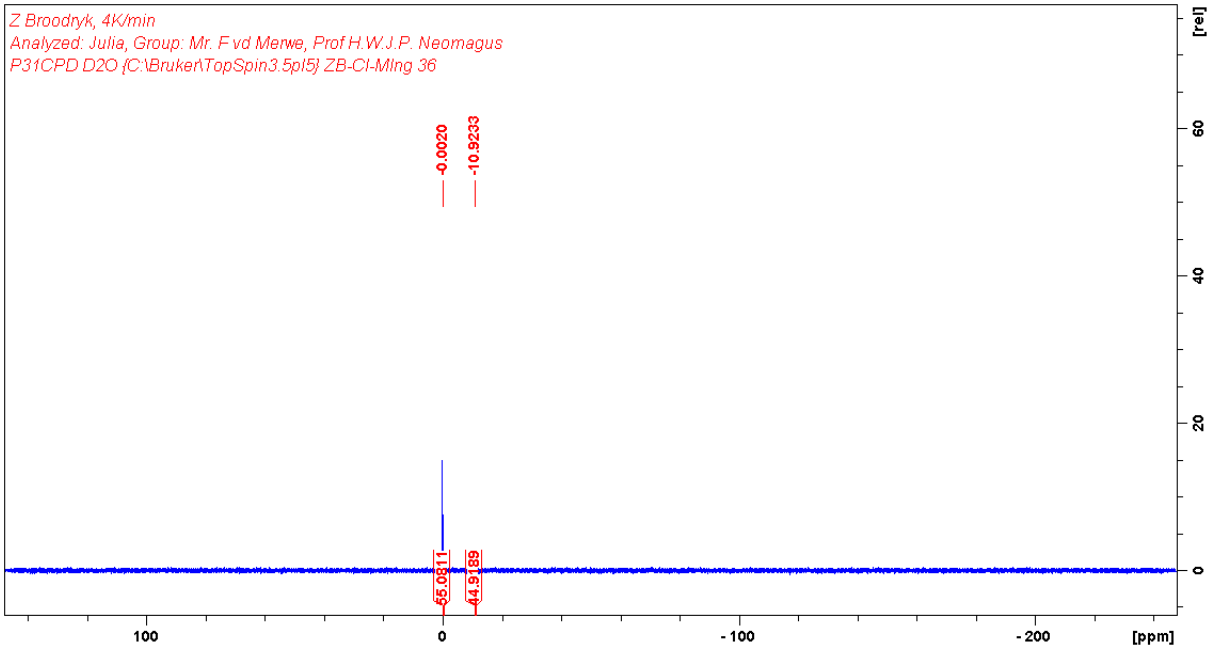

Figure E.60: NMR spectrum of the 122 °C isothermal 60 min sample

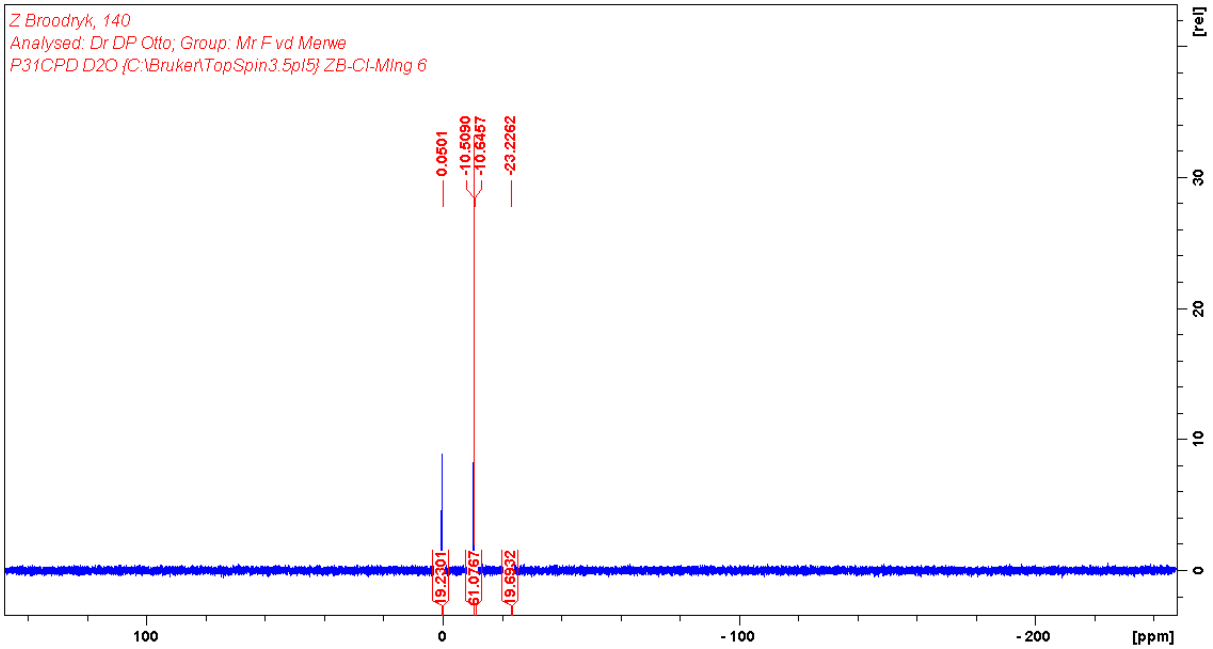

Figure E.61: NMR spectrum of the 0.5K/min sample

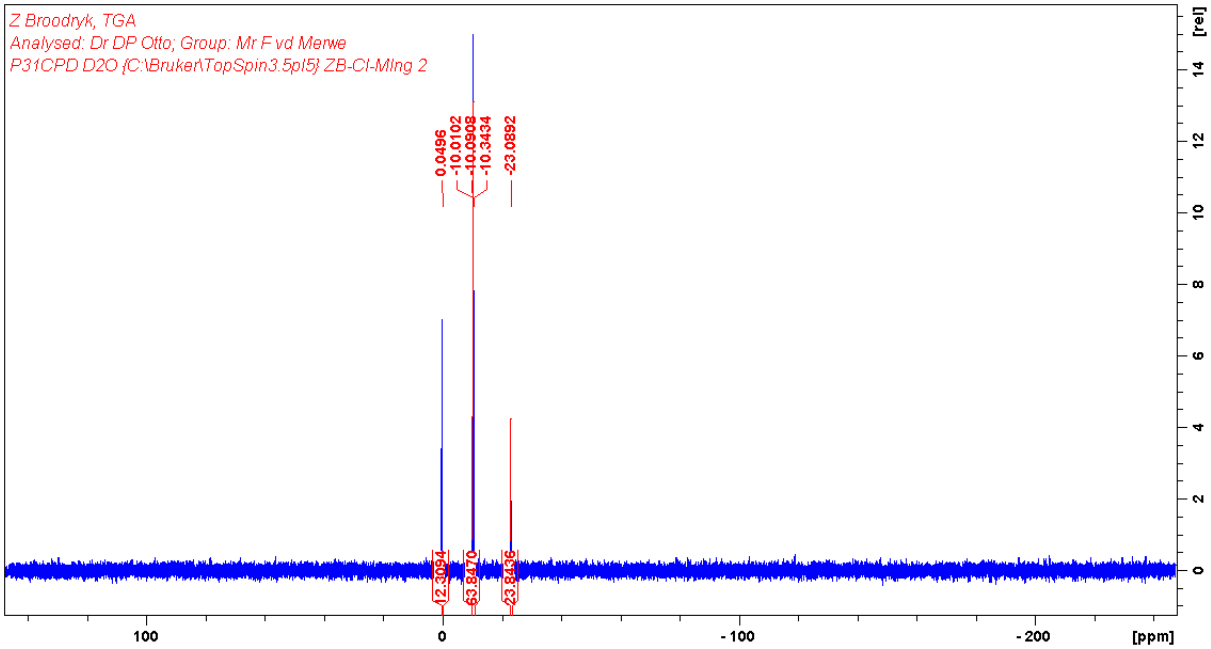

Figure E.62: NMR spectrum of the 1K/min sample

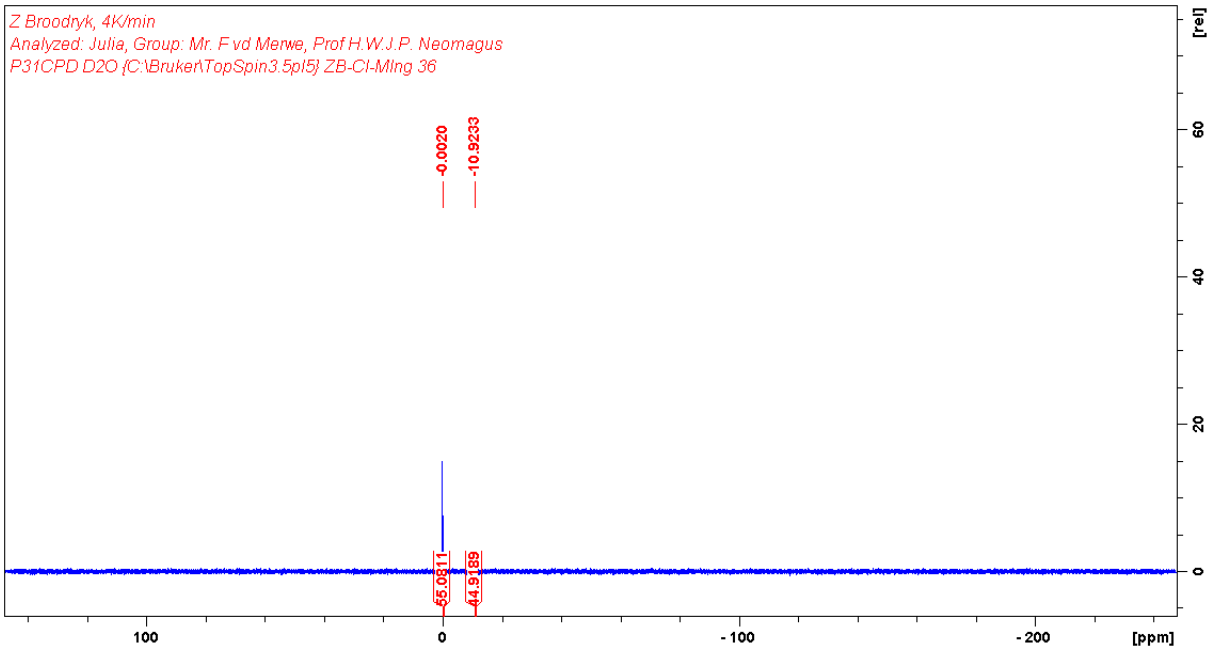

Figure E.63: NMR spectrum of the 4K/min sample